MESENCHYMAL STEM CELL DIFFERENTIATION ON BIOMIMETIC SURFACES FOR ORTHOPAEDIC APPLICATIONS

LIM TEE YONG

(B.Sc., Auckland)

[M.Sc. (Biomedical Engineering), NTU]

A THESIS SUBMITTED

FOR THE DEGREE OF DOCTOR OF PHILOSOPHY

DEPARTMENT OF ORTHOPAEDIC SURGERY

NATIONAL UNIVERSITY OF SINGAPORE

2009

Acknowledgements

The work for this thesis has been made possible with much assistance rendered by various persons to whom I owe my gratitude. Hence, I wish to sincerely thank the following persons who have assisted me in various ways:

- Dr. Wang Ee Jen, Wilson, for the opportunity to carry out my work in our laboratory, for the well-established collaboration with the Department of Chemical and Biomolecular Engineering Laboratory of Prof. Neoh Koon Gee, for his advice, encouragement and guidance throughout the project, and for reading my journal manuscripts, conference abstracts and posters, and this thesis;
- Prof. Neoh Koon Gee for facilitating my access to her laboratory at the Department of Chemical and Biomolecular Engineering to carry out work on the fabrication of titanium substrates, and for her advice and guidance;
- Shi Zhilong, Ph.D., for his assistance and guidance in the work on the fabrication of titanium substrates, and for the advice and discussions on techniques and the underlying chemical reaction mechanisms, and,
- Poh Chye Khoon, for his assistance in the acquisition of equipment and materials for my thesis work and the fabrication of titanium substrates, and for his encouragement and great companionship.

I also wish to express my gratitude to many other persons whose names are not listed here, who have assisted me in various other ways, and whose assistance, advice and guidance over the past few years have benefited me greatly, culminating in the much-needed confidence to undertake this project.

Acknowledgement is also given to the following sources:

- Fig. 1.3 is adapted from [1];
- Fig. 1.4 is adapted from [2];
- Fig. 5.3 is adapted from [2, 3];
- Fig. 8.1 is adapted from [3].

Contents

Summary of thesis

A large number of people require surgery, including total joint replacements, to treat bone and joint degenerative and inflammatory diseases. Implant-related infections and failure of an implant to osseointegrate with the bone tissue are common causes of implant failure. Despite efforts to avoid initial bacterial adhesion on an implant surface, nosocomial infections do occur. Hence, it is crucial to have the means to down-modulate the deleterious effects of bacterial endotoxins like lipopolysaccharide (LPS) on differentiating osteoblasts on the implant surface while treatment for the infection is given. Implant failure is also partly attributed to the poor vascularization around the healing bone. Thus, in the present thesis, the aims are to develop an anti-bacterial, osteogenic substrate for bone cell differentiation, and to develop an angiogenic substrate to promote endothelial cell differentiation, as an adjunct to osteogenesis. To address the concern of opportunistic bacterial infections at the bone-implant interface, a study is also done to evaluate the effects of a bioactive lysophospholipid on differentiating osteoblasts growing on the osteogenic substrate in the presence of a selected bacterial endotoxin. Taken together, the work in the present thesis forms the basis for future work to be done in order to take the functionalized substrates closer to clinical applications.

List of tables

Chapter 3

Chapter 4

Chapter 6

List of figures

Chapter 1

Chapter 3

Chapter 4

Chapter 5

Chapter 6

List of publications and abstracts derived from work on this thesis

Journals

T. Y. Lim, W. Wang, Z. Shi, C. K. Poh and K. G. Neoh, Human bone marrow-derived mesenchymal stem cells and osteoblast differentiation on titanium with surface-grafted chitosan and immobilized bone morphogenetic protein-2, *J Mater Sci Mater Med* **20(1)** (2009), pp. 1-10.

T. Y. Lim, C. K. Poh and W. Wang, Poly (lactic-co-glycolic acid) as a controlled release delivery device, *J Mater Sci Mater Med* **20(8)** (2009), pp. 1669-1675.

T. Y. Lim, C. K. Poh, Z. Shi, K. G. Neoh and W. Wang, Effect of Sphingosine-1-phosphate on LPS-treated human mesenchymal stem cell-derived osteoblasts cultured on bone morphogenetic protein-2-linked chitosan-grafted titanium substrate, *Under review*.

Abstracts

T. Y. Lim, W. Wang, Z. Shi, C. K. Poh and K. G. Neoh, Human bone marrow-derived mesenchymal stem cells and osteoblast differentiation on titanium with surface-grafted chitosan and immobilized bone morphogenetic protein-2, 2nd International Congress on Stem Cells and Tissue Formation, 2008, Dresden, Germany.

Chapter 1

General Introduction

The initiative for the modification of bone implants

Bone and joint degenerative and inflammatory problems affect a large number of people worldwide. It is believed that the number of afflicted people will continue to rise. These diseases usually require surgical treatment, including total joint replacements in cases of severe degeneration of natural joints. Orthopaedic biomaterials are used in the fabrication of implantable medical devices to substitute, replace, or repair bones, cartilage or ligaments and tendons. However, current bone implants have a limited lifespan. An average implant lasts only about one to two decades. Implant failure can result from the repeated cyclic mechanical stress of motion, which fragments the cement used to secure the implant to the bone. Biomaterial debris around the bone-implant interface can cause osteolysis, a condition in which bone is gradually resorbed. Although osteolysis is a low-grade form of bone resorption, it eventually results in the loosening of an implant. Revision surgery to replace the failed implant with a new one is a painful and costly procedure for the patient. Besides the inconvenience of revision surgery, each replaced implant also has a shorter lifespan than the one which immediately precedes it. Although non-cemented implant components have been used to get around the problem of cement failure, the success of this approach is not consistent. This technique relies on the physical modification of the implant surface to render it porous, in an attempt to encourage bone growth into the porous surface. Implant components are

fabricated from titanium, but bone often recedes from the cementless components as well.

Bacterial infection of a bone implant surface is another major cause of implant failure. During surgical insertion of an orthopaedic implant, bacteria from the patient's own skin and mucosa can enter the wound site. Upon adhesion on the implant surface, the bacteria secrete a thick extracellular matrix and this leads to the formation of a bioflim. The protective biofilm delays the action of antimicrobial agents, making the bacteria within the biofilm very resistant to host defence mechanisms and antibiotics [4]. Bacterial infection at an implant site can eventually result in localized bone destruction, leading to implant failure. Furthermore, the evolution of antibiotic-resistant bacteria limits the availability of effective antibiotics for the treatment of implant-related infections.

The failure of implant to osseointegrate with the host bone tissue and bacterial infection are the main reasons for much research into making implant surfaces that retard initial bacterial adhesion and promote bone formation at the tissue-implant interface. The concept of using a cementless component bone implant, despite its present short-comings, is an attractive option to pursue in the quest for a longer-lasting prosthesis. To this end, researchers have explored the idea of coating an implant surface with a bone-growth stimulating factor to encourage bone attachment onto the surface. However, such biomimetic coatings have to be firmly attached to the implant surface to be resistant to any abrasions that the prosthesis may be subjected to during surgery. The coating must also be resistant to the wear and tear of repeated cyclic mechanical stress,

and not delaminate at the implant metal interface. Due to the highly corrosive environment of the human body, implantable devices consequently need to fulfill stringent requirements so that they do not corrode and release cytotoxic by-products. A biomaterial also must not induce an immunogenic response when it is implanted in a host. Undesirable host response to an implant can result in implant failure due to host rejection of the prosthesis. The process of bone regeneration is a unique one in the human body, in which angiogenesis plays a role. A chapter in this thesis is dedicated to the surface functionalization of poly-(lactic-co-glycolic acid) (PLGA) substrates with an angiogenic growth factor, to promote the differentiation of endothelial cells. Thus, in this thesis the purpose of surface modification is to render the titanium substrates osteogenic and the PLGA substrates angiogenic, as an adjunct to osteogenesis.

Introduction to biomaterials

An overview of biomaterials in orthopaedics

The choice of biomaterials for use in an implant is a crucial process that involves rigorous tests to assess their mechanical and biochemical properties, and their biological interaction with tissues. Hence, along the guidelines of mechanical properties and biocompatibility, the development of orthopaedic biomaterials conceptually evolved over three generations. A review of the evolution of biomaterials over three generations will allow a better appreciation of the initiative and the subsequent aims of the work undertaken for this thesis. The

wide range of orthopaedic biomaterials available necessitates the discussion to be focused on a few selected metals and biodegradable materials.

The first generation biomaterials

The first generation of orthopaedic biomaterials was mainly bioinert materials. This generation of biomaterials was designed to match the physical properties of the replaced tissues, and would not elicit an immune response [5]. Metallic materials of this generation that were successfully employed in orthopaedic applications were stainless steel and cobalt chrome-based alloys. Stainless steel implants were used in movable joints replacement parts but their poor wear resistance generated wear debris which resulted in osteolysis and local bone destruction, eventually leading to implant loosening. Thus, stainless steel was replaced by the wear resistant cobalt chrome alloys for the fabrication of replacement parts that were subjected to constant cyclical stress. Cobalt-chrome-molybdenum (Co-Cr-Mo) alloys have exceptional corrosion resistance [6]. However, it is difficult to fabricate complex shapes using this alloy. Another problem is the occurrence of large grain sizes despite the use of special casting techniques. Notwithstanding these disadvantages, Co-Cr-Mo alloys possess properties superior to stainless steel. Co-Cr-Mo alloys have higher intrinsic resistance to corrosion compared to stainless steel. Metallic transfer which results in galvanic corrosion, which is thought to occur between surgical tool and implant is much less for Co-Cr-Mo implants than for stainless steel ones. Surface damage to the implant which inevitably occurs during the surgical insertion of the implant can lead to corrosive damage in stainless steel implants but does not seem to similarly damage Co-Cr-Mo ones. However, the elastic modulus of these metals is higher than that of cortical bone. Hence, when

placed in contact with cortical bone, these metals will take much of the load that originally acts on the bone, resulting in reduced loading on the bone. This is known as the load sharing principle of the composite theory, and results in stress shielding. Bone is a natural composite material comprising an organic phase, made up mainly of Type I collagen, and a mineral phase, made up of hydroxyapatite. According to Wolff's Law, bone that is subjected to stresses higher than baseline physiological levels responds with osteogenesis. Conversely, when subjected to stresses lower than physiological levels, bone atrophy occurs as the bone resorbs, eventually leading to implant failure. Although hydroxyapatite, which has the chemical formula, $Ca_{10}(PO_4)_6(OH)_2$, does not have the mechanical strength to be used for load bearing purposes, it is often used as a ceramic coating on metallic implant surfaces. Being a bioactive material, a hydroxyapatite coating on the implant surface may serve to enhance osseointegration between implant and bone [7].

The use of titanium and its alloys in orthopaedics became popular after Branemark discovered the phenomenon of osseointegration [8]. Titanium and its alloys can tightly integrate into bone, greatly increasing the long-term behaviour of titanium-based implants and reducing the risks of implant failure. Titanium is a strong metal, and is very resistant to heat and corrosion. However, it is very difficult to machine into desired shapes. Its hardness, together with its high chemical reactivity with air, and other factors, has made titanium components very costly. Nevertheless, titanium, due to its biocompatibility, in addition to its strength and excellent resistance to corrosion, is used in the

fabrication of components in implants and prosthetics. There are several types of titanium alloys which have been developed for use. The most commonly used titanium alloy is Ti-6Al-4V. Another type of titanium alloy is Ti-4Al-4Mo-2Sn-0.5Si, which is less commonly used. Titanium and titanium alloys possess characteristics which make them a popular choice as a biomaterial for orthopaedic applications. Their hardness confers strength which allows them to be used for load-bearing applications. They also possess bend strength and fatigue resistance, which are important in load-bearing structures that are constantly subjected to the cyclic stress of motion. Ti-6Al-4V has a lower density than other metals that are used as biomaterials, making it comparably lighter. As an example, Ti-6Al-4V has a density of 4.40 g cm^{-3} while cobalt-chrome alloy has a density of approximately 8.5 g cm^{-3}. In terms of their elastic modulus, Ti-6Al-4V has a magnitude of 106 GPa while that of cobalt-chrome alloy is 230 GPa. Elastic modulus is a measure of a substance's tendency to be deformed non-permanently, that is, elastically. A substance with a low elastic modulus is flexible. A rigid biomaterial may cause bone atropy due to stess shielding and interference with blood circulation, which causes the bone to weaken. Hence, Ti-6Al-4V would be a more suitable choice than cobalt-chrome alloys for use in regions of the body which experience bending stresses. From a biomechanical perspective, Ti-6Al-4V would thus be less likely to cause bone atrophy and resorption. Although titanium has excellent corrosion resistance, its wear properties are poor. There are concerns that wear debris from titanium-based joint replacement implants could be cytotoxic or cause tissue reactions [9, 10].

A common feature of first generation biomaterials is the adsorption of unspecific proteins on the surface of the materials. A diverse array of unspecific proteins thus elicits the unspecific signaling to the cellular environment. Ultimately, a fibrous layer forms and encapsulates the implant. Thus, in the second generation of biomaterials, the aim is to develop bioactive interfaces which elicit a specific biological response.

The second generation biomaterials

The second generation of biomaterials is characterized as bioactive materials which interact with the biological environment to induce specific responses, as well as resorbable materials which support tissue development while progressively degrading into harmless products. The development of bioactive surfaces which promote mineralization and bonding between bone and implant is a common functionalization process to enhance osseointegration.

Although no metallic surface is bioactive *per se*, metals can be rendered bioactive by anchoring bioactive molecules onto their surface (surface functionalization). Metals can be functionalized using methods of physical or chemical modification of the surface. Physical surface modification includes electrophoretic deposition, plasma spraying and laser ablation [11-13]. Various chemical methods have also been developed to activate a material surface. Kokubo *et. al.* developed a thermochemical treatment which results in the formation of a thin titanate layer on a material surface that is able to form a dense bone-like apatite layer when immersed in a physiological medium [14]. Various

other chemical treatment methods including etching with hydrogen peroxide have also been developed [15, 16].

Resorbable polymers are the focus of the second generation of polymers. These biodegradable polymers undergo a controlled chemical breakdown and the polymer chains are resorbed. Examples of biodegradable polymers are polyglycolide (PGA), polylactide (PLA), poly(ε-carprolactone) (PCL), chitosan and hyaluronic acid. Kulkarni *et. al.* introduced the concept of biodegradable polymers, and these materials have been used in many orthopaedic applications such as repair of bone fractures and bone substitution [17, 18]. These polymers are also used for making sutures, screws and pins [19]. The use of biodegradable polymers in orthopaedic application has several advantages over metallic ones. As the polymers gradually degrade, they help to reduce the problem of stress shielding that are typical of metallic implants. Biodegradable polymers also eliminate the need for subsequent surgeries that may sometimes be necessary to remove metallic implants. Finally, biodegradable polymers enable post-operative diagnostic imaging without artefacts, unlike metals.

Due to the hydrolytic sensitivity of biodegradable polymers, moisture must be avoided during thermal processing of the polymers [20]. The biodegradation of these polymers is mainly initiated by hydrolysis, although enzymatic activity may to a lesser extent, play a role [21, 22]. Various factors control the degradation times of the polymers. The molecular weight of the polymer, polymer crystallinity, monomer concentration, porosity, geometry and location of the implant are factors that determine how quickly a polymer will degrade. In

what is termed ‘bulk degradation’, when an implant is in an aqueous environment, water will enter the bulk of the polymer and preferentially attack the chemical bonds of the amorphous phase, thereby shortening the polymer chain, following which water attacks the chemical bonds in the crystalline regions of the polymer [23]. In the second stage of degradation the acidic breakdown products autocatalyse the degradation process. The resulting lower crystallinity and size of the implanted device, and the presence of a larger amount of reactive hydrolytic groups in the polymer backbone eventually contribute to hastening the degradation process [24, 25]. A relevant example of this form of degradation is poly (lactic-co-glycolic acid) (PLGA). The breakdown products are lactic acid and glycolic acid which are enzymatically converted and fed into the tricarboxylic acid (TCA) cycle in the mitochondria. The final products are ATP, water and carbon dioxide. Water and carbon dioxide are then excreted by the lungs and kidneys [26, 27]. Another consideration of the use of a degradable polymer like PLGA for orthopaedic applications is mechanical strength, which can be improved by self-reinforcing the material with oriented fibres or fibrils of the same material. Some natural polymers like chitosan and collagen have intrinsic bioactive activity in some tissues, for example, cartilage tissue. The bioactivity of polymers depends on the functional groups and binding sites available on the polymer surface. Hence, the bioactivity of polymers can be modified by coupling certain polymers or biomolecules onto their surface. Metals and ceramic surfaces can be similarly modified in this way. For second generation biomaterials, the modification of polymer surfaces is achieved by physical adsorption of proteins and peptides

onto the surface, by dip-coating, or by amino- and carboxyl-directed immobilization of biomolecules [16]. The surfaces of polymers can also be chemically modified to induce their mineralization with HA layers [15].

The third generation biomaterials

The third generation biomaterials are materials engineered to be able to stimulate specific cellular responses at the molecular level [18, 28]. Third generation biomaterials debuted at about the same time as scaffolds were developed for tissue engineering applications. Temporary three-dimensional porous scaffolds that are able to promote cell adhesion, proliferation and differentiation are being developed [26, 29, 30]. Biomaterial surfaces functionalized with peptide sequences to mimic the extra-cellular matrix (ECM) are being developed as well. Due to the limitations of tissue transplantation and grafting such as rejection, costs, disease transfer, donor scarcity and post-operative morbidity, tissue engineering is seen as an attractive alternative solution [28, 31, 32]. There is current active research in tissue engineering and regenerative medicine to repair organs and tissues, using stem cells, growth factors and peptide sequences, in conjunction with synthetic scaffolds [33]. Other issues like angiogenesis and nutrient delivery which are crucial to tissue regeneration also need to be addressed. Despite the promising therapeutic potentials that tissue engineering offers, there are many concerns that still need to be addressed. Tissue engineering necessitates the manipulation of cells, which requires technical competence. Cell manipulation could also raise ethical

concerns. Very often, tissue engineering is a multi- and inter-disciplinary field, and work must be well-coordinated among workers in the relevant fields like biology, chemistry, physics, engineering and medicine. Clinically, new surgical procedures may need to be developed to complement the advancements in the tissue engineering field.

Modified biomaterials

The outcome of the interaction between biological systems and materials is dependent in large part upon the surface properties of the materials. Important properties to be considered include the physico-chemical nature, the topography, the mechanical properties, and the bio-functionality of the material surface. The surface properties of a material interact with biological entities like water, biological molecules, cells, and tissues, which come into contact with it. Many techniques are available to modify a material surface for the desired effect. Some examples of the current techniques include gas plasma treatments, ion bombardment, chemical and physical vapour deposition, coating of ceramics, metals and polymers, as well as coating of material surfaces with peptides, lipids and sugars.

In the subsequent chapters, details of the techniques used to functionalize selected titanium substrates and to coat the poly (lactic-co-glycolic acid) (PLGA) substrate with a bioactive molecule will be discussed.

Choice of biomaterials for osteoblast differentiation

Titanium

Titanium alloys are widely used in the fabrication of orthopaedic implants, owing to their strength-to-weight ratio and biological inertness. Besides being biocompatible, titanium alloys are also able to osseointegrate. Bone cells have been known to attach onto the surface of titanium-based hip and joint replacement implants. Although inherently osteogenic, bone cell attachment onto untreated titanium alloy surface is often insufficient for full osseointegration to occur. Hence, improvements in the techniques of surface modification of titanium alloys are continually being made to enhance bone cell adhesion and proliferation properties. Other modifications include the grafting of osteogenic factors onto the metal surface to further promote osteogenesis on the implant surface. Besides enhancing bone formation on the implant surface, biomimetic coatings are also used to counter titanium implant-related bacterial infections.

Chitosan

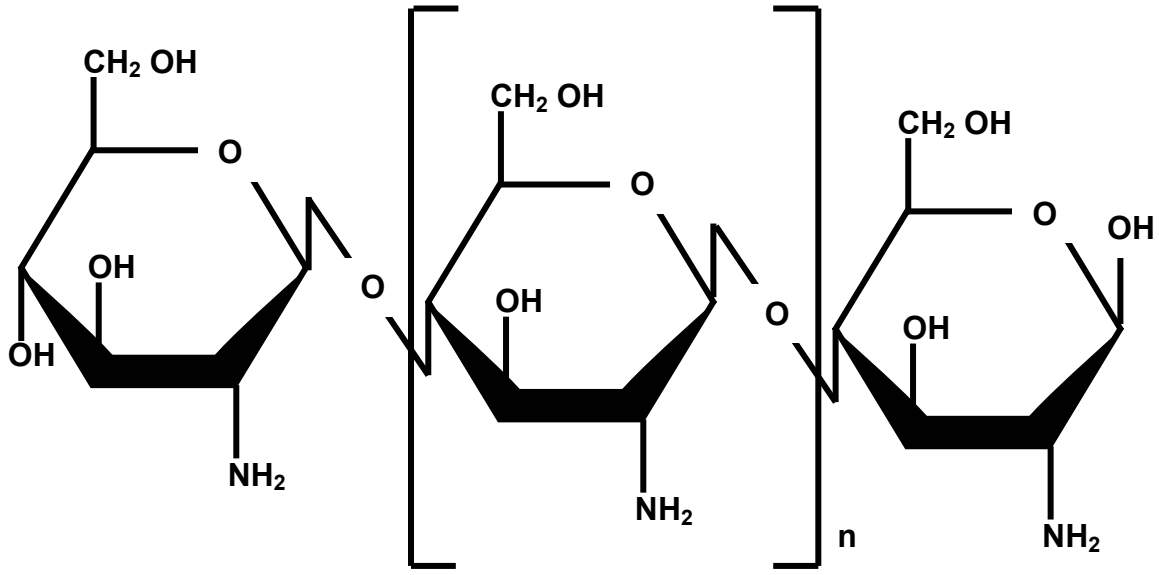

Fig. 1.1. Structural formula of chitosan in Haworth's projection.

Chitosan is a linear polysaccharide comprising randomly distributed β–(1-4)-linked D-glucosamine, which is the deacetylated unit, and N-acetyl--glucosamine, the acetylated unit. It has the potential to be used in biomedical applications. Chitosan is derived from chitin, the structural element in the exoskeleton of crustaceans, and is commercially produced by the deacetylation

of chitin. The degree of deacetylation of commercially produced chitosan ranges between 60% and 100%.

The amino group of chitosan has a pKa value of approximately 6.5. Thus, chitosan is positively charged, and is soluble in acidic to neutral solution, depending on the pH of the solution and the degree of deacetylation of the chitosan used. The positive charge makes chitosan bioadhesive, binding to negatively charged surfaces like mucosal membranes. Chitosan is a biocompatible and biodegradable substance. Its biocompatibility and its bioadhesive property make chitosan a potentially useful coating material for the functionalization of other biomaterials. Studies have shown that chitosan possesses osteoinductive potential [34-37]. Composite scaffolds containing chitosan have also been shown to support for the attachment and proliferation of osteoblast cells [24, 38-40]. In another approach, chitosan was chemically linked onto a polylactic acid membrane surface using carbodiimide chemistry. This membrane was shown to support the growth of osteoblasts [33, 41]. Another very important attribute of chitosan is its anti-bacterial property [36, 42]. A composite film of keratin-chitosan showed resistance against bacteria while supporting fibroblast attachment and proliferation [37].

Dextran

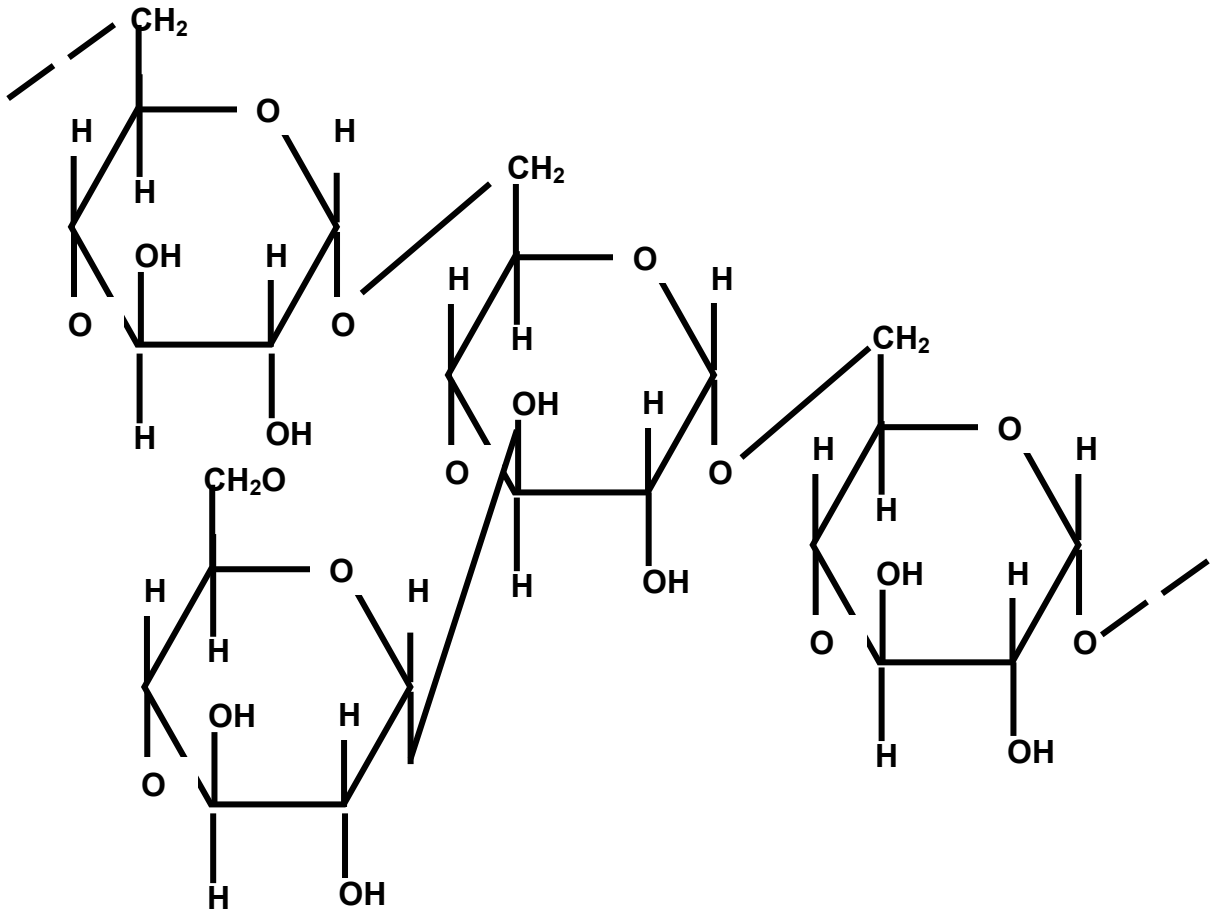

Fig. 1.2. Structure of fragment of dextran molecule.

Dextran is a complex, branched polysaccharide comprising glucose chains of varying lengths. Dextran immobilized onto material surfaces has been found to limit cell adhesion and spreading [43]. Thus dextran has been suggested for use as an effective low protein-binding, cell-resistant coating on biomaterial surfaces [44]. Hence, it is reasonable to speculate that dextran would similarly resist bacterial cell adhesion. However, the disadvantage of using dextran for surface coating biomaterials is due to the highly toxic and expensive sulfonyl chloride reagents used [45, 46]. The reactions also need to be carried out under stringent anhydrous conditions. These difficulties have been largely overcome with the availability of a method described that requires less toxic reagents and less stringent reaction conditions [43].

Immobilized dextran possesses the potential for multivalent, high density immobilization of bioactive molecules [44, 47]. This distinct advantage of dextran makes it an attractive polymer to be used as a biointeractive coating on bone implant surfaces. Dextran has also been shown to be a biocompatible molecule and therefore should not induce an adverse response if used *in vivo*. Dextran mimics the glycocalyx on cell surfaces and has been shown to be well-tolerated in animal studies [43]. Furthermore, dextranase, the enzyme that degrades dextran, is produced by bacteria and not by tissues [48]. Hence, other than tissues that have significant microbial populations, dextran implants and dextran-coated material surfaces will not degrade enzymatically in most tissues [48]. Recent studies have further shown that surface-immobilized dextran on biomaterials are resistant to dextranase-mediated degradation and thus should

be stable in most tissue environments [49]. Thus, dextran coated surfaces prevent non-specific protein and cell attachment, and can be grafted with cell adhesion ligands to promote the attachment of specific cell types, to develop well-defined surface modifications that promote specific cell interactions [44]. This could potentially result in well-defined surface modifications to bring about the better performance of long-term biomaterial implants.

Choice of biomaterials for angiogenesis

Poly (lactic-co-glycolic acid) (PLGA)

PLGA has been widely used to fabricate drug delivery matrices in the forms of microspheres, microparticles, nanoparticles, tablets, wafers and scaffolds [50-60]. The potential uses of PLGA include tissue engineering applications, medical therapy and drug delivery. PLGA biomaterials degrade *in vivo* by hydrolysis into lactic acid and glycolic acid. These two breakdown products are fed into the tricarboxylic acid cycle and excreted [61]. PLGA degradation occurs in four steps. Initially, water penetrates the amorphous region of the polymer and disrupts the secondary forces. This is followed by the cleavage of the covalent bonds in the polymer backbone by hydrolysis. As hydrolysis proceeds, the carboxylic end groups of the polymer autocatalyse the hydrolysis reaction. As massive cleavage of the covalent bonds in the polymer backbone ensues, there is significant mass loss. Finally, erosion occurs as monomers and oligomers leave the polymer bulk, resulting in the loss of weight [23]. Chemical degradation by hydrolysis is an important degradation mechanism in PLGA structures. However, PLGA structures contain hydrolysable ester bonds. Hence enzyme-catalyzed hydrolysis also contributes to the chemical degradation process of PLGA [62]. Enzyme-catalyzed hydrolysis is an important consideration in the design of PLGA-based biomaterial implants and devices with PLGA coatings for *in vivo* applications. Serum albumin, an important protein of blood plasma, has an esterase-like activity. While serum albumin may not alter the degradation mechanism, it increases the initial velocity

of the hydrolytic de-esterification process of glycolic acid-containing copolymers like PLGA [63]. Thus, when PLGA comes into contact with blood *in vivo*, its degradation rate may be significantly altered, which in turn will affect the release kinetics of a drug or bioactive molecules that are attached onto the PLGA matrix.

Besides water permeability and enzyme-mediated hydrolysis, the degradation of PLGA depends on a multitude of other factors [64, 65]. Temperature, pH, monomer ratio of the constituent lactic acid and glycolic acid, site of implantation, attachment of bioactive molecules and inflammation are some other factors that may affect the degradation kinectics of PLGA, and consequently alter the release kinectics of any bioactive molecule loaded onto the PLGA surface [65]. In previous studies elevated temperatures have been used to accelerate PLGA degradation and drug release from PLGA devices. [65]. Besides the effect of temperature, the thickness of the PLGA material also affects its degradation rate [66]. The degradation rate of PLGA *in vitro* is likely to differ from that *in vivo*. This is because the degradation process of PLGA is autocatalytic [67, 68]. The accumulation of acidic degradation products of PLGA causes a decrease in pH, and autocatalyzes the degradation process *in vitro*. However, this accumulation of acidic breakdown products is unlikely to occur *in vivo*. *In vivo* environments are dynamic, where body fluids and circulating blood would carry away the breakdown products constantly, preventing the build-up of acidity around the PLGA implant. Thus, a PLGA material would degrade comparatively more rapidly *in vitro* compared to that *in vivo*, which demonstrates that environmental conditions affect the degradation rate of PLGA [68]. A study

has shown that PLGA degradation rates *in vitro* are greater if no media change was done, which removes the acidic breakdown products, than if media was changed periodically [63]. Furthermore, the polymer composition of the monomeric units of PLGA also contributes to the differences in degradation rates [68].

Thus, the degradation of PLGA is dependent upon a number of factors operating simultaneously. *In vitro* studies conducted on PLGA degradation may yield results that do not actually reflect the *in vivo* situation. Unlike static conditions *in vitro*, the *in vivo* environment, by virtue of its dynamic nature, constantly changes and the PLGA degradation rate is thus correspondingly altered. Nevertheless, *in vitro* studies using a series of combinations of variables to simulate specific *in vivo* situations can yield a reasonable amount of useful information for the fabrication of PLGA-based biomaterials, like controlled release devices.

Introduction to the biological aspects of implants

Mesenchymal stem cells (MSCs)

MSCs are a population of multipotent, heterogeneous mesenchymal stromal cells [69]. These cells can proliferate *in vitro* as plastic-adherent cells. MSCs have a fibroflast-like morphology, can form colonies and can differentiate into bone, cartilage and fat cells. Although MSCs have been isolated from almost every type of connective tissue, the characterization of these cells is based mainly on bone marrow-derived MSCs [70]. The general consensus is that human MSCs lack the haematopoietic markers CD45, CD34 and CD14, as well as the co-stimulatory molecules CD80, CD86 and CD40. MSCs express variable levels of CD105, otherwise known as endoglin, CD 44, which is a cell surface glycoprotein that acts as a receptor for hyaluronic acid and other ligands like collagen, osteopontin and matrix metalloproteinases, and CD271, which is the low affinity nerve growth receptor, alternatively known as the LNGFR or p75 neurotrophin receptor. Besides the ability to differentiate into osteoblasts, MSCs have also been shown to differentiate into pericytes and endothelial cells, implicating their potential role in supporting haematopoieis [71]. The migratory capability of MSCs is a useful feature that has been demonstrated in *in vivo* studies [72]. Hence, the homing ability of MSCs is an attractive feature to exploit for potential therapeutic purposes in orthopaedic applications.

Bone morphogenetic proteins (BMP)

Bone morphogenetic proteins are cytokines belonging to the transforming growth factor beta (TGF-β) family, and more than 20 BMPs have been identified to date [73]. BMPs are synthesized as prepropeptides comprising 400 – 500 amino acids consisting of a signal domain, a predomain and a mature domain. BMPs dimerize by forming disulphide bridges. Upon cleavage of a Arg-X-X-Arg sequence in the C terminal domain, BMPs become active cytokines. Demineralized bone contains BMPs which have been found to stimulate ectopic bone formation *in vivo* [33]. Some BMPs like BMP2 can also be produced by preosteoblasts [73]. Besides their roles in the development of the skeleton and the maintenance of homeostasis during bone remodeling, BMP2 is also implicated in other biological processes like embryogenesis and angiogenesis [74]. Thus, BMPs have potential biomedical role as therapeutic agents.

BMPs prevent mesenchymal progenitor cell differentiation into myoblasts, and the transcription factor, Runx2, appears to play an important role in this process, by inducing matrix gene products and inhibiting myotube formation [1]. Runx2 expression seems to be low in mesenchymal progenitor cells. BMPs act on these progenitor cells to induce the upregulate Runx2 expression. However, Runx2 alone is insufficient in inducing osteoblastic differentiation. Runx2 subsequently needs to interact with BMP-specifc transcription factors called receptor-regulated Smads (R-Smads) to induce the mesenchymal progenitor cells into osteoblastic cells. In summary, the synergistic action of BMPs with

Runx2 and R-Smads is essential in inducing osteoblastic cell differentiation from mesenchymal progenitor cells.

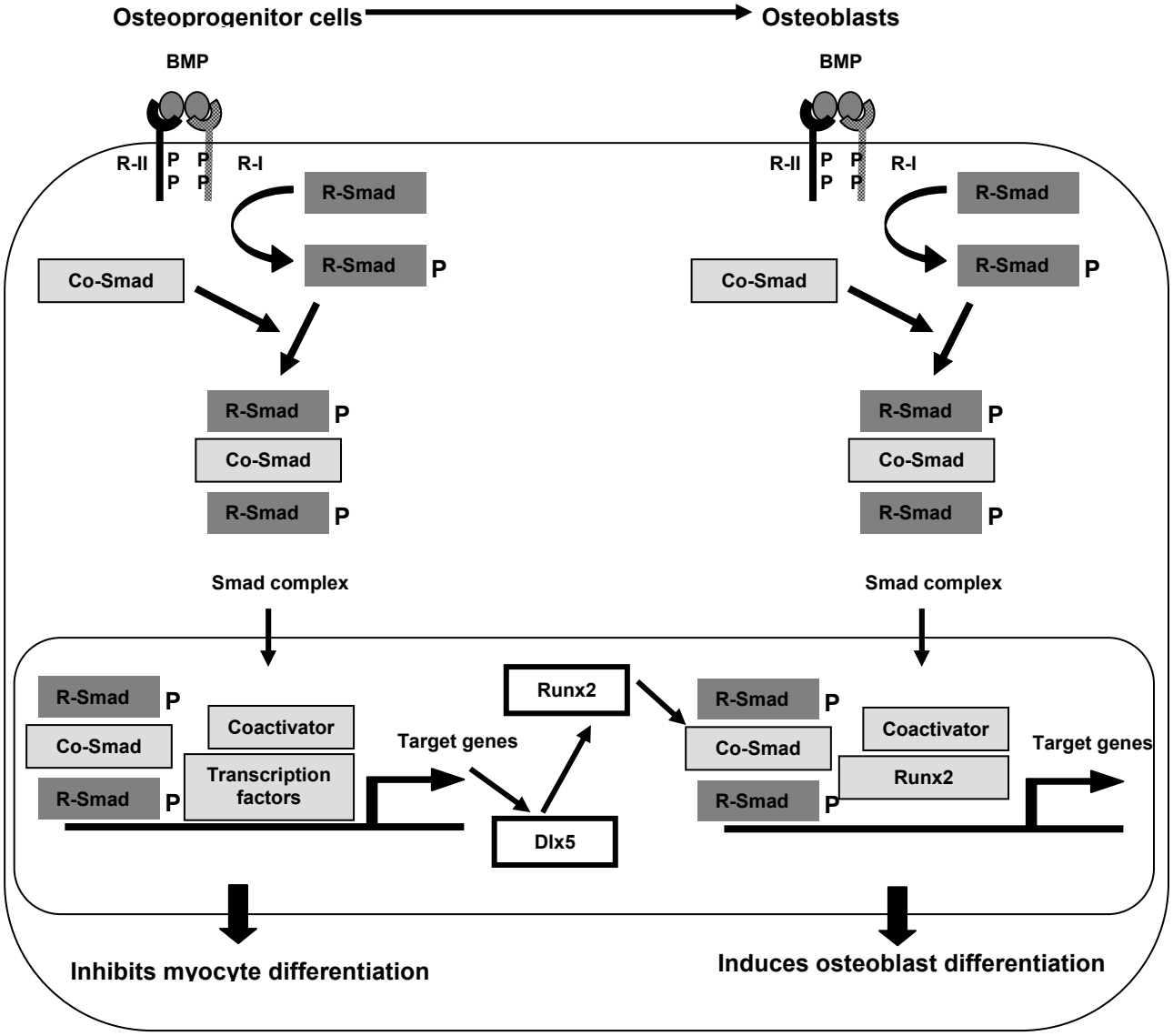

Fig. 1.3. Induction of osteoblast differentiation by BMPs through Runx proteins. Upon ligand binding onto the types I and II serine/threonine kinase receptors (R-I, R-II), the R-II receptor transphosphorylates the R-I receptor. The activated R-I receptor then phosphorylates the R-Smad, which in turn complexes with common-partner Smads (Co-Smads) to form the Smad complex. The Smad complex translocates into the nucleus. In the nucleus, the Smad complex binds directly to specific DNA sequences as well as interact with various transcription factors and transcriptional coactivators/corepressors, leading to the transcriptional regulation of target genes. BMPs induce the expression of Runx2 through Dlx5 in the osteoprogenitor cells and inhibits myoblast differentiation. BMP-specific R-Smads then interact with Runx2 and other proteins to induce osteoblast differentiation. (Adapted from Miyazono *et. al. Oncogene* **23** (2004). pp. 4232-4237.)

Vascular endothelial growth factor (VEGF)

Bone healing is a multistep regenerative process which involves coordinating angiogenesis with bone homeostasis [75]. Angiogenesis plays a central role in the bone regeneration process [76]. Angiogenesis is regulated by two main hormonal pathways, namely, the VEGF pathway and the angiopoietin pathway [77]. However, the VEGF pathway is the more important of the two pathways. Originally described as the tumour vascular permeability factor, VEGF was finally discovered and characterized in 1989 [78, 79]. Human VEGF exists as isomers, the most important VEGF isomers being $VEGF_{121}$, $VEGF_{165}$, $VEGF_{189}$ and $VEGF_{206}$. Angiogenesis has an especially important role in endochondral ossification [80]. During this process, avascular cartilagenous tissue is gradually transformed into vascular osseous tissue. VEGF is expressed by the hypertrophic chondrocytes in the epiphyseal growth plate. VEGF promotes vascularization of the cartilage by metaphyseal vessels. This results in new bone formation. Blocking VEGF binding to the VEGF receptors resulted in the suppression of vascularization of the cartilage and bone formation, which are restored upon termination of anti-VEGF treatment [81]. Thus, VEGF mediates the essential condition of vascularization that is required for the complex endochondral ossification. There is also evidence of the role of VEGF in intramembraneous ossification [75].

The mechanism of action of VEGF in endothelial cells begins with the binding of VEGF to the VEGF receptor. Following which, a cascade of intracellular signaling events begins with the dimerization and

autophosphorylation of the intracellular receptor tyrosine kinases [2]. This results in the activation of several downstream protein pathways, leading to some of the key biologic effects on endothelial cells (Fig. 1.3). The protein kinase c (PKC)-mediated activation of the protein kinase Akt, otherwise known as protein kinase B (PKB), mediates VEGF-dependent endothelial cell signaling and function [82]. This PKC-dependent Akt activation by VEGF was demonstrated through the use of several PKC inhibitors, which prevented the VEGF-stimulated Akt activation [82]. Endothelial cell migration has been shown to be regulated by the p38 mitogen-activated protein kinase (p38MAPK) pathway [83]. P38MAPK regulates the expression of urokinase plasminogen activator (uPA), which mediates the migration of several cell types including endothelial cells. uPA involvement in endothelial cell migration has been demonstrated by the use of agents that disrupt the uPA-uPA receptor interaction, which abrogated the cell migration process. Thus, VEGF-mediated endothelial cell migration is regulated through uPA, whose expression is in turn regulated by p38MAPK. The process of endothelial cell proliferation has been investigated in a study which found that the transcription factor serum response factor (SRF) is critical for endothelial cell proliferation and angiogenesis [84]. Also through the use of specific inhibitors, it was found that the activation of SRF requires the MEK/ERK and Rho signaling [ERK – extracellular signal regulated kinase; MEK – the immediate upstream activator kinase of ERK, otherwise known as MAP kinase (MAPK) or ERK kinase; Rho is a member of the family of small GTPases, which are G-proteins found in the cytosol]. Treatment of endothelial cells with each type of specific

inhibitor abrogated the VEGF-induced SRF expression. Furthermore, *in vivo* experiments using SRF antisense RNA to knock down SRF protein levels demonstrated that SRF deficiency inhibits angiogenesis. Taken together, SRF is a critical requirement for VEGF-induced angiogenesis and endothelial cell migration and proliferation. VEGF induces the SRF protein expression, its nuclear translocation and DNA binding activity in endothelial cells, a process that requires MEK-ERK and Rho GTPase signaling.

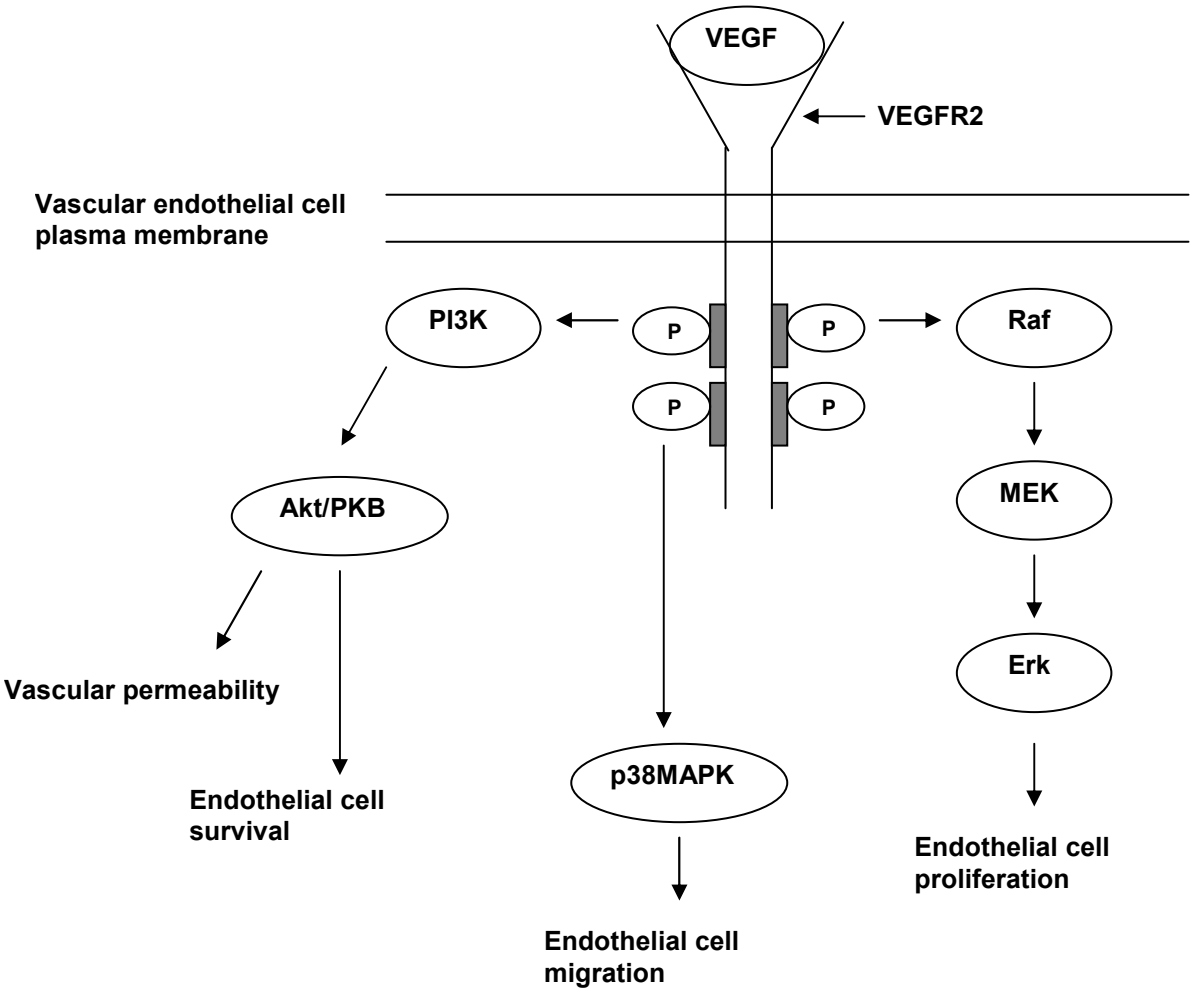

Fig. 1.4. VEGF receptor binding and intracellular signaling. (Adapted from Rini *et. al. J Clin Oncol* **23** (2005), pp. 1028-1043.)

Much work has been done on VEGF in recent years [85]. However, the role of VEGF in bone formation and angiogenesis is still not fully understood. VEGF has potential clinical applications as an adjunct to the osseointegration of bone and implant in areas of poor vascular supply. Hence, the use of VEGF to functionalize biomaterials for clinical applications remains to be explored. In this work, the release of VEGF from a PLGA substrate and the ability of the released VEGF to mediate endothelial cell differentiation from hMSCs are studied.

Introduction to the relevant aspects of osteoimmunology

In order to better appreciate the significance of the work done in chapter 6, the relevant aspects of osteoimmunology in the chapter wherein the LPS-CD14/TLR4/MD2 interaction, TNFα and S1P are discussed below.

(LPS – Lipopolysaccharide, TLR4 – Toll-like receptor-4, tumour necrosis factor-α (TNFα) and sphingosine-1-phosphate (S1P))

The LPS-CD14/TLR4/MD2 interaction

LPS is a major component of the outer cell membrane of Gram-negative bacteria, acts as an endotoxin and is able to elicit strong immune responses in the body. Dendritic cells stimulated with LPS showed an increase in the expression of TNFα mRNA and protein levels [86]. LPS comprises three structural components: a core oligosaccharide, an O-specific chain made up of repeating sequences of polysaccharides and a lipid A component, which is responsible for the proinflammatory properties of LPS [87]. LPS has been reported to activate Toll-like receptor-4 (TLR4/CD284) [88]. Toll-like receptors

(TLR) are a family of mammalian proteins. Mammalian Toll-like receptors are Microbe Associated Molecular Pattern (MAMP) receptors and thus recognise bacterial common structures [89]. TLR4 is an LPS ligand and has been found to be essential for LPS responsiveness *in vivo* [90]. TLR4 is part of a receptor complex comprising two other molecules, CD14 and MD2. Like the other mammalian Toll-like receptors, TLR4 is a MAMP receptor which recognizes LPS and thus functions as a LPS ligand [89, 91, 92]. CD14 is also a pattern recognition receptor and LPS is its main ligand. CD14 thus functions as a co-receptor of the CD14/TLR4/MD2 receptor complex. The MD2 protein is encoded by the human gene, Lymphocyte antigen 96. MD2 associates with the TLR4 to confer responsiveness to LPS, thereby mediating the extracellular to intracellular LPS signalling [93]. Fig. 6.7 is a schematic to illustrate the association of LPS with the CD14/TLR4/MD2 receptor complex on the cell surface.

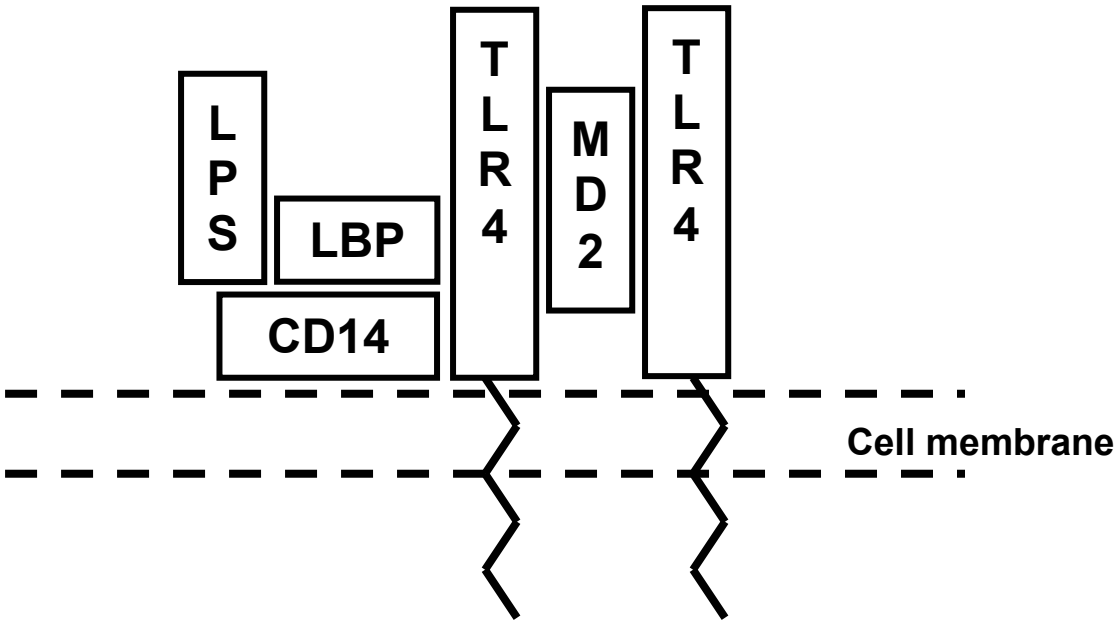

Fig. 1.5. This schematic illustrates the association of LPS with the CD14/TLR4/MD2 receptor complex on the cell surface. CD14 and TLR4 are pattern recognition receptors which recognise LPS. MD2 is a protein which interacts with TLR4 to mediate the extracellular to intracellular LPS signaling. LBP (lipopolysaccharide binding protein) is an integral membrane protein which is involved in the acute-phase immunologic response to Gram-negative bacterial infections. LBP binds LPS and interacts with the CD14 co-receptor.

TNFα

TNFα is a member of a large family of inflammatory cytokines that share common signal pathways [94]. Like the other inflammatory cytokines, it activates the transcription factor NFκB and stimulates the apoptotic pathway. In bone, TNFα plays a central role in bone pathophysiology, and attacks bone at many levels [94]. It stimulates osteoclastogenesis and simultaneously inhibits OB function. TNFα inhibits the recruitment of osteoprogenitors from the bone marrow, suppresses the expression of matrix protein genes while upregulating the expression of genes that mediates osteoclastogenesis, and inducing OB resistance to 1,25-dihydroxyvitamin D. Bone-related genes like Runx2 and OCN have also been reported to be downregulated by TNFα [95, 96]. At the same time, RANKL expression is upregulated by TNFα [97].

S1P

S1P is a bioactive lysophospholipid that acts both intracellularly and extracellularly [98]. It induces a wide spectrum of biological responses like cell survival, growth and migration [99-103]. S1P has been shown to be a potent OB mitogen [104]. It has been proposed that S1P functions to regulate the migration of osteoprogenitors from the bone marrow to the bone formation site, through its receptor, S1P2 [105]. Thus, S1P helps to preserve the osteoprogenitor pool in marrow by ensuring that only mature osteoprogenitors are mobilized. It also regulates osteoclastogenesis by increasing RANKL in OBs [98].

Besides its roles in bone cell related functions, S1P appears to also mediate important roles in vascular biology. Experiments were conducted using transgenic mice that overproduce endogenous S1P, as well as mice with ischaemic limbs given intramuscular administration of S1P. The results showed that S1P promotes post-ischaemic angiogenesis and blood flow recovery [106]. It has also been proposed to embed S1P in polymeric thin films to be gradually released for therapeutic arteriogenesis [107].

S1P has also been indicated to be able to protect against damage caused by endotoxin-induced inflammation [108]. One of the receptors for S1P is S1P1, which has been shown to act in unison with TLR4 to regulate IFNβ in human primary gingival epithelial cells [109]. IFNβ exerts an anti-inflammatory effect by inhibiting TNFα production [110]. Interestingly, S1P has also been shown to induce an anti-inflammatory phenotype in macrophages through the S1P1 receptor on the macrophages [111]. S1P is also able to cross-activate the TGFβ

signaling pathway in renal mesangial cells and mimic TGFβ induced cell responses, including the inhibition of proinflammatory gene induction [112].

Conclusion

Although biomaterials are continually being improved upon, currently, biomaterials from all three generations still have a relevant role to play. Developments in materials science must match the biological complexity at the molecular level, so that biomaterial surfaces can be tailored for different specific purposes of implant integration and tissue regeneration. Such tasks would need the synergistic, coordinated efforts of the various scientific, engineering and medical disciplines. The purpose of functionalizing an implant surface by the physical or chemical modification of its surface is to render it capable of supporting various cellular functions. Beside the engineering perspective of biomaterials, the biological aspect of tissue engineering also plays a critical role in regenerative medicine. Thus, the choice of the appropriate cell type for use with functionalized biomaterials will synergize with the body's physiology to enhance the integration of an implant with host tissues. Due to wide range of orthopaedic biomaterials available, the scope of work and discussion in this thesis will focus on Ti-6Al-4V, a metallic biomaterial, with a chapter dedicated to the studies using PLGA, a bioresorbable polymer. Within this scope, discussions on the work done will include the surface modification of Ti-6Al-4V to render it anti-bacterial and osteogenic. An osteoconductive titanium surface may have a better potential to osseointegrate with host bone tissue and thus reduce the chances of implant loosening. Following the initial work to render the titanium surface osteogenic and resistant to bacteria, further work is done to improve on the technique of attaching BMP2 onto the titanium surface. This improved

substrate is then used to simulate the effects of bacterial infection on differentiating osteoblasts, and to study the ability of a selected bioactive molecule in countering the deleterious effects of the bacterial endotoxin, LPS. The discussion will also include the use of PLGA for the fabrication of a controlled release angiogenic substrate. The process of angiogenesis is important to the proper healing of bone repair and wound healing. Together, an implant with an osteoconductive surface and a biomimetic material that supports angiogenesis, coupled with cells that possess multi-lineage differentiation potential could promote more efficient bone repair and healing after surgery.

Chapter 2

General materials and methods

Materials and methods common to chapters 3, 4, 5, 6 and 7 are described below. Materials and methods specific to each of the chapters mentioned above are described in the corresponding chapters (denoted by # against the appropriate sub-headings below).

Materials

Ti-6Al-4V (subsequently denoted as Ti) foils were purchased from Goodfellow of Cambridge (UK). Chitosan (CS) was purchased from CarboMer (San Diego, US) and refined twice by dissolving it in dilute acetic acid solution, filtered, then precipitated with aqueous sodium hydroxide and dried in a vacuum oven for 24 h at 40^{o}C. The viscosity-average molecular weight was approximately 2.2 X 10^5 as determined by the viscometric method. The degree of deacetylation was 84% as determined by elemental analysis using the Perkin-Elmer Model 2400 elemental analyzer [113]. 3,4-dihydroxyphenylalanine (dopamine), glutaraldehyde, dextran (MW = 70 000), sodium periodate, sodium borohydride, dexamethasone, β-glycerophosphate and ascorbic acid were purchased from Sigma-Aldrich Chemical Co. (Singapore). Ultrapure water (>18.2 MΩ cm, Millipore Milli-Q system, Singapore) was used in the experiments. All materials used in cell culture were purchased from Gibco, Invitrogen (Singapore). Flow cytometry was done using the CyAn^{TM} ADP Analyzer. Fluoroisothiocynate (FITC)-conjugated CD44 and phycoerythrin (PE)-conjugated

CD105 antibodies were purchased from eBioscience (San Diego, US), CD271-FITC was purchased from Miltenyi Biotec (GmbH, Germany), and CD34-FITC and CD45-FITC were purchased from AbD Serotec (UK). BMP2 was purchased from USBiological (US). The intensity and stability of BMP2 attached onto the chitosan-grafted titanium substrate surface were assessed using the Bio-Rad DC Protein Assay (US). RNA and protein concentrations were measured using the NanoDrop ND1000 spectrophotometer. RT-PCR was done using the BIORAD iCycler. The CellQuanti-MTT™ cell viability assay kit and the QuantiChrom™ alkaline phosphatase (ALP) assay kit were purchased from BioAssay Systems (US). Human mesenchymal stem cells (hMSC) were purchased from Lonza (Lonza Walkersville Inc., USA. Product number: PT-2501). Human osteoblasts (hFOB) were purchased from the American Type Culture Collection (ATCC, USA. Product number: CRL-11372).

Preparation of surface modified titanium substrates [#]

The preparation of each specific type of surface modified titanium substrate is described in the corresponding specific chapters.

Characterization of the titanium substrates

The characterization of the Ti-CS and Ti-Dex substrates was done by the staff of Department of Chemical and Biomolecular Engineering, Faculty of Engineering, National University of Singapore [114, 115]. The chemical composition of the surfaces was analyzed by X-ray photoelectron spectroscopy (XPS) on an AXIS HSi spectrometer (Kratos Analytical Ltd., UK) with an AlKα X-ray source (1486.6 eV photons). The details for the XPS measurements are similar to those reported earlier [116]. All binding energies (BEs) were referenced to the C 1s hydrocarbon peak at 284.6 eV. In the peak synthesis, the line width (full width at half-maximum) of the Gaussian peaks was kept constant for all components in a particular spectrum.

Stability and surface density of BMP2 on the surface modified titanium substrates

To assess the stability of BMP2 on the surface modified titanium substrates, the substrates were placed individually in a 24-well plate containing 1 ml of PBS per well. The intensity of the BMP2 on the substrate surface was assessed on days 0, 1, 3, 5 and 7. At each respective point in time, the substrates were removed and placed in a new well each. 1 ml of PBS was then added to each well, and the attached BMP2 was scrapped off the substrate surface with 20 strokes of a cell scraper. An alternative method of detaching the bound BMP2 is to immerse the substrates individually in a 1N HCl solution at 50^{o}C for 24 hours [117]. The solution is then neutralized with 0.1 NaOH to pH

7.0 before the concentration of BMP2 is determined. However, the use of HCl could possibly result in some degree of denaturation of the BMP2 [117]. In the case of the Ti-Dex-BMP2 substrate, the interference by the dextran chains could also result in inaccurate determination of the amount of BMP2 [117]. Hence, the method of detaching the bound BMP2 from the substrate surface by scrapping is chosen for this study. The amount of BMP2 in solution was then measured using the Bio-Rad DC Protein Assay, following the manufacturer's instructions. The colour intensity of the reaction mixture was measured at 700 nm using an absorbance plate reader after an incubation period of 15 min. The amount of attached BMP2 on day 0 is the initial coating density, while those on days 1, 3, 5 and 7 give an indication of the stability of BMP2 on the substrate surface. The absolute amount of BMP2 adsorbed onto the substrate surface, that is, the initial coating density, was measured as described above, using a series of BMP2 solutions of known concentrations as standards.

Culture of bone marrow-derived stromal cells (BMMSC)

Bone marrow was taken with written consent from patients undergoing surgery for rheumatoid arthritis. The marrow was washed 3 times with copious Hanks Balanced Salt Solution (HBSS). Erythrocytes were lysed with a 0.8% ammonium chloride solution and the bone marrow cells were centrifuged at 300 g for 10 min. The cell pellet was then washed 3 times with HBSS, resuspended and cultured in a medium comprising Minimal Essential Medium-alpha (MEM-α), supplemented with 10% foetal bovine serum (FBS), L-glutamine (2mmol/l),

penicillin (100 U/ml) and streptomycin sulphate (100 μg/ml), and incubated at 37°C in a humidified atmosphere of 5% CO_2 and 95% air. Unattached cells were removed on the following day. The attached cells were then denoted BMMSCs. Cell colonies that formed during culture were identified and removed by gentle trypsinization (0.25% trypsin-EDTA). Trypsin was removed by centrifugation. Each colony of BMMSCs was re-seeded in a new culture flask. Half of the culture medium was replaced by a fresh aliquot of medium once every 2 days. The BMMSCs were then allowed to grow to about 75% confluence before use. Passage 2 cells were used throughout the study. Attached cells were detached by trypsinization and resuspended in fresh culture medium for subsequent experiments. Although the experiments were done using bone marrow donated by three different patients, the results are a representative from one sample which had consistent cell morphology and a high cell proliferation rate by passage 2.

Culture of bone chip-derived osteoblasts (BC-OBs)

BC-OBs were obtained from bone chips of the same patients from whom bone marrow was taken for the culture of BMMSCs. The bone chips were washed 3 times in HBSS, cut into smaller fragments before being placed in tissue culture flasks and cultured under the same conditions as BMMSCs. Upon reaching approximately 75% confluence, the bone chips were removed and the cells were washed 3 times with HBSS, trypsinized and reseeded in new tissue culture flasks for further expansion. Passage 2 BC-OBs were used for RT-PCR.

Culture of human mesenchymal stem cells (hMSC) (Lonza, USA)

Human mesenchymal stem cells (hMSC) were seeded into cell culture flasks and cultured in a medium comprising Minimal Essential Medium-alpha (MEM-α), supplemented with 10% foetal bovine serum (FBS), L-glutamine (2mmol/l), penicillin (100 U/ml) and streptomycin sulphate (100 μg/ml), and incubated at 37^{o}C in a humidified atmosphere of 5% CO_2 and 95% air. Unattached cells were removed on the following day. Half of the culture medium was replaced by a fresh aliquot of medium once every 2 days. The attached cells were allowed to grow to about 75% confluence. Cells colonies that were formed were identified and individually removed by gentle trypsinization, seeded into a new flask each and allowed to grow to about 75% confluence before being used. Passage 2 hMSCs were used throughout the study. Attached cells were detached by trypsinization and resuspended in fresh culture medium for subsequent experiments described below. Undifferentiated hMSCs were used as a negative control in the alkaline phosphatase (ALP) assay.

Culture of human osteoblasts (hFOBs) (ATCC, USA)

hFOBs were cultured in a medium comprising a 1:1 mixture of Ham's F12 Medium and Dulbecco's Modified Eagle's Medium without phenol red, supplemented with 10% FBS and 0.3 mg / ml of G418. The hFOBs were maintained at a permissive temperature of 34^{o}C in 5% CO_2 in a humidified atmosphere. For differentiation into osteoblasts, the hFOBs were maintained at

a restrictive temperature of 39.5^{o}C. Differentiated osteoblasts were used as a positive control in assays for bone-cell differentiation.

Cell attachment

Cell attachment on the various titanium substrates was evaluated by counting the number of attached cells (BMMSCs or hMSCs) 6 hours after cell seeding. The substrates were placed into a 24-well plate and seeded with cells at a density of 5 000 cells / cm^2. The number of attached cells on the substrates was evaluated, and compared to the number of attached cells on the bottom of a similar well without any titanium substrate (control). At the time of cell counting, unattached cells were rinsed off with PBS. The attached cells were detached with trypsin. Tryspin was removed by centrifugation. The cells were resuspended in an appropriate amount of cell culture medium and counted using a haemocytometer.

Cell proliferation

Cell proliferation on the substrates was evaluated by counting the number of attached cells on days 1, 3, 5 and 7. The number of attached cells on the bottom of a similar well without any titanium substrate was counted at the respective points in time and was used as a control. At each designated point in time, the unattached cells were rinsed off with PBS. Attached cells were detached and counted as described above. The number of attached cells is reported as number of cells / cm^2.

Flow cytometry [#]

Flow cytometry is a technique used in the work described in chapter 3 to detect cell surface markers on the BMMSCs to confirm the cell lineage. The procedure is described in chapter 3. Flow cytometry is also used in chapter 7, to rule out the presence of CD133+ cells, which are endothelial progenitors.

Cytotoxicity assay

The MTT assay was carried out at day 7 of culture of the cells on the different titanium substrates to assess the effect of the substrates on cell viability. The assay is based on the conversion of yellow MTT (3-(4,5-Dimethylthiazol-2-yl)-2,5-diphenyltetrazolium bromide) to purple formazan in the mitochondria of living cells. A suitable quantity of MTT reagent was added to the cells at day 7 of culture on the different substrates and then incubated for 4 hours at 37^{o}C. At the end of the incubation period, an appropriate amount of solubilization solution (supplied in the MTT assay kit) was added to respective cultures and then gently mixed on an orbital shaker for one hour at room temperature. The insoluble purple formazan product was dissolved in the solubilization reagent to give a purple solution. The intensity of the colour in each well was measured at 570 nm on an absorbance plate reader.

Alkaline phosphatase (ALP) assay

The level of ALP of the cells was assessed using an ALP assay kit. The ALP assay is used in the studies to assess the level of osteoblast differentiation from BMMSCs or hMSCs. This assay relies on the ALP hydrolysis of *p*-nitrophenyl phosphate into a yellow product, the intensity of which was measured at 405nm on an absorbance plate reader. Briefly, BMMSCs or hMSCs were seeded onto the substrates at a density of 5,000 cells / cm^2. At day 7 of culture, the cell layers were washed with HBSS and gently scraped off from the surfaces of the substrates. HBSS was removed by centrifugation and cell lysis buffer was then added to the cells. The cells were sonicated to disrupt the cell membranes. After sonication, cellular debris was removed by centrifugation and aliquots of the cell lysates were collected for the analysis of the ALP activity and the quantification of total protein level. The assay was carried out at room temperature. For each sample well of a 96-well plate, 50μl of the respective cell lysate was added. A further 150 μl of the kit's working reagent comprising 5 mM of magnesium acetate and 10 mM of p-nitrophenyl phosphate were then added to each sample well. The colour intensity of the reaction mixture was measured at 4 minute intervals. The ALP activity of each sample was calculated according to a formula provided in the kit. The readings at the 20-minute interval were used to determine the respective levels of ALP activity. ALP activity was determined as the rate of *p*-nitrophenol liberation from *p*-nitrophenyl phosphate, normalized with respect to the total protein content obtained from the same cell lysate, and

expressed as number of IU of *p*-nitrophenol formation per minute per milligram of total proteins (IU min^{-1} mg^{-1} protein).

Reverse transcription-polymerase chain reaction (RT-PCR)

RNA was extracted from cells on day 10 of culture using the NucleoSpin® RNA / Protein isolation kit (Macherey-Nagel, GmbH, Germany) according to the manufacturer's instructions. Each sample of RNA was diluted 50X with DEPC (diethypyrocarbonate) water and the RNA concentration was measured using the NanoDrop ND1000 spectrophotometer. 1 μg of each sample of total RNA was used for the RT-PCR reaction. Reverse transcription of mRNA to cDNA and subsequent cDNA amplification was done using the TITANIUM™ One-step RT-PCR Kit (Clontech Laboratories, Inc., US), through one cycle at 50°C for 1h and 94°C for 5 minutes. This was followed by 32 cycles at 94°C for 30 seconds, 60°C for 30 seconds and 68°C for 1 minute, with a final extention at 68°C for 2 minutes. The expression of glyceraldehyde 3-phosphate dehydrogenase (GAPDH) was used to check RNA integrity. The amplified products were subjected to electrophoresis in a 2% agarose gel and stained with ethidium bromide (Sigma-Aldrich, Singapore). Cells grown on the titanium substrates were compared with BC-OBs or human osteoblasts (hFOBs), and untreated BMMSCs or hMSCs, both cultured in normal tissue culture flasks. BC-OBs or hFOBs were used as a positive control while BMMSCs or hMSCs were used as a negative control. Densitometry was done to quantify the relative levels of the bone-related genes, normalized to the respective levels of GADPH.

Alizarin red staining

Cells were grown on the titanium substrates for 21 days and removed by trypsinization, then re-seeded into individual wells of a new 24-well plate. At 48 hours after re-plating, the cells were stained with 1% alizarin red S for 2 minutes and then washed with PBS. The stained cells were observed under a light microscope to detect intracellular calcium deposits.

Statistical analysis

The results were assessed statistically using one-way analysis of variance. Statistical significance was accepted at $p < 0.05$.

Chapter 3

A Preliminary Study

Human bone marrow-derived mesenchymal stem cells differentiation into osteoblasts on titanium with surface-grafted chitosan and immobilized bone morphogenetic protein-2

Introduction

Circulating mesenchymal stem cells (MSC) are known to migrate and home to various organs to mediate tissue repair [69, 118]. Similarly, it is possible that circulating bone progenitor cells can home to a bone implant and differentiate into bone-forming cells, eventually leading to osseointegration with the prosthesis. However, bacterial infection following surgical implantation of biomaterials and devices poses a risk to an implant. It has been shown that titanium (Ti) with surface-grafted chitosan (CS) prevents bacterial adhesion, the mechanism of which has been proposed to be due to the interaction between the oppositely charged bacterial cell wall and the CS [119, 120]. This interaction results in a change in bacterial membrane permeability, leading to the fatal leakage of cellular contents. Previous work has shown that bone morphogenetic protein-2 (BMP2)-adsorbed onto titanium porous oxide implant surfaces had an osteoconductive effect which was surface- and dose-dependent [121]. The incorporation of BMP2 into biomimetic coatings like calcium phosphate has been shown to result in the formation of bone cells at the implant site [120, 121]. However, others have also reported that BMP2 immoblized onto implants does not increase bone formation [122]. In the present study, the aim was to investigate if BMP2 immobilized onto bacteria-resistant chitosan-grafted titanium substrate will enhance BMMSC adhesion on the substrate surface and further induce their differentiation into osteoblasts.

Materials and methods

Materials

Materials and methods specific to this chapter are described below. All the other materials and methods used in this chapter are described in Chapter 2 (General materials and methods).

Preparation of chitosan-grafted titanium substrate with immobilized BMP2 (Ti-CS-BMP2 substrate)

Ti foils of 0.52-mm thickness were cut to a size of 1 cm X 1 cm, and cleaned with sandpaper, followed by sonication sequentially in Knoll's reagent (4.0% HF, 7.2% HNO_3, 88.8% water), dichloromethane, acetone and water. After surface passivation in 40% HNO_3, dopamine was anchored to the surface of the Ti substrates by immersion in a 1 mg / ml solution of dopamine at room temperature in the dark overnight, as described elsewhere [123]. Unbound dopamine was washed off with copious PBS and the substrates were air dried in a sterile environment. Subsequently, the substrates were immersed in a stirred 3% glutaraldehyde solution at room temperature overnight. Glutaraldehyde serves as a cross-linker, providing the reactive aldehyde groups for covalently bonding dopamine and CS. Unbound glutaraldehye was removed by rinsing the substrates in water. CS was dissolved in a 0.1% dilute acetic acid to a concentration of 5 mg / ml. The glutaraldehyde-treated substrates were then immersed in the CS solution. Imine bonds are formed between the aldehyde groups on the Ti surface and the primary amino groups at the C-2 position of CS.

The resulting substrates were then washed with water and dried under vacuum. Some of the chitosan-grafted Ti substrates were then individually coated with BMP2 at a concentration of 50 μg / ml and allowed to air dry in a sterile environment. Following which, the substrates were rinsed 3 times with sterile PBS to remove unattached BMP2 and left to air dry in a sterile environment before use. The present author used a BMP2 concentration of 50 μg / ml to coat the titanium substrates to ensure that the growth factor was adequately adsorbed onto the substrate surface. The substrates are denoted Ti (pristine titanium), Ti-CS (chitosan-grafted Ti) and Ti-CS-BMP2 (BMP2-coated, chitosan-grafted Ti) in subsequent discussions. Fig. 3.1a is a schematic to illustrate the preparation of the substrates. Fig. 3.1b is a photograph of the sterilized finished substrates ready for use.

Preparation of substrates

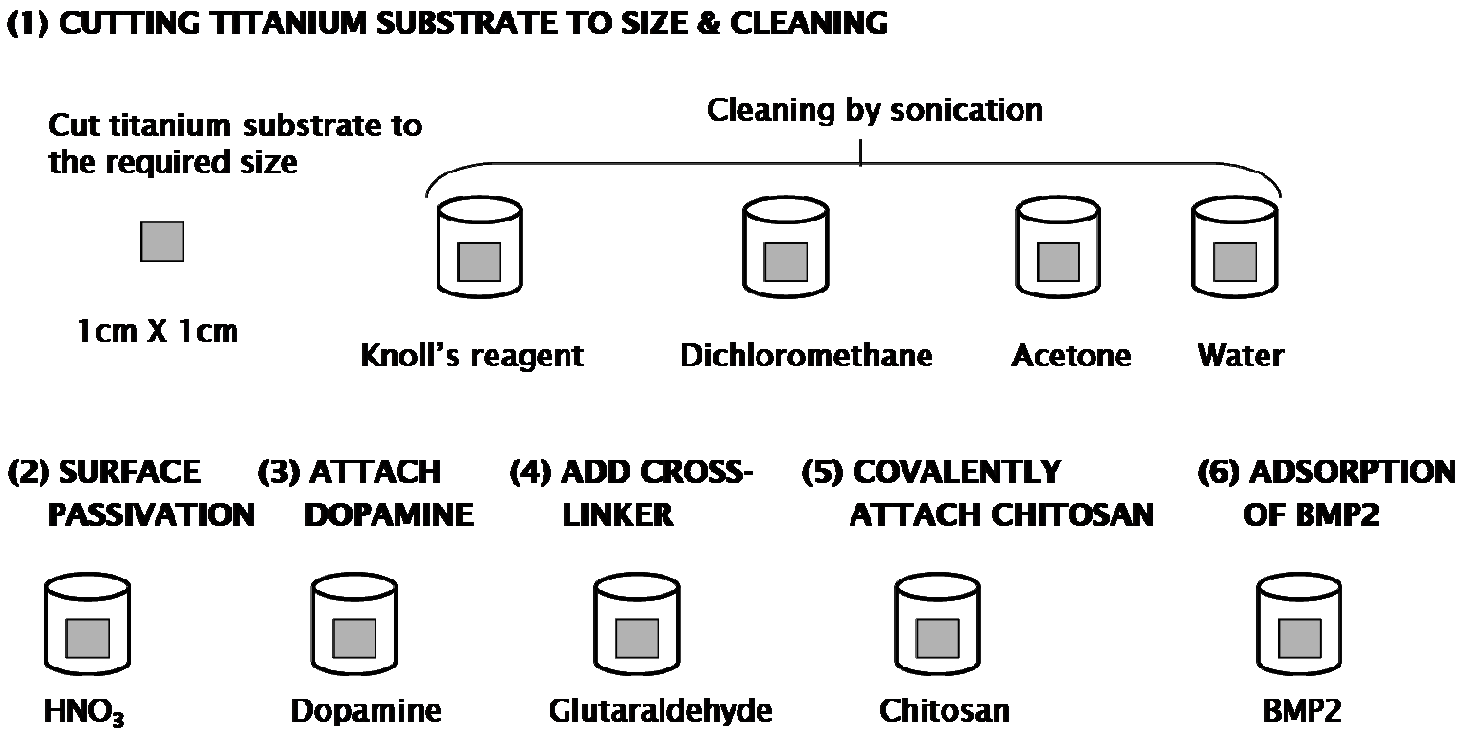

Fig. 3.1a. Schematic illustrates the preparation of titanium substrates

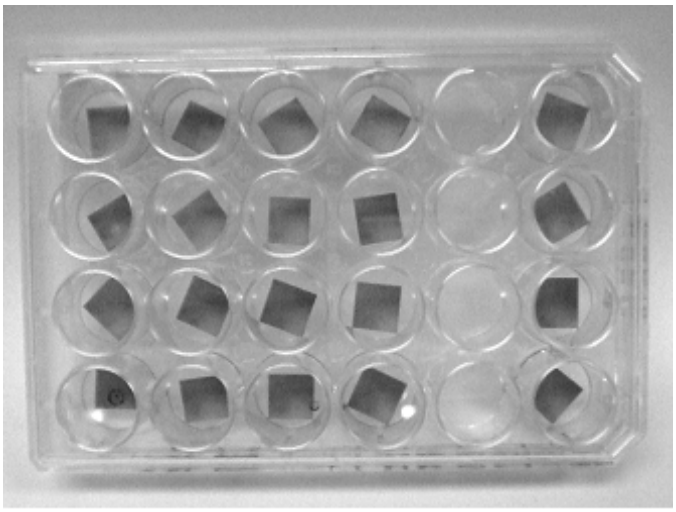

Fig. 3.1b. Photograph of finished Ti-CS-BMP2 substrates in 24-well plate, sterilized and ready for use.

After the preparation of the Ti-CS-BMP2 substrates, the following were subsequently done, the procedures of which are described in chapter 2:

Stability and surface density of BMP2 on the Ti-CS-BMP2 substrate

Culture of BMMSCs

Culture of BC-OBs

Cell attachment

BMMSCs attached on the Ti, Ti-CS and Ti-CS-BMP2 substrates will subsequently be denoted Ti cells, Ti-CS cells and Ti-CS-BMP2 cells respectively.

Cell proliferation

Flow cytometry

Flow cytometry was done to confirm the cell lineage of the BMMSCs prior to further work. The BMMSCs were detached by gentle trypsinization. The detached cells were resuspended and incubated in PBS with 2% FBS for 10 minutes in an ice bath. 1μl each of CD44-FITC, CD105-PE, CD271-FITC, CD34-FITC and CD45-FITC antibodies was added to the cells suspended in 100μl of PBS with 2% FBS each in separate tubes. The tubes were incubated for 10 minutes in an ice bath in the dark. The cells were then washed and resuspended in 1 ml of PBS, and analysed using flow cytometry. 10,000 events were collected for the analysis of each marker.

After the flow cytometry, further work was done to check for any adverse effects that the substrate may have on the attached cells. Work was also done to assess the osteogenic potential of the Ti-CS-BMP2 substrates. The procedures, listed below, for the above mentioned work are described in chapter 2:

Cytotoxicity

ALP assay

RT-PCR

Alizarin red staining

Results

Stability and surface density of adsorbed BMP2 on Ti-CS-BMP2 substrates

Other researchers have physically modified the surface of the titanium substrate and allowed BMP2 to be adsorbed onto the surface. Upon immersion of the substrate in a solution, only a small percentage of the initially adsorbed BMP2 remained firmly attached to the substrate surface [5]. In this study, chitosan has been covalently linked onto the surface of titanium. These substrates were then immersed in a solution containing a high concentration of BMP2 to allow sufficient BMP2 to be adsorbed onto the substrate surface. BMP2 adsorption on the Ti-CS substrates is probably via strong electrostatic interaction. It can be expected that most of the BMP2 molecules would be detached from the substrate surface upon immersion in a liquid. It was found that only about 1%, or 500 ng of the initial coating solution concentration of 50 μg, was firmly attached onto the substrate surface. Approximately 81% of the 500 ng of BMP2 that was initially attached on day 0 remained attached to the substrate surface on day 1. The attached BMP2 was slowly released into solution over time, at a rate of about 2% per day from day 3 to day 7, as is shown by the results of the surface density assessment in Fig. 3.2. From Fig. 3.2, it can also be seen that the BMP2 rate of release was not consistent from day 0 to the start of day 3. This could probably be due to the overcrowding of BMP2 molecules on the substrate surface, resulting in some of the BMP2 molecules being loosely attached. By day 7, the amount of attached BMP2 was still more than 50% of the initial coating density, suggesting that enough BMP2 can remain attached on the Ti-CS surface

for a length of time, and released slowly to support osteoblast differentiation. The surface density of BMP2 adsorbed onto the Ti-CS surface is comparable to that of covalently linked BMP2 on titanium surfaces, as reported by other researchers [114].

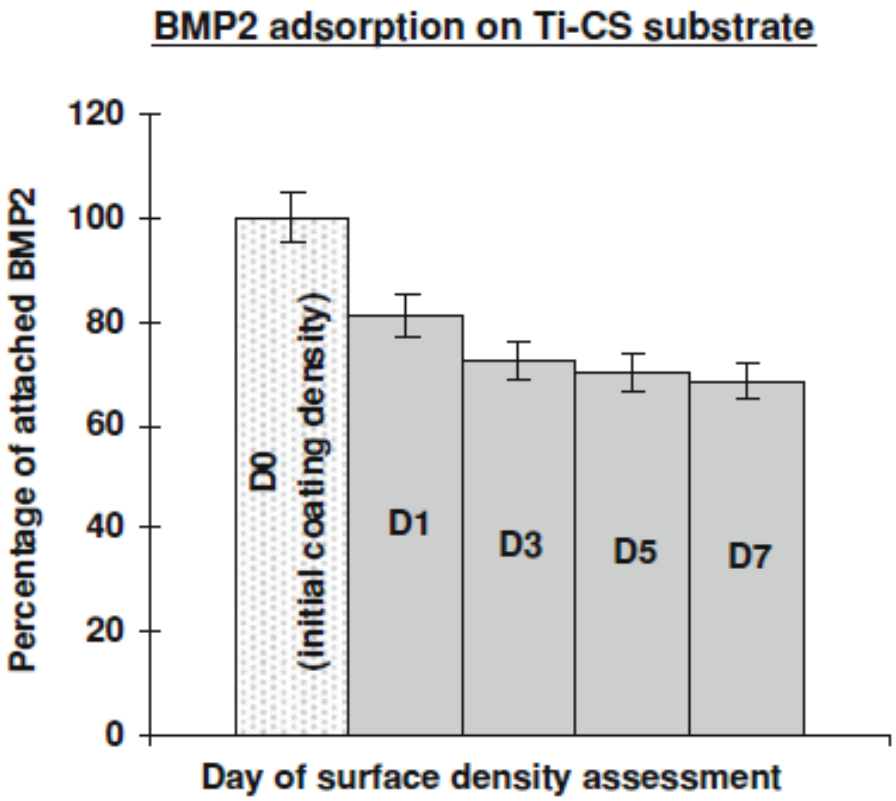

Fig. 3.2. Data reported as percentage of BMP2 that remained adsorbed on the Ti-CS substrate (n = 2) ($p < 0.05$). Error bars represent the standard deviations of each group. About 70% of the initial coating of BMP2 remained attached to the Ti-CS substrate surface after 7 days of submersion in PBS, indicating that BMP2 can potentially remain attached for a sufficient period of time to enhance osteoblast differentiation.

Cell attachment and proliferation

The number of BMMSCs attached on the various titanium surfaces was assessed 6 h after cell seeding, and compared to the control, where the cells are directly attached to the bottom of the culture well (Fig. 3.3). Cell attachment on Ti-CS substrates was comparable to that in the control (without any titanium substrate), while the number of cells attached to the pristine Ti substrate was less compared to that on either the Ti-CS substrate or in the control. This suggests that the chitosan that is grafted onto the titanium enhances initial cell attachment. However, the Ti-CS-BMP2 substrates had the least number of attached cells. This can probably be attributed to the fact that the adsorbed BMP2 molecules occupied a proportion of the available area on the chitosan-grafted titanium surface, altering its surface topology. Substrate surface topology is known to affect cell attachment [124]. Cell proliferation progressed steadily over the following 7 days of culture, as shown in Fig. 3.5. Except for the control on day 7, the cell proliferation rates were not significantly different on all the titanium substrates and in the controls ($p < 0.05$). This apparent anomaly could be due to the fact that cells on the substrates were undergoing differentiation, as differentiating cells are known to slow down in proliferation rate or even leave the cell cycle [125]. Others have shown that cell attachment is significantly affected by the presence of phosphate and apatite groups on the titanium surface [126]. This suggests that the presence of certain types of molecules on the titanium substrate surface can affect the degree of cell attachment. Besides the presence of certain preferred molecules, the technique employed in applying coatings on a

titanium substrate can alter the substrate surface topology, and hence, cell attachment efficiency [124]. Despite much work done, there is still no unanimous agreement as to the optimal surface topology of an implant surface [127]. However, there is a positive correlation between implant surface topology and bone attachment [127]. In comparison, the chitosan on the Ti-CS substrate is a stable, covalently attached layer which should confer anti-bacterial properties to the titanium substrate for an extended period of time, while promoting cell attachment on the substrate surface.

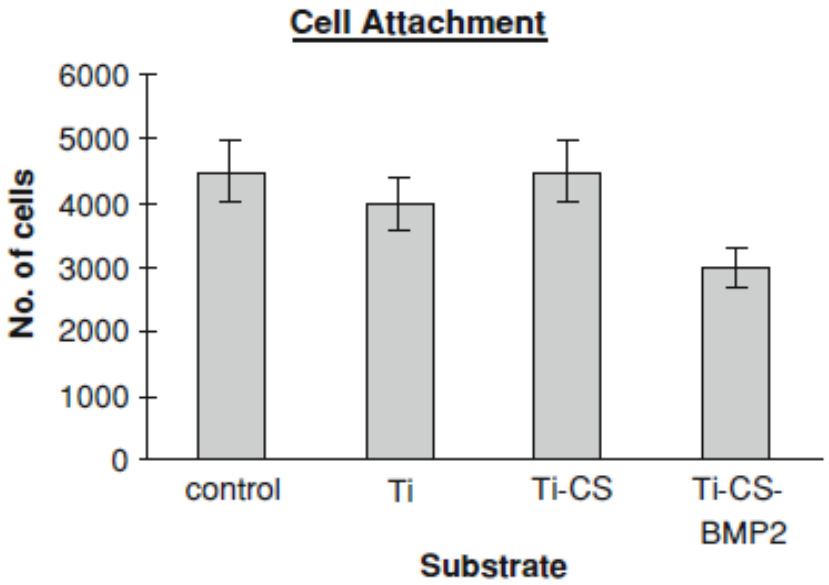

Fig. 3.3. The number of attached BMMSCs on each type of titanium substrate ($n = 2$) ($p < 0.05$) was evaluated after 6 hours. Error bars represent the standard deviations of each group. As shown, BMMSCs can adhere to the titanium substrates as effectively as on the plastic surface of culture flasks, suggesting that bone implants constructed with these substrates can possibly support BMMSC adhesion on the prosthesis, where further cellular developments can occur.

Flow cytometry

Passage 2 BMMSCs were subjected to flow cytometry analysis after being separately stained with CD271, CD44, CD105, CD34 and CD45 antibodies to assess their lineage (Table 3.1). About 64% of the cells were CD44+ while approximately 86% of them were CD105+. About 1.3% of CD34+ cells and 1.1% of CD45+ cells were present among the BMMSCs. The rare population of CD271 cells which has been described as one of the most specific markers of BMMSCs constituted about 3.4% of the cell population [128, 129].

Table 3.1. This analysis shows the profile of the surface markers of the bone marrow stromal cells.

Marker	CD34	CD45	CD271	CD44	CD105
Percentage	1.3	1.1	3.4	64.0	86.0

Flow cytometry analysis of these passage 2 BMMSCs shows the presence of mesenchymal stem cell markers CD271, CD44 and CD105, suggesting that there is a population of progenitor cells in bone marrow that can possibly contribute to osteoblast differentiation and osseointegrate with the titanium substrates. A small fraction of CD34+ and CD45+ haematopoietic cells was present among the BMMSCs.

Cytotoxicity

Cell viability on the 3 types of substrates was assessed using the MTT assay (Fig. 3.4), to give an indication of the effect of the substrates on the survival and proliferation of the attached cells. The assay was done on day 7 of culture and the results suggest that all the 3 types of titanium substrates do not seem to be cytotoxic to the cells, and can support cell growth and proliferation almost as effectively as plastic culture flasks (control), as shown in Fig. 3.5.

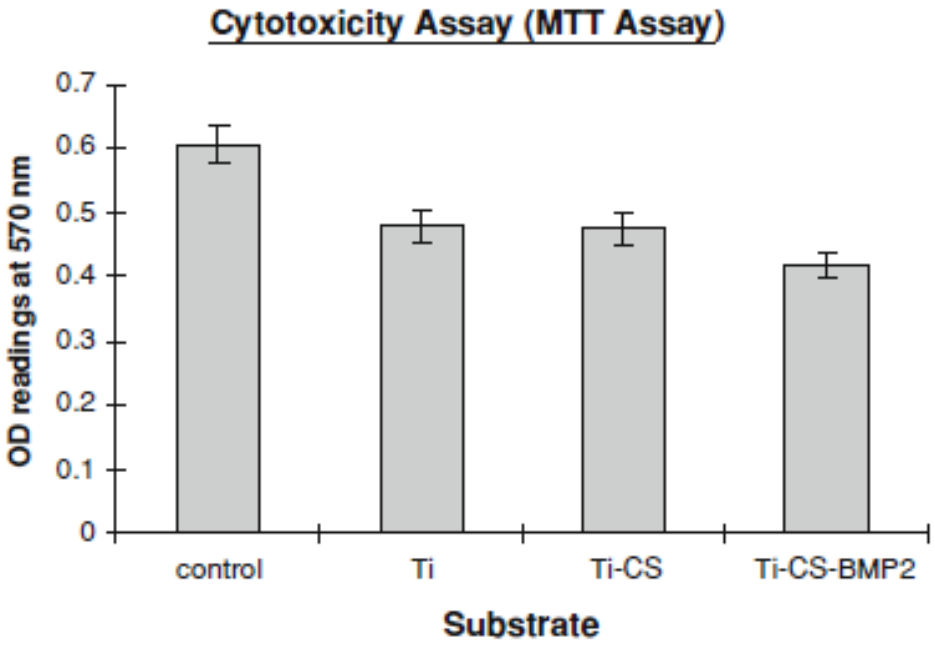

Fig. 3.4. The MTT assay shows that the three types of titanium substrates (n = 2) do not adversely affect cell viability, suggesting that these substrates are probably not cytotoxic *in vivo*, and can possibly be used to fabricate bone implants. Error bars represent the standard deviations of each group.

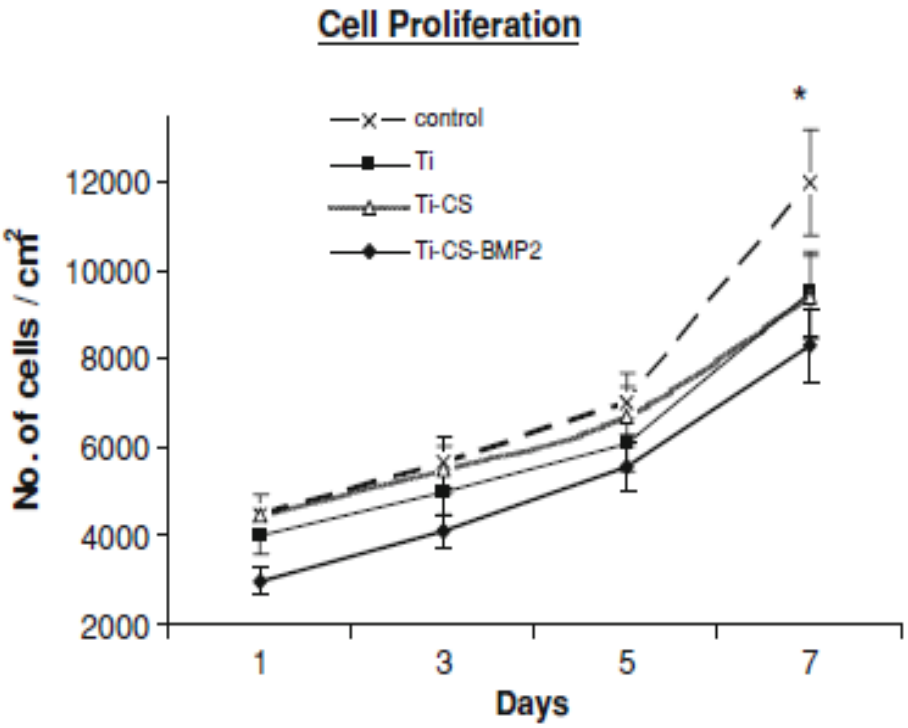

Fig. 3.5. The ability of the titanium substrates to support cell proliferation was assessed by counting the number of attached BMMSCs on each type of substrate (n = 2) on days 1, 3, 5 and 7. The cell proliferation rates are consistent on all the three types of substrates. By day 7, most of the cells on the substrates are probably differentiating, hence the slow-down in proliferation rates as compared with that in the control (denoted by *). Error bars represent the standard deviations of each group.

Alkaline phosphatase activity

The results in Fig. 3.6 indicate that osteoblast differentiation occurred on all the substrates, with the ALP activity of the cells on the various substrates in the ascending order Ti, Ti-CS, and Ti-CS-BMP2. Chitosan has been shown to enhance the ALP activity of osteoblasts [130, 131]. The results show that although there was a higher ALP activity in the Ti-CS cells compared with the Ti cells, the increase was not significant. However, Ti-CS-BMP2 cells showed a significantly higher ALP activity over both Ti cells and Ti-CS cells ($p < 0.05$). Thus, the results suggest that CS and BMP2 on the Ti-CS-BMP2 substrate surface may have a synergistic effect in enhancing osteoblast differentiation from BMMSCs. Based on the above results, RT-PCR was carried out using BMMSCs cultured on the Ti-CS-BMP2 substrate.

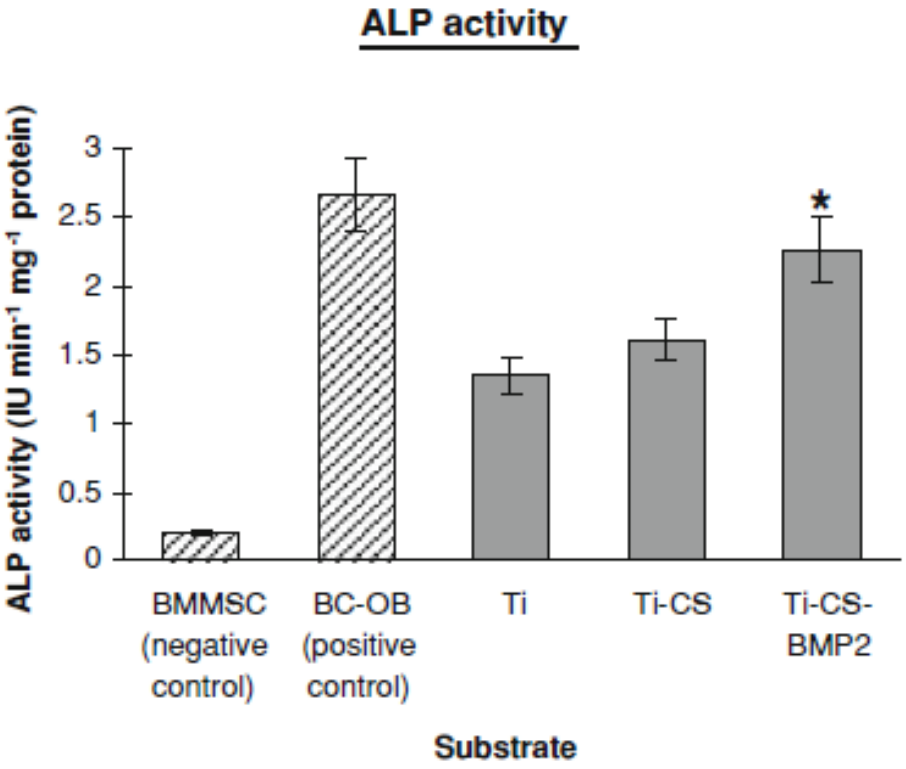

Fig. 3.6. ALP activity (Day 7) in the cells attached to each type of titanium substrate (n = 2) indicates osteoblast differentiation. Although cells on the Ti-CS substrates had a higher ALP activity than those on the Ti substrates, this was not significant. Only cells on the Ti-CS-BMP2 substrates show a significantly higher ALP activity than cell on either of the other 2 types of substrates (denoted by *), indicating that CS and BMP2 may synergistically work to enhance BMMSC differentiation into osteoblasts. In contrast, BMMSCs cultured in normal tissue culture flasks showed almost no ALP activity. The ALP activity of BC-OBs serves as a positive control. Error bars represent the standard deviations of each group.

RT-PCR

RT-PCR was carried out to assess the expression of the genetic markers, Runx2, collagen type I (Col I) and osteocalcin (OCN), to confirm osteoblast differentiation on the Ti-CS-BMP2 substrate (Fig. 3.7a). The results were compared with those from BC-OBs and untreated BMMSCs cultured in normal tissue culture flasks. In addition, BC-OBs were also assessed for the expression of endogenous BMP2, a key growth factor involved in bone formation, to confirm the bone cell lineage of the BC-OBs. Fig. 3.7b shows the relative levels of expression of the 3 genes in BC-OBs and Ti-CS-BMP2 cells, normalized to the expression level of GAPDH.

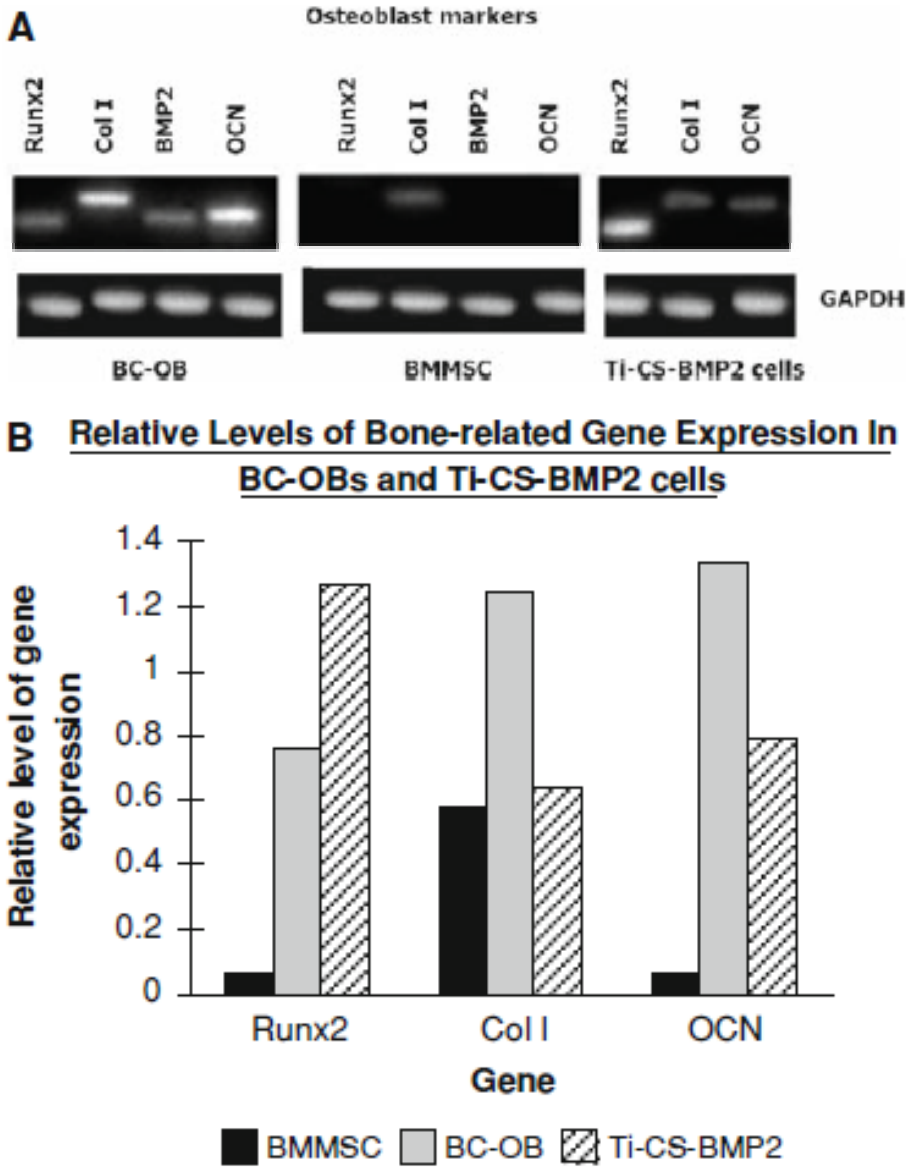

Fig. 3.7a and Fig. 3.7b. RT-PCR of Runx2, Col I and OCN suggests that Ti-CS-BMP2 cells are undergoing osteoblast differentiation, unlike BC-OBs (positive control), which are mature osteoblasts. This is evident from the comparatively higher level of Runx2, indicating a higher transcription level of this gene, and the relatively lower levels of Col I and OCN, indicating that the Ti-CS-BMP2 cells are not fully differentiated osteoblasts yet. Conversely, untreated BMMSCs cultured in plastic tissue culture flasks (negative control) do not differentiate and hence have no detectable level of bone-related markers except for Col I.

Table 3.2. Primers used for the RT-PCR reaction of bone-related genes.

Gene (Ascension number)	Sequence		T_{anneal} (^{o}C)	Product size (bp)
RUNX2 (NM_004348)	Forward	tttgcactgggtcatgtgtt	58	156
	Reverse	tggctgcattgaaaagactg	58	
Collagen I (NM_000088)	Forward	ccaaatctgtctccccagaa	60	214
	Reverse	tcaaaaacgaaggggagatg	58	
BMP2 (NM_001200)	Forward	cccagcgtgaaaagagagac	62	168
	Reverse	gagaccgcagtccgtctaag	64	
Osteocalcin (NM_199173)	Forward	gtgcagagtccagcaaaggt	62	175
	Reverse	tcagccaactcgtcacagtc	62	
GAPDH (NM_002046)	Forward	gagtcaacggatttggtcgt	60	238
	Reverse	ttgattttggagggatctcg	60	

Alizarin Red staining

The Ti-CS-BMP2 cells were stained with Alizarin Red S to detect calcium deposits in the cells. Fig. 3.8a shows some of the positively-stained cells, while untreated BMMSCs stained negative with Alizarin Red S.

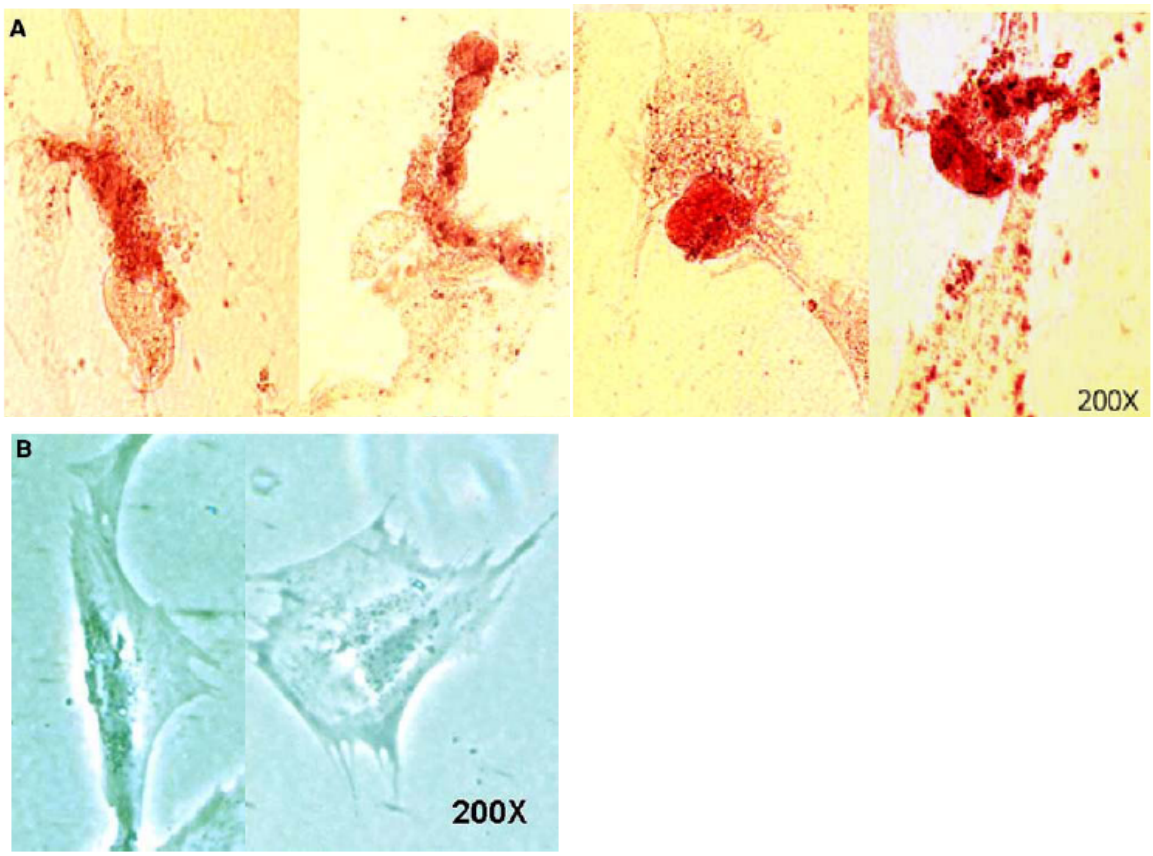

Fig. 3.8. **(a)** Ti-CS-BMP2 cells that stain positive for the presence of calcium deposits with alizarin red S indicate osteoblast differentiation. **(b)** Untreated, cultured BMMSCs do not differentiate and hence stain negative for Alizarin Red S.

Discussion

MSCs have been reported to retain their undifferentiated phenotype and remain capable of osteogenic differentiation during *ex vivo* expansion through multiple passages [132]. Their surface marker expression profiles remain consistent, and their gene expression profiles do not change significantly during long-term expansion [132]. The well-established MSC markers, CD44 and CD105, used to confirm the MSC lineage of the BMMSCs in the present study reveal that there is a population of relatively undifferentiated progenitors that can possibly contribute to osteoblast differentiation [132-134]. In addition, a small population of the cells were found to be CD271+. CD271 is one of the most specific and novel markers of BMMSCs [128]. CD271+ cells are highly proliferative, and possess multilineage differentiation potential [129, 134, 135]. Unfortunately, CD271+ cells are rare in a population of bone marrow-derived cells, and would have to be immunomagnetically isolated, and then expanded *in vitro*. Thus, a relatively large volume of bone marrow would have to be extracted in order that a feasible number of CD271+ cells can be magnetically isolated to constitute the starting cells for *in vitro* expansion.

While osteoblast differentiation from BMMSCs may occur on the surface of titanium substrates, it is paramount that BMMSCs must first be able to firmly attach to the substrate surface. This is to ensure that osseointegration of a bone implant can take place *in vivo*. MSCs are known to adhere strongly to plastic surfaces and this characteristic has enabled them to be easily isolated and investigated for potential therapeutic applications [136]. The patient-derived

BMMSCs used in the present study also similarly adhere to plastic surfaces and to the various titanium substrates. Firm cell attachment is evidenced by the prolonged trypsinization required to detach them from the substrates. Together with the consistent cell proliferation rates, this indicates that BMMSCs can be a potential source of progenitors to initiate osseointegration with functionalized titanium-based implants *in vivo*. However, such surface-modified implants must be biocompatible. The results of the MTT assay show that the titanium-based substrates do not adversely affect cell viability, indicating that these substrates probably would not be cytotoxic *in vivo*.

An assessment of the ALP activity of the cells on the various types of substrate surfaces on day 7 of culture suggests that osteoblast differentiation can possibly occur soon after cell attachment. While others have used calcium phosphate-coated, collagen-coated, or chondroitin sulphate-coated titanium to enhance the retention of BMP2 on the substrate surface, BMP2 in this case was allowed to be adsorbed onto the chitosan-grafted titanium substrates. [122, 137, 138]. Besides being able to promote osteoblast differentiation, chitosan also possesses anti-bacterial properties [139-142]. Thus, it can be hypothesized that chitosan and BMP2 would act synergistically to improve osteoblast differentiation on titanium surfaces. Based on the results of the ALP assay, it would be reasonable to expect that the Ti-CS-BMP2 substrates would be the most osteogenic among the 3 types of titanium substrates. The expression levels of three bone genetic markers in the BMMSCs grown on Ti-CS-BMP2 substrates was then assessed. RT-PCR was carried out to assess the expression levels of

three key bone markers, Runx2, Col I and OCN. Runx2 is the trasnscription gene of the osteoblast specific protein, osteocalcin. Together, Runx2 and OCN are the key regulators of osteoblast differentiation and function [143-145]. Runx2 is regulated by a number of factors including bone morphogenetic protein (BMP). It functions as a scaffold protein for nucleic acids and regulatory factors involved in skeletal gene expression. Osteocalcin is the major noncollagenous protein of bone matrix [146]. Interestingly, besides being used as a biomarker of osteoblast differentiation, this gene has been implicated in human osteoarthritis and its presence could possibly mark the stage of the development of this disease at a point of dysregulation of cellular behaviour and failure of repair mechanisms [146]. Thus, the detection of OCN in the serum may potentially be used as a clinical indicator of the need for a bone implant. Collagen I is the major constituent in bone extracellular matrix [147]. Cells of the bone lineage express Col I in all their developmental stages. Collagen I interacts with the $\alpha_2\beta_1$ integrin receptor on the cell membrane to mediate transduction of extracellular signals into the cell [148]. The interruption of this collagen-integrin interaction inhibits osteoblast differentiation from bone marrow cells [148]. The RT-PCR results show that these three key genes were expressed in the Ti-CS-BMP2 cells, and only Col I was expressed in the untreated BMMSCs, indicating that the Ti-CS-BMP2 substrate promotes osteoblast differentiation in the BMMSCs that adhered to its surface. A densitometry of the band intensities of Runx2, Col I and OCN suggests that the Ti-CS-BMP2 cells were in the early stages of osteoblast differentiation (Fig. 3b). This is evident from the relatively lower levels of Col I

and OCN in the Ti-CS-BMP2 cells as compared with those from the BC-OBs. Furthermore, the relatively higher level of the transcription factor, Runx2, in the Ti-CS-BMP2 cells suggests a higher gene transcription activity level of bone-related genes than that in the BC-OBs. Additionally, the BC-OBs were assessed for the expression of endogenous BMP2, which is a key gene in bone cells, as BMP2 also serves to regulate the Runx2 gene. Finally, the Ti-CS-BMP2 cells were stained with Alizarin Red S to detect calcium deposits in the cells.

Besides chemically modifying the substrate surface, others have also physically modified the titanium substrate surface to enhance the adsorption of BMP2 [121]. While most of these modified surfaces have been reported to support osteoblast differentiation, others have also reported that immobilized BMP2 on titanium substrates with biomimetic coatings does not enhance bone formation [122].

Conclusion

Circulating progenitor cells are known to home to various organs to repair injured tissues or to routinely replace old cells and maintain tissue integrity. Similarly, circulating progenitor bone cells can possibly home to a bone implant, differentiate, and eventually osseointegrate with the prosthesis. Osseointegration of bone cells with the prosthesis can help to reduce the risk of implant failure due to constant movement between bone tissue and implant surface. The aim of this preliminary study is to investigate if Ti-CS-BMP2 will enhance BMMSC adhesion onto the substrate surface and further induce their differentiation into osteoblasts.

The results show that the Ti-CSBMP2 substrate is able to retain adsorbed BMP2, and is capable of slow release of this growth factor. Despite the lesser number of BMMSCs initially attached onto the Ti-CS-BMP2 substrates and consequently the lower level of cell proliferation, Ti-CS-BMP2 cells had the highest level of ALP activity. RT-PCR results show that Ti-CSBMP2cells had a relatively higher level of transcription activity of Runx2, compared with that of bone cell-derived osteoblasts (BC-OB), an indication that the BMMSCs were actively differentiating into osteoblasts. Finally, Alizarin Red staining reveals the presence of calcium deposits in the differentiated cells. Hence, Ti-CS-BMP2 substrates possess an osteoconductive effect and can possibly be used to fabricate bone implants that can osseointegrate with host bone tissue.

The method of immobilizing BMP2 onto chitosan-grafted titanium surfaces in the present study is convenient and effective in promoting BMMSC-derived osteoblast differentiation. Although only a small proportion of the initial amount of BMP2 used for adsorption onto the chitosan-grafted titanium surface was firmly attached, this amount was sufficient to promote osteoblast differentiation. Nevertheless, one very distinct advantage of the chitosan-grafted titanium substrates is their bacteria-resistant property. The Ti-CS-BMP2 substrate therefore has the potential to be used to fabricate anti-bacteria, osteoconductive bone implants.

Chapter 4

A Comparative Study

Human bone marrow-derived mesenchymal stem cells differentiation into osteoblasts on titanium with surface-grafted dextran and immobilized bone morphogenetic protein-2

Introduction

Titanium and its alloys are widely used in orthopaedic and dental implants. Although titanium surface is biocompatible and possesses bioactivity, the bioactivity level is insufficient to encourage osseointegration of implant with host bone tissue [149]. Failure of an implant to osseointegrate with host bone tissue can ultimately result in implant failure [149]. Past attempts have thus been made to activate titanium surface to facilitate the attachment and proliferation of bone cells, so that osseointegration may occur. Currently, the focus is on the biochemical modification of titanium surface with the incorporation of bioactive molecules [150]. As mentioned in chapter 3, while others have incorporated BMP2 into biomimetic coatings and successfully induced the formation of bone cells at the implant site, there are also contradictory reports [122].

Besides the difficulties encountered in the surface modification of titanium, another major clinical problem is titanium implant-related infections. Bacteria attached to an implant surface during surgery forms a resistant biofilm which confers protection upon the bacteria by delaying the action of anti-microbial agents [4]. Bacterial infection at an implant site can eventually result in localized bone destruction, leading to implant failure. A failed implant may then need to be removed, a costly and painful process for the patient.

Thus, a biomaterial which possesses osteoconductive and anti-bacterial properties would have the potential to be used for the fabrication of longer-lasting bone implants. In the present study, work is done to assess the effectiveness of a surface-modified titanium alloy in promoting osteoblast differentiation. Previous

work has shown that the dextran-grafted titanium (Ti-Dex) substrate possesses anti-bacterial properties [114]. The Ti-Dex substrate has been further functionalized with bone morphogenetic protein-2 (BMP2) to enhance osteoblast functions. The present study shows that hMSCs can adhere to the Ti-Dex-BMP2 substrate, proliferate, and differentiate into osteoblasts. The methodology and results of the various experiments in this study, which are discussed in chapter 5, will be considered in the context of the anti-bacterial mechanism and the complexity of the substrate fabrication procedure, and compared similarly to that of the study in chapter 3, in order to select either the Ti-CS-BMP2 substrate or the Ti-Dex-BMP2 substrate for further work.

Materials and Methods

Materials

Materials and methods specific to this chapter are described below. All the other materials and methods used in this chapter are described in Chapter 2 (General materials and methods).

In order to avoid implicating factors due to patient variability, patient bone marrow-derived mesenchymal stem cells and patient bone chip-derived osteoblasts were not used in the present study. Instead, appropriately characterized human mesenchymal stem cells (hMSC) and human osteoblasts (hFOB) were purchased from Lonza, USA, a commercial source and used for all the experiments.

Preparation of the Ti-Dex-BMP2 substrate

Ti foils of 0.52-mm thickness were cut to a size of 1 cm X 1 cm, and cleaned with sandpaper, followed by sonication sequentially in Knoll's reagent (4.0% HF, 7.2% HNO_3, 88.8% water), dichloromethane, acetone and water. After surface passivation in 40% HNO_3, dopamine was anchored to the surface of the Ti substrates as described elsewhere [123]. The Ti substrates were immersed in a 1 mg / ml solution of dopamine overnight in the dark. Unattached dopamine was washed off with copious amounts of ultra-pure water and the substrates were dried under nitrogen flow.

Dextran was oxidized using periodate oxidation to produce aldehyde groups [151, 152]. Briefly, 2.18 g of sodium periodate ($NaIO_4$) were added to 50

ml of dextran solution (33.33 mg / ml). The reaction mixture was continuously stirred for 24 h at room temperature, protected from light. The resulting solution was purified by exhaustive dialysis against water at 4^{o}C. The purified dextran solution was lyophilized and stored at 4^{o}C.

The immobilization of dextran onto the Ti substrates was carried out using a reductive amination process [49, 133, 134]. Oxidized dextran was dissolved in 0.1 M PBS to a concentration of 2 mg / ml. Dopamine-modified Ti substrates were individually placed in each well of a 24-well plate. Two ml of the dissolved dextran solution was added to each well and the substrates were incubated overnight at room temperature, protected from light. After incubation, the reaction mixture was decanted from the wells and replaced with freshly prepared sodium borohydride ($NaBH_4$) solution (0.1 M) to reduce the Schiff bases formed to secondary amine bonds. Any free unreacted aldehyde groups on the oxidized dextran chain would be reduced to hydroxyl groups. The substrates were incubated for 2 h with slight shaking. The $NaBH_4$ solution was then removed and the substrates were gently rinsed with ultra-pure water to remove unbound dextran, and allowed to dry before proceeding to the subsequent steps.

The dextran-grafted Ti substrates were further functionalized with BMP2 through a second reductive amination reaction. After treatment with 0.1 M $NaIO_4$ at room temperature for 2 h, the substrates were washed with steirle water and allowed to dry. The substrates were then incubated in a BMP2 solution (50 μg / ml) overnight at room temperature. The BMP2 solution was then decanted and replaced with freshly prepared 0.1 M $NaBH_4$ and left for 2 h. The substrates

were then rinsed with water containing 0.1% sodium dodecyl sulphate to remove the unreacted BMP2. After which, the substrates were incubated overnight in 0.1 M ethanolamine in PBS to quench any unreacted hemiacetal groups that could immobilize serum matrix and cell surface proteins and thus promoting non-specific cell adhesion [43]. The substrates were allowed to dry before use. In subsequent discussions, the substrates are denoted as Ti-Dex-BMP2.

After the preparation of the Ti-Dex-BMP2 substrates, the following were subsequently done, and the procedures are described in chapter 2:

Stability and surface density of BMP2 on the Ti-Dex-BMP2 substrate

Culture of hMSCs

Culture of hFOBs

Cell attachment

hMSCs attached on the Ti, Ti-Dex and Ti-Dex-BMP2 substrates will subsequently be denoted Ti cells, Ti-Dex cells and Ti-Dex-BMP2 cells respectively.

Cell proliferation

Differentiation of hMSCs into osteoblasts on the Ti-Dex-BMP2 substrate

The Ti-Dex-BMP2 substrate has been shown to support cell adhesion and is therefore not cytotoxic [114]. The substrates were placed into a 24-well plate and seeded with hMSCs at a density of 10 000 cells / cm^2. Two ml of osteogenic medium comprising normal hMSC culture medium supplemented with 10 nM dexamethasone, 7 mM β-glycerophosphate and 0.2 mM ascorbic acid were added to each well. Half of the medium was removed and replaced with fresh medium after every 2 days. The cells were allowed to differentiate for 7 days before being used for the following subsequent experiments, to assess the osteogenic potential of the Ti-Dex-BMP2 substrates. The procedures, listed below, for the above mentioned work is described in chapter 2:

ALP assay

RT-PCR

Alizarin Red staining

Results

Stability and surface density of adsorbed BMP2 on Ti-Dex-BMP2 substrates

Titanium has previously been modified to allow BMP2 to be adsorbed onto the surface. Upon immersion of the substrate in a solution, only a small percentage of the initially adsorbed amount of BMP2 remained firmly attached to the substrate surface [121, 153]. In the current study, oxidized dextran was covalently linked onto dopamine coated Ti (Ti-Dex) substrates. BMP2 was then covalently linked to the Ti-Dex substrate surface. It is expected that chemical attachment would help to retain a relatively higher percentage of BMP2 on the substrate. About 2.33%, or 1.164 μg of the initial coating solution concentration of 50 μg, were firmly attached onto the substrate surface. There was a loss of 2% of the BMP2 from the substrate surface from day 0 to day 1 which could probably be attributed to the detachment of some loosely bound BMP2. However, by day 14, the surface density was almost 95%, indicating the stability of the covalently bound BMP2 molecules on the substrate, which contrasts sharply with adsorbed BMP2 on the Ti-CS substrate described in chapter 3. This suggests that BMP2 can be stably retained on the substrate for a substantially long period to support osteoblast differentiation.

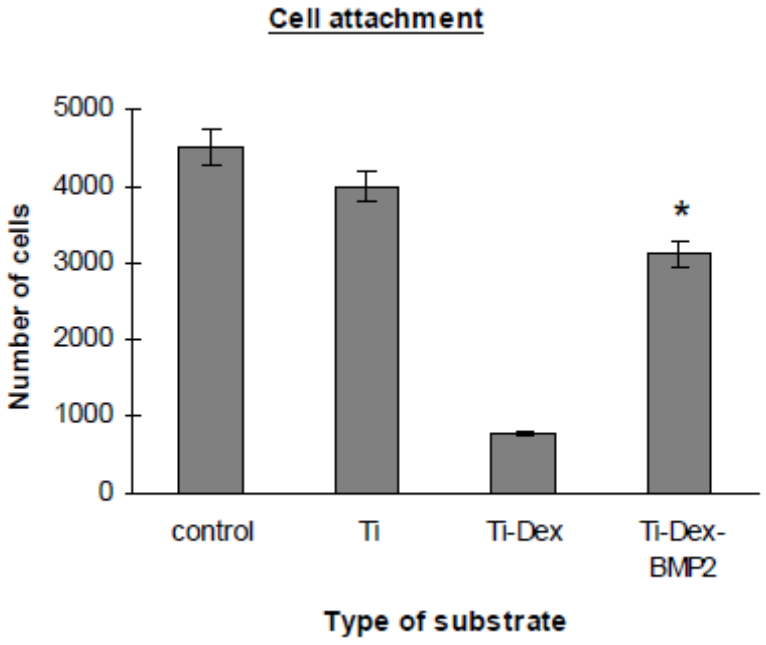

Fig. 4,1. The number of attached hMSCs on each type of titanium substrate (n = 2) was evaluated 6h after cell seeding. Error bars represent the standard deviations of each group. Adhesion of hMSCs to the Ti and Ti-Dex-BMP2 is comparable to that on plastic culture flasks (control), suggesting that bone implants constructed with these substrates can possibly support hMSC adhesion and further cellular developments. Immobilized BMP2 restores the adhesion capability of hMSCs on the Ti-Dex surface.

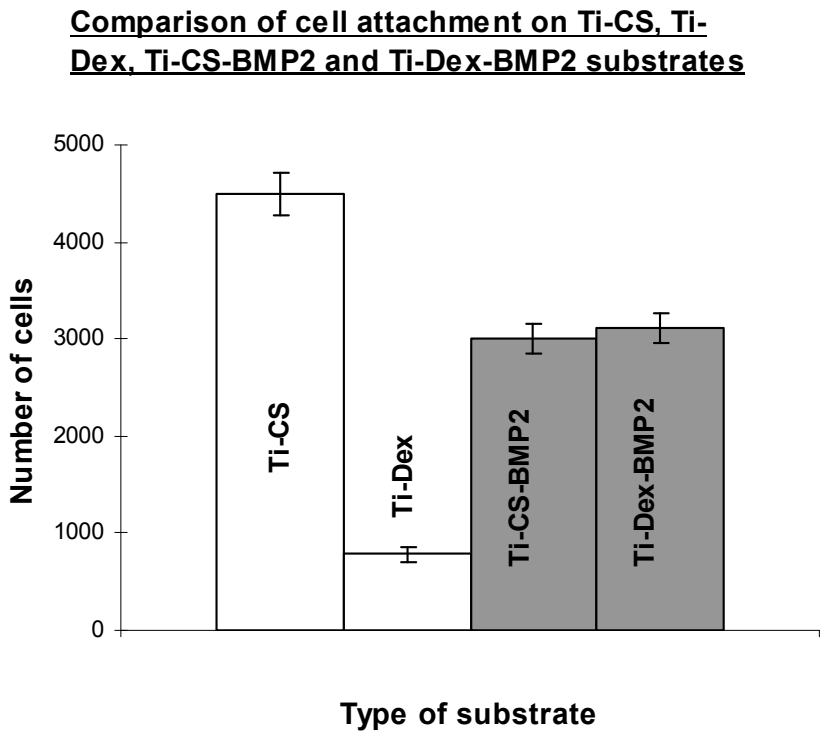

Fig. 4,1a. A comparison of the number of cells attached on the Ti-CS and Ti-CS-BMP2 (done in chapter 3), and, Ti-Dex and Ti-Dex-BMP2 substrates show that only the Ti-Dex substrate had a significant decrease in the number of attached cells, suggesting that dextran prevents initial cell attachment. Error bars represent the standard deviations of each group.

Cell attachment and proliferation

The number of hMSCs attached on the substrate surfaces was assessed 6 h after cell seeding, and compared to the control, where the cells were directly attached to the bottom of the culture well (Fig. 4.1). The results show that cell attachment on the Ti-Dex substrate was only about 20% of that on the pristine Ti substrate. This is consistent with the results obtained by others [43]. The low cell adhesion rate could be due to the repulsion of cells from the negatively-charged dextran coat on the Ti substrate surface. However, cell attachment was considerably enhanced on the Ti-Dex-BMP2 substrate surface. This suggests that BMP2 possesses the ability to enhance cell attachment on a surface that otherwise does not promote initial cell attachment. Firm cell attachment on the substrate surface is a prerequisite for osteoblast differentiation, and subsequently, osseointegration to occur. The increased cell attachment in the presence of BMP2 could also be due to the altered substrate surface topology following the attachment of BMP2. Substrate surface topology and the type of molecules attached on the substrate is known to affect cell attachment [106, 108]. The technique employed in coating a substrate is also known to alter the substrate surface topology and hence the initial cell attachment efficiency [124]. The results of the cell attachment assay are comparable with those of the Ti-CS-BMP2 substrate (Fig. 4.1a). Although the cell adhesion rates on the chitosan surface of the Ti-CS substrate is higher than that of BMP2 on the Ti-CS-BMP2 and Ti-Dex-BMP2 substrates, BMP2 has the dual advantage of promoting cell adhesion and enhancing bone cell differentiation (Fig. 4.1a).

Cell proliferation progressed steadily over the following 7 days of culture, as shown in Fig. 4.2. On day 7, the cell proliferation rate in the control was significantly higher than that on all the titanium substrates ($p < 0.05$). Conversely, cell proliferation on the Ti and Ti-Dex-BMP2 substrates by day 7 had noticeably decreased (Fig. 4.2).

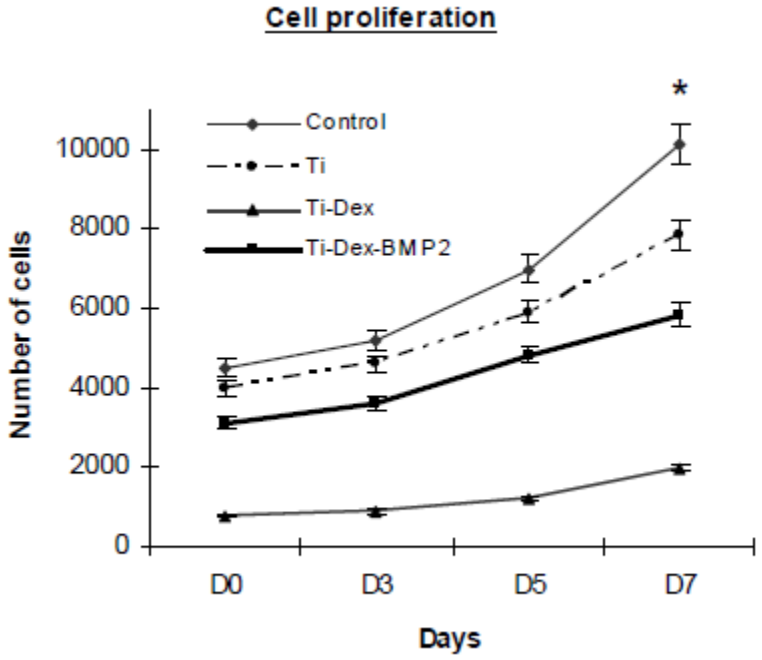

Fig. 4.2. The ability of the titanium substrates to support cell proliferation was assessed by counting the number of attached hMSCs on each type of substrate (n = 2) on days 0, 3, 5 and 7. The cell proliferation rates are consistent on all the substrates except on Ti-Dex. By day 7, most of the Ti cells and Ti-Dex-BMP2 cells are probably differentiating, hence the slow-down in proliferation rates as compared with that in the control (denoted by *). Error bars represent the standard deviations of each group.

Alkaline phosphatase activity

The results in Fig. 4.3 indicate that osteoblast differentiation occurred on both the Ti and Ti-Dex-BMP2 substrates. The ALP activity of the Ti-Dex-BMP2 cells was significantly higher than that of the Ti cells. Based on this result, RT-PCR was carried out using the Ti-Dex-BMP2 cells.

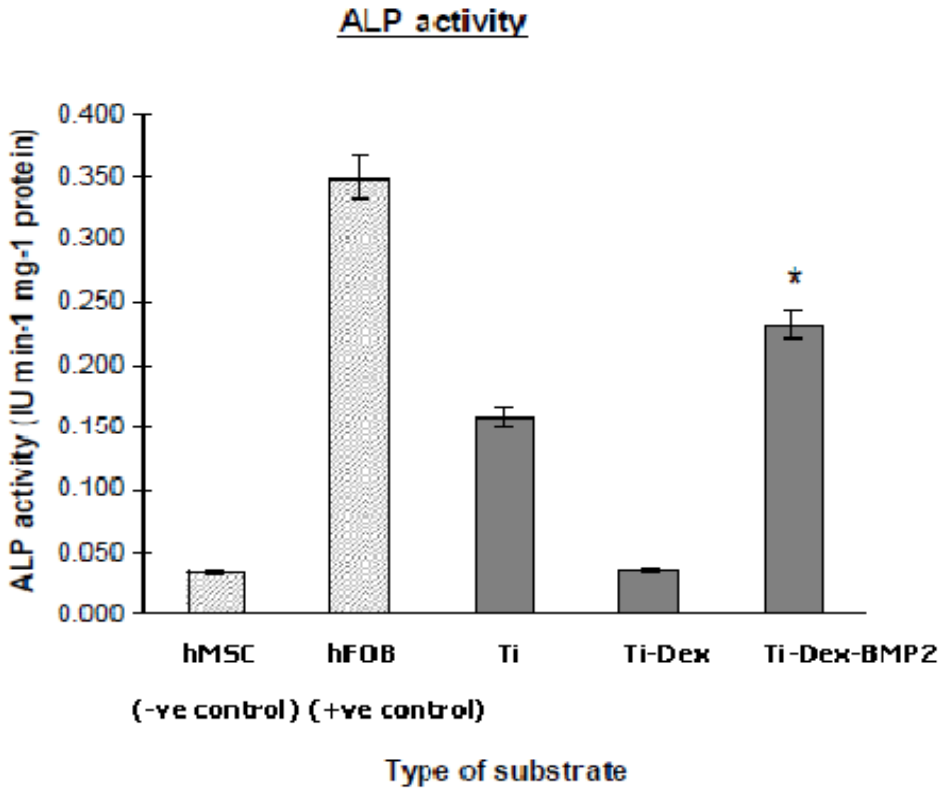

Fig. 4.3. ALP activity in the cells attached to each type of titanium substrate (n = 2) indicates osteoblast differentiation. Ti-Dex-BMP2 cells show a significantly higher ALP activity than that of the Ti cells (denoted by *), indicating that BMP2 retains its osteogenic inductive properties after immobilization on the substrate surface. In contrast, hMSCs cultured in plastic culture flasks and on Ti-Dex show almost no ALP activity. The ALP activity of hFOBs and hMSCs serve as the positive and negative controls respectively. Error bars represent the standard deviations of each group.

RT-PCR

RT-PCR was carried out to assess the expression of the genetic markers, Runx2, collagen type I (Col I) and osteocalcin (OCN), to confirm osteoblast differentiation on the Ti-Dex-BMP2 substrate (Fig. 4.4a). The results were compared with those from hFOBs (positive control) and untreated hMSCs (negative control) cultured on plastic. Fig. 4.4b shows the relative levels of expression of the 3 genes in hMSCs, hFOBs and Ti-Dex-BMP2 cells, normalized to the expression level of GAPDH. Other than Col I, hMSCs had no detectable levels of Runx2 and OCN. Table 4.1 shows the primers used for the RT-PCR reaction of bone-related genes.

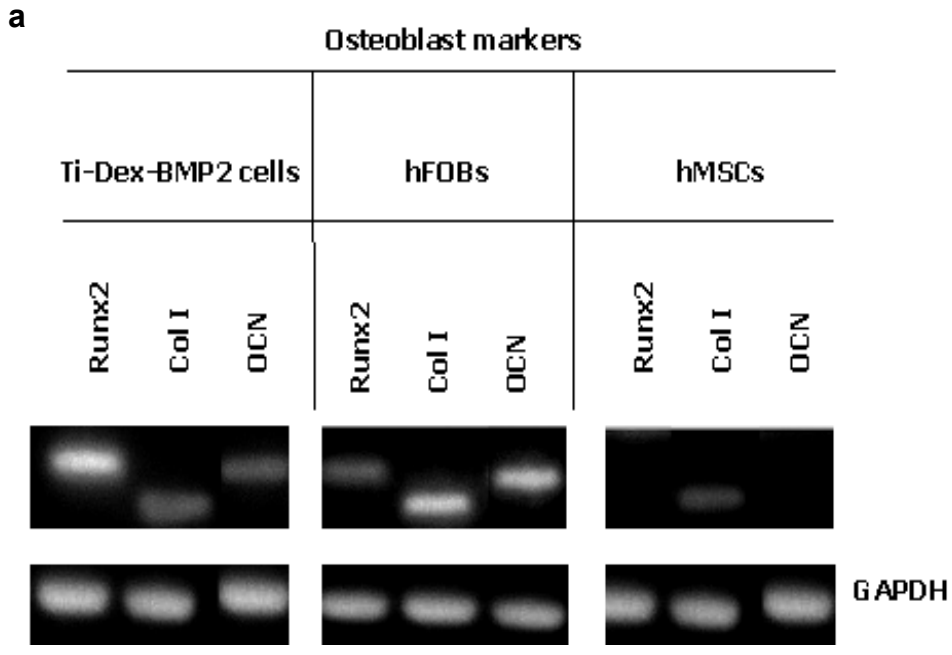

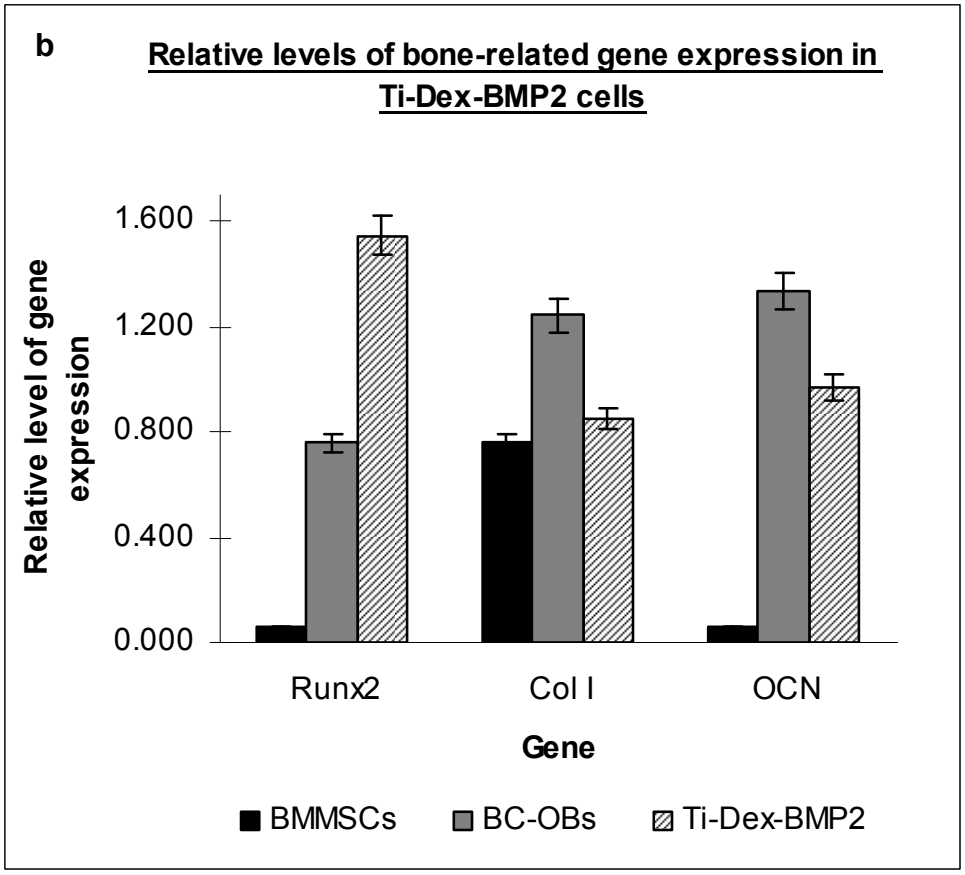

Fig. 4.4a & 4.4b. RT-PCR of Runx2, Col I and OCN suggests that Ti-Dex-BMP2 cells are undergoing osteoblast differentiation, unlike hFOBs (positive control), which are mature osteoblasts. This is evident from the comparatively higher level of Runx2, indicating a higher transcription activity level of this gene, and the relatively lower levels of Col I and OCN, indicating that the Ti-Dex-BMP2 cells are not fully differentiated osteoblasts yet. Conversely, untreated, hMSCs cultured in plastic culture flasks (negative control) do not differentiate and hence have no detectable level of bone-related markers except for Col I.

Table 4.1. Primers used for the reverse transcription-polymerase chain reaction of bone-related genes.

Gene (Ascension number)	Sequence		T_{anneal} (^{o}C)	Product size (bp)
RUNX2 (NM_004348)	Forward	tttgcactgggtcatgtgtt	58	156
	Reverse	tggctgcattgaaaagactg	58	
Collagen I (NM_000088)	Forward	ccaaatctgtctccccagaa	60	214
	Reverse	tcaaaaacgaaggggagatg	58	
Osteocalcin (NM_199173)	Forward	gtgcagagtccagcaaaggt	62	175
	Reverse	tcagccaactcgtcacagtc	62	
GAPDH (NM_002046)	Forward	gagtcaacggatttggtcgt	60	238
	Reverse	ttgattttggagggatctcg	60	

Alizarin Red staining

The Ti-CS-BMP2 cells were stained with Alizarin Red S to detect calcium deposits in the cells. Fig. 4.5a shows the some of the positively-stained cells. Untreated hMSCs stained negative with Alizarin Red S, as shown in Fig. 4.5b.

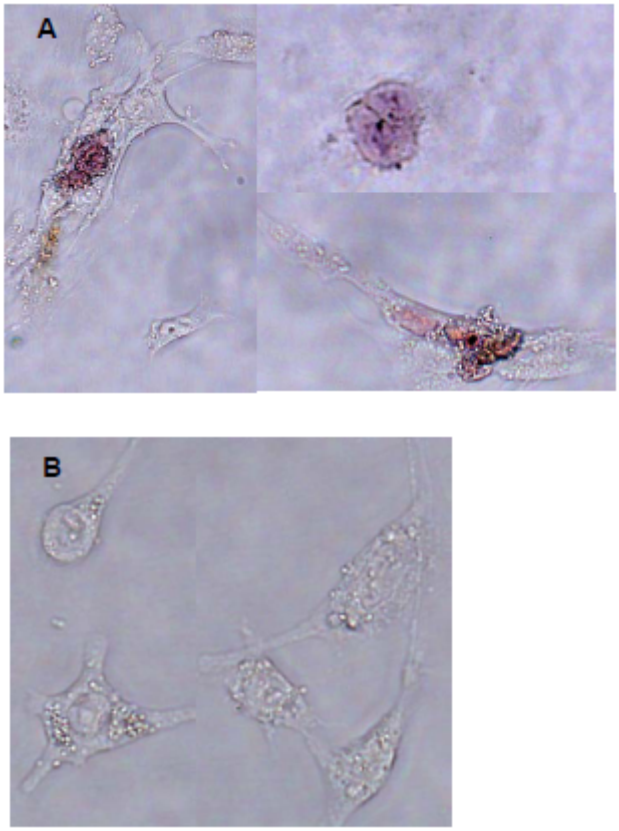

Fig. 4.5a & Fig. 4.5b. Ti-Dex-BMP2 cells that stain positive for the presence of calcium deposits with Alizarin Red S indicate osteoblast differentiation (Fig. 4.5a), while untreated, cultured hMSCs do not differentiate and hence stain negative for Alizarin Red S (Fig. 4.5b).

Discussion

MSCs are a heterogenous mix of cells with different proliferation capacities [154]. Despite their varying differentiation potential, the default differentiation pathway is usually osteogenesis [155-159]. These cells have been reported to retain their undifferentiated phenotype and remain capable of osteogenic differentiation during *ex vivo* expansion through multiple passages [132]. Their surface marker expression profiles remain consistent, and their gene expression profiles do not change significantly during long-term expansion [132].

Initial attachment of hMSCs onto the surface of the titanium substrates is paramount for cell proliferation and osteoblast differentiation to take place *in vivo*. The present results show that upon cell attachment on all the titanium substrates except the Ti-Dex substrate, the hMSCs steadily proliferated until day 7, when proliferation was seen to slow down. This suggests that the cells were undergoing differentiation, since differentiating cells are known to slow down in proliferation rate or even leave the cell cycle [125]. The BMP2 coating on the Ti-Dex-BMP2 substrates appears to have enhanced initial cell attachment, probably by stimulating biological responses in the cells which come into contact with the substrates. BMP2 is known to increase the expression of cytoskeletal proteins [160]. An increase in the expression of cytoskeletal proteins probably contributes to improved cell spreading and migration, thereby encouraging a strong and evenly distributed cell attachment over the substrate surface.

Osteoblast differentiation possibly occurred on the Ti and Ti-Dex-BMP2 substrates soon after cell attachment, as suggested by the results of the ALP activity assay on day 7 of culture (Fig. 3). Others have used calcium phosphate-coated, collagen-coated, or chondroitin sulphate-coated titanium to enhance the retention of BMP2 on the substrate surface [121, 122, 137]. BMP2 was covalently attached to dextran-grafted titanium substrates and achieved almost 95% retention of the BMP2 on the substrate surface after 14 days. Whereas physically adsorbed BMP2 may gradually detached and diffuse into the surrounding tissue fluids, covalently attached BMP2 can remain on the substrate for a sufficiently long period of time to support osteoblast differentiation. Thus, localized BMP2 can possibly enhance osteoblast differentiation at the implant site since in clinical practice, osteoblast attachment and bone formation are known to occur on unmodified titanium implants.

Based on the ALP assay which showed that the Ti-Dex-BMP2 cells had the highest level of activity, the expression levels of three bone genetic markers in the cells on the Ti-Dex-BMP2 substrates were assessed. RT-PCR was carried out to assess the expression levels of three key bone markers, Runx2, Col I and OCN. Runx2 is the trasnscription gene of the osteoblast specific protein, osteocalcin. Together, Runx2 and OCN are the key regulators of osteoblast differentiation and function [143-145]. Runx2 functions as a scaffold protein for nucleic acids and regulatory factors involved in skeletal gene expression. Osteocalcin is the major noncollagenous protein of bone matrix and thus serves as a convenient biomarker of osteoblast differentiation [146]. Interestingly,

serum OCN levels may indicate the point of severity of the disease at which a bone implant should be considered, as OCN has been implicated in human osteoarthritis [146]. The major constituent in bone extracellular matrix, collagen I, mediates the transduction of extracellular signals into the cells through its interaction with the $\alpha_2\beta_1$ integrin receptor on the cell membrane [147, 148]. Disruption to this collagen-integrin interaction can thus inhibit osteoblast differentiation from bone marrow cells [148]. RT-PCR analysis shows that Runx2, Col I and OCN are expressed in the Ti-Dex-BMP2 cells, whereas only Col I is expressed in the untreated hMSCs. The comparatively lower levels of Col I and OCN in the Ti-Dex-BMP2 cells as compared with those from the hFOBs suggests that the Ti-Dex-BMP2 cells are in the early stages of osteoblast differentiation (Fig. 4b). This is further corroborated by the relatively higher level of the transcription factor, Runx2, indicating a higher bone related gene transcription activity level in Ti-Dex-BMP2 cells than in hFOBs. Additionally, the hFOBs were assessed for the expression of endogenous BMP2, which is a key gene in bone cells, as BMP2 also serves to regulate the Runx2 gene. Finally, the Ti-Dex-BMP2 cells were stained with Alizarin Red S to detect intracellular calcium deposits. There could be a possibility that there exists in the hMSCs, a small population of cells that are already committed to the osteoblast lineage. However, the results show that by day 7, the cells attached onto the Ti-Dex-BMP2 substrates did not continue to proliferate. Furthermore, RT-PCR results from the untreated hMSCs do not reveal the expression of Runx2 and OCN.

Thus, the hMSCs differentiated into osteoblasts under the influence of the immoblilized BMP2 on the substrate.

Conclusion

Implant related bacterial infections and the lack of osseointegration between implant and host bone tissue can result in implant failure. Hence, a favoured strategy to combat bacterial infections and to promote osseointegration would be to develop an implant surface that is anti-bacterial and osteoconductive. In Chapter 3, it has been shown that the Ti-CS-BMP2 substrate is able to support the differentiation of mesenchymal stem cells into osteoblasts. In this chapter, work is done to study another method to surface modify the titanium substrate. The titanium substrate is first surface modified by covalently grafting dextran onto the titanium surface. Subsequently, BMP2 is covalently grafted onto the dextran coat. While dextran-grafted titanium has been shown to resist bacteria adhesion, it does not favour human mesenchymal stem cell (hMSC) adhesion. However, further modification with covalently grafted BMP2 on the dextran coat enhanced hMSC adhesion and proliferation. The attached hMSCs also underwent active differentiation into osteoblasts. This is evident from their relatively higher level of transcription activity of Runx2 and lower levels of collagen I and osteocalcin expressions, as compared with human osteoblasts (hFOB). Osteoblast differentiation is confirmed by Alizarin Red staining, which revealed the presence of intracellular calcium deposits.

Although surface modification of titanium has been reported to enhance the attachment of BMP2 on the substrate surface, there are concerns that biomimetic coatings do not enhance bone formation [121, 122]. It is shown in this chapter that the method of covalently attaching BMP2 onto dextran-grafted titanium is an effective way to confer upon the substrate surface anti-bacterial and osteogenic properties. The Ti-Dex-BMP2 substrate therefore has the potential to be used to fabricate anti-bacterial, osteoconductive bone implants. The work done in Chapters 3 and 4 has enabled a selection of one of the two titanium substrates in this thesis for further studies to be done.

Chapter 5

Improvement to the Ti-CS-BMP2 substrate

Glutaraldehyde crosslinking of BMP2 to chitosan-grafted titanium substrate

Introduction

In chapter 4, the Ti-Dex-BMP2 substrate is found to be osteogenic. However, the substrate requires a tedious preparation process as compared with the Ti-CS-BMP2 substrate described in chapter 3. Chitosan is proposed to alter the surface charge on the bacterial cell wall, leading to bacterial cell lysis and leakage of cellular contents. On the other hand, dextran only prevents initial bacterial cell adhesion. Hence, on the basis of the anti-bacterial mechanism and the complexity of the substrate fabrication procedure, the Ti-CS-BMP2 substrate is chosen for further studies on a method to enhance the firmer attachment of BMP2 on the Ti-CS surface, and the subsequent work in chapter 6.

Physical adsorption of BMP2 onto the Ti-CS substrate surface is a relatively simple and convenient method. However, adsorption is probably mediated by electrostatic forces which results in a substrate with a low surface density of BMP2. Adsorbed BMP2 is also progressively lost from the substrate surface. Loss of BMP2 molecules from the substrate surface could potentially give rise to implicating factors if the substrate is to be used for other studies. Thus, an improved method to firmly attach BMP2 onto the Ti-CS surface is required. In the present study, glutaraldehyde, a common crosslinker used to crosslink proteins, is used to crosslink BMP2 to the Ti-CS surface. Glutaraldehyde crosslinking effectively anchors a high density of BMP2 onto the chitosan layer of the Ti-CS substrate surface. Crosslinked BMP2 molecules are also more firmly attached than those which are physically adsorbed. Consequently, a relatively consistent and high percentage of attached BMP2

remains available for osteogenic differentiation for a substantially longer period of time. Implicating factors due to substrate variability resulting from the loss of BMP2 molecules from the substrate surface would also be reduced.

Materials and methods

Materials and methods specific to this chapter are described below. All the other materials and methods used in this chapter are described in Chapter 2 (General materials and methods).

In order to avoid implicating factors due to patient variability, patient bone marrow-derived mesenchymal stem cells and patient bone chip-derived osteoblasts were not used in the present study. Instead, appropriately characterized human mesenchymal stem cells (hMSC) and human osteoblasts (hFOB) were purchased from Lonza, USA, a commercial source and used for all the experiments in this study.

Preparation of the Ti-CS-BMP2(gluta) substrates

Ti foils of 0.52-mm thickness were cut to a size of 1 cm X 1 cm, and cleaned with sandpaper, followed by sonication sequentially in Knoll's reagent (4.0% HF, 7.2% HNO_3, 88.8% water), dichloromethane, acetone and water. After surface passivation in 40% HNO_3, dopamine was anchored to the surface of the Ti substrates by immersion in a 1 mg / ml solution of dopamine at room temperature in the dark overnight, as described elsewhere [123]. Unbound dopamine was washed off with copious PBS and the substrates were air dried in a sterile environment. Subsequently, the substrates were immersed in a stirred 3% glutaraldehyde solution at room temperature overnight. Glutaraldehyde serves as a cross-linker, providing the reactive aldehyde groups for covalently bonding dopamine and CS. Unbound glutaraldehye was removed by rinsing the

substrates in water. CS was dissolved in a 0.1% dilute acetic acid to a concentration of 5 mg / ml. The glutaraldehyde-treated substrates were then immersed in the CS solution. Imine bonds are formed between the aldehyde groups on the Ti surface and the primary amino groups at the C-2 position of CS. The resulting substrates were then washed with water and dried under vacuum. The Ti-CS substrates were subsequently immersed in a 3% glutaraldehyde solution (pH = 8.0) and left at room temperature overnight. After washing to remove unbound glutaraldehyde, the substrates were individually coated with BMP2 (from a 50 μg / ml BMP2 solution) and left at room temperature overnight. Following which, the substrates were rinsed with sterile PBS to remove unbound BMP2 and left to air dry in a sterile environment before use. The substrates are denoted Ti-CS-BMP2(gluta) in all subsequent discussions. All the biological assays were done in duplicates, and each assay was done twice.

After the preparation of the Ti-CS-BMP2(gluta) substrates, the following were subsequently done, and the procedures are described in chapter 2:

Stability and surface density of BMP2 on Ti-CS-BMP2(gluta) substrates

Culture of hMSCs

Culture of hFOBs

Differentiation of hMSCs into osteoblasts on the Ti-CS-BMP2(gluta) substrate

The substrates were placed into a 24-well plate and seeded with hMSCs at a density of 10 000 cells / cm^2. Two ml of osteogenic medium comprising normal hMSC culture medium supplemented with 10 nM dexamethasone, 7 mM β-glycerophosphate and 0.2 mM ascorbic acid were added to each well. Half of the medium was removed and replaced with fresh medium after every 2 days. The cells were allowed to differentiate for 7 days before being used for the ALP assay, to ascertain if the Ti-CS-BMP2(gluta) cells have differentiated into osteoblasts. The ALP assay procedure is described in chapter 2. As a control, hMSCs were also cultured on Ti-CS-BMP2(gluta) substrates with the BMP2 heat-denatured at 80^{o}C for 10 minutes in an oven. hFOBs and hMSCs, grown on normal plastic culture dish, were used as the positive control and the negative control respectively.

Results

Stability and surface density of BMP2 on Ti-CS-BMP2(gluta) substrate

In this chapter, an improved technique of attaching BMP2 onto the Ti-CS substrate is described. BMP2 is crosslinked to the grafted chitosan layer on the Ti-CS substrate using glutaraldehyde. The results show that about 46% of the BMP2 used to coat each substrate, or 23 μg, is stably attached onto the Ti-CS surface. By day 9, about 95% of the originally attached BMP2 remains attached (Fig. 5.1).

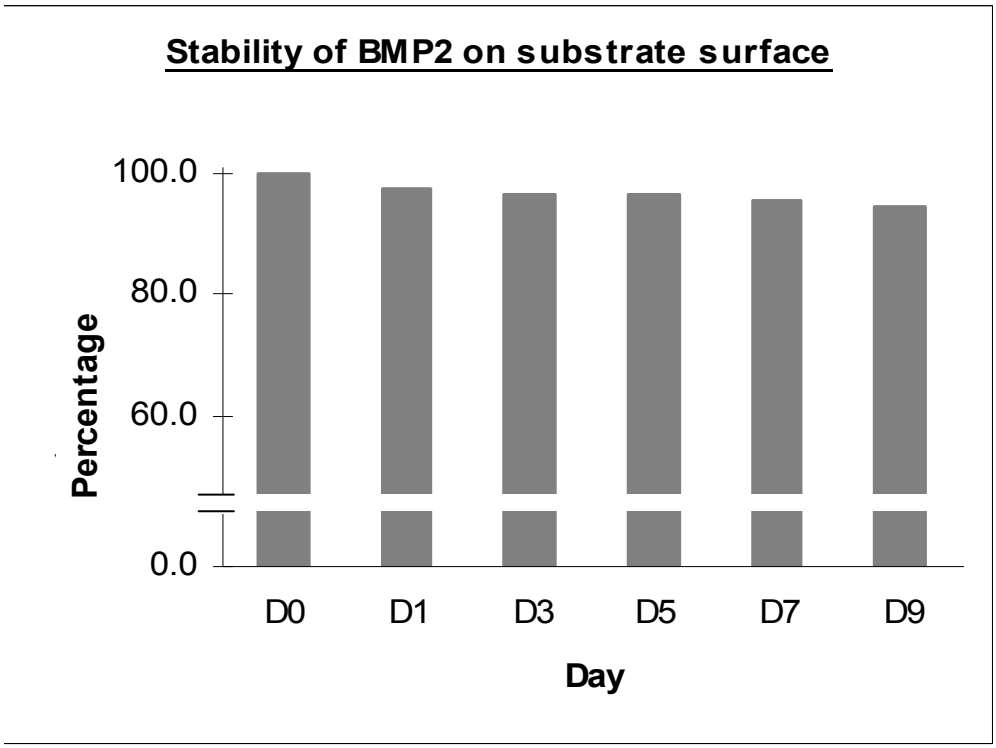

Fig. 5.1. BMP2 is crosslinked to the Ti-CS substrate surface using glutaraldehyde. Approximately 46% of the BMP2 used to coat the surface is firmly attached. By day 9, about 95% of the attached BMP2 remains stably adhered to the substrate surface.

Alkaline phosphatase assay

The results show that the hMSCs growing on the Ti-CS-BMP2(gluta) substrate had differentiated into osteoblasts by day 7 (Fig. 5.2).

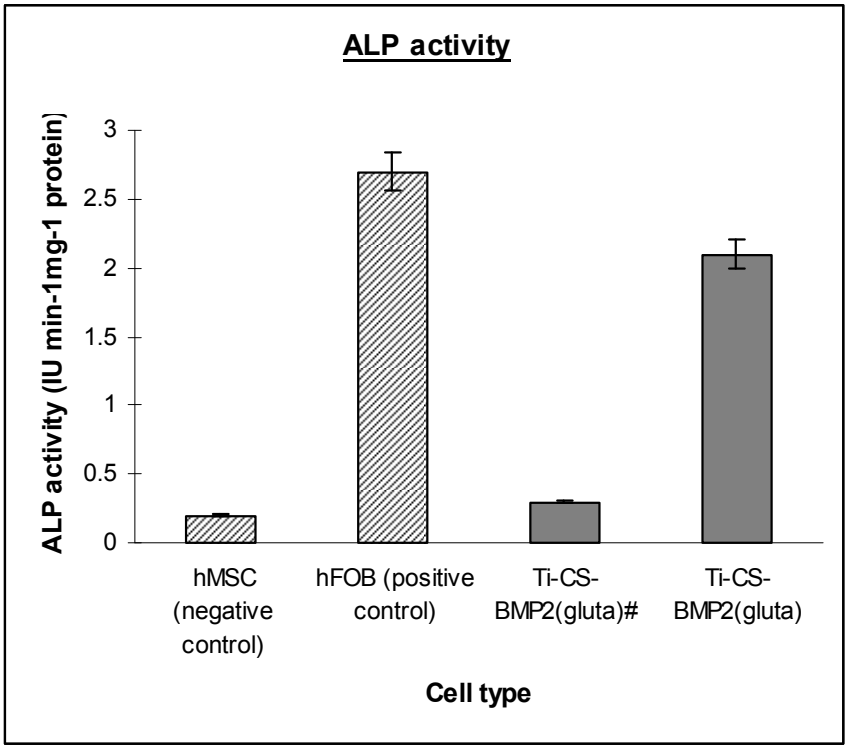

Fig. 5.2. By day 7, hMSC grown on the Ti-CS-BMP2(gluta) substrate had begun differentiating into osteoblasts, as shown by the ALP assay. hMSCs grown on the Ti-CS-BMP2(gluta) substrates with heat-denatured BMP2 (denoted by Ti-CS-BMP2(gluta)#) did not differentiate into osteoblasts. Untreated hMSCs cultured on normal plastic culture dish were used as a negative control while cells from a human foetal osteoblast (hFOB) cell line were used as a positive control. Statistical significance was accepted at $p < 0.05$. Error bars represent the standard deviation of each group.

Discussion

In the preliminary study in Chapter 3, BMP2 was allowed to adsorb onto the Ti-CS substrate. Adsorption of BMP2 is probably mediated by electrostatic forces. Hence, the surface density of BMP2 on the substrate surface is low. Weak binding forces probably also contribute to the gradual loss of BMP2 from the substrate. The gradual loss of BMP2 may present other implicating variables if the substrate is used to study the response of differentiating osteoblasts subjected to LPS treatment (Chapter 6). Therefore, an improved method is devised to attach BMP2 onto the Ti-CS substrate. A 3% aqueous solution of glutaraldehyde at pH 8.0 is used to crosslink BMP2 to the chitosan layer on the Ti-CS surface to achieve a stable, high surface density coating of BMP2. This improved substrate is then used for the study in Chapter 6. Studies of collagen crosslinking with aldehydes of various carbon lengths have established that the highest reactivity occurs at five carbons. Hence, glutaraldehyde, being a 5-carbon dialdehyde, is an effective crosslinking agent. It is more efficient than other aldehydes in generating thermally and chemically stable crosslinks [161]. This is due to the formation of intra- and inter-molecular crosslinks which results in a more rigid protein molecule that is resistant to conformational changes. However, the reaction conditions must be carefully chosen so that inter-molecular crosslinks between the BMP2 molecules are favoured. During the crosslinking process, covalent bonds are formed. These bonds are stable in the presence of substrates or solutions of high ionic strength. Crosslinked protein molecules remain stable over a wide range of pH and temperature, without

dissolution or deterioriation. The fragile proteins after being crosslinked are more sturdy and robust, and are thus less susceptible to damage during physical handling. Yet, their crystal structure remains permeable to dissolved solutes. The process of crosslinking thus confers mechanical advantages to proteins, which otherwise are easily damaged and lose their biological activity.

Glutaraldehyde exists in multi-molecular forms

Various molecular forms of glutaraldehyde in aqueous solution can exist [162]. Hence, commercially available glutaraldehyde consists of a mixture of multi-molecular forms. Under acidic or neutral conditions, glutaraldehyde can exist as a free aldehyde monomer (Structure I), as a cyclic hemiacetal monomer (Structure II), or as cyclic hemiacetal oligomers (Structure III) (Fig. 5.4) [163]. In alkaline solutions, as in the present study, where the pH value of the glutaraldehyde solution is 8.0, glutaraldehyde forms polymers (Structure IV) (Fig. 5.4) [164]. Thus, the effectiveness of glutaraldehyde immobilization and the reaction mechanism involved is possibly a consequence of the existence of the glutaraldehyde structures depending on the solution conditions.

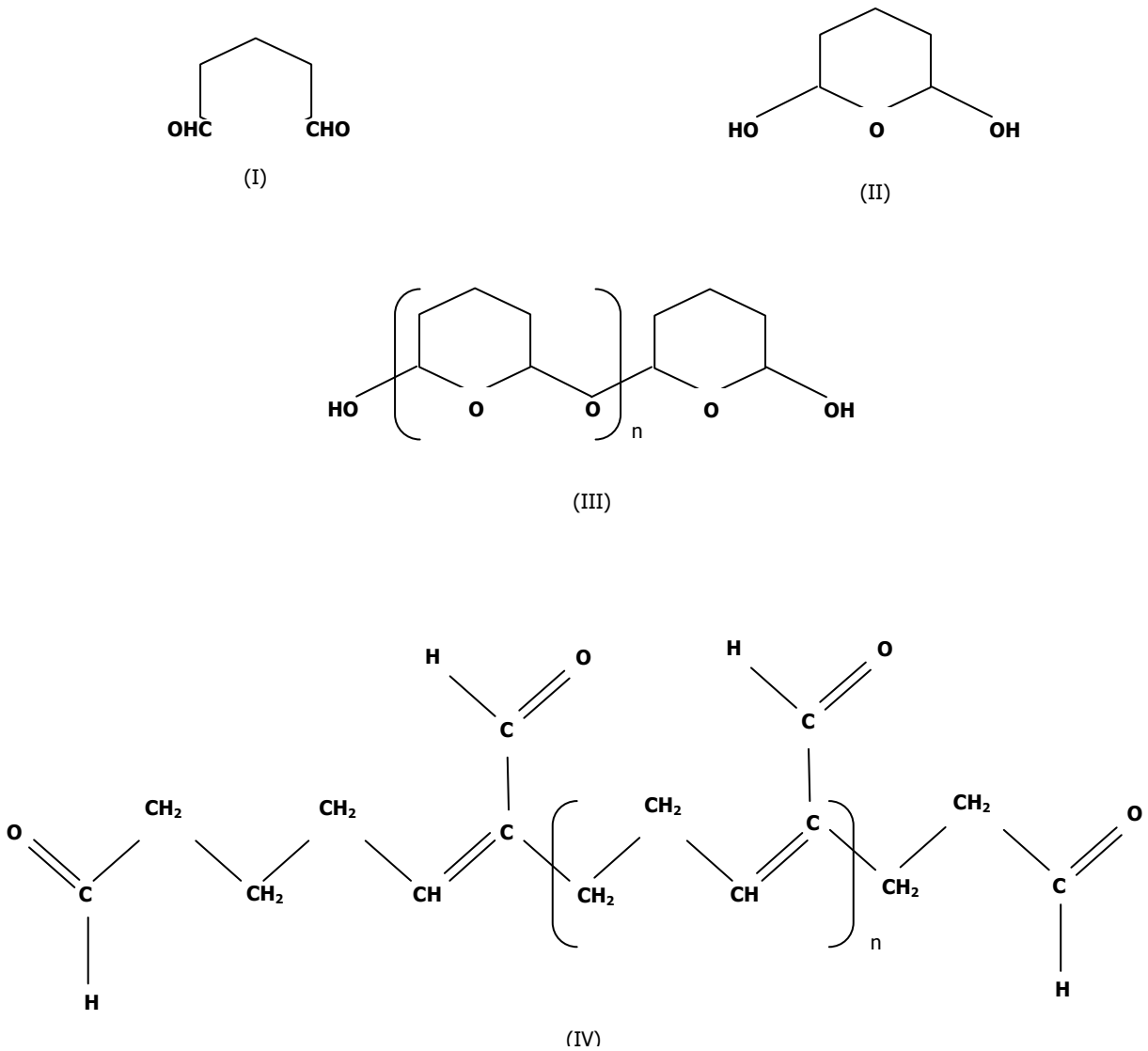

Fig. 5.3. Under acidic or neutral conditions, glutaraldehyde can exist as a free aldehyde monomer (Structure I), as a cyclic hemiacetal monomer (Structure II), or as cyclic hemiacetal oligomers (Structure III). In alkaline solutions, glutaraldehyde forms polymers (Structure IV). (Adapted from Rini *et. al. J Clin Oncol* **23** (2005), pp. 1028-1043 and Barrère *et. al. Materials Science and Engineering: R: Reports* **59** (2008), pp. 38-71.)

The reactivity of glutaraldehyde toward proteins

The chemical behaviour of glutaraldehyde in aqueous solutions has been intensively studied [162]. In acidic conditions, the kinetics of glutaraldehyde crosslinking is slower than that in alkaline conditions [164]. For example, the mildly acidic pH value of 4.5 is considered to be unfavourable for glutaraldehyde crosslinking as the amino groups of the protein are likely to be protonated [165]. Accumulated data show that in alkaline solutions, glutaraldehyde undergoes polymerization, resulting in a mixture of polymeric chains consisting of CH=C(CHO) groups [166]. it is possible that during crosslinking of proteins, glutaraldehyde or its polymerization products may react with several functional groups like amine, thiol, phenol and imidazole [167]. These amino acid side-chains are reactive because they are nucleophiles. The crosslinking is attributed mainly to the reactions with the ε-amino groups of the lysine residues [168]. When crosslinking is carried out under alkaline conditions, the polymeric glutaraldehyde affects crosslinking by way of two reactions, namely, Schiff base formation with an amino group from one protein molecule and a C-N bond formation by Michael addition to the β-carbon of its adjunct double bond by another amino group from a neighbouring protein molecule (Fig. 5.4a & Fig. 5.4b) [164]. Thus, the probable mechanism in the crosslinking of BMP2 to the chitosan layer on the Ti-CS substrate involves Schiff base formation between the glutaraldehyde polymer and the amino groups of BMP2 and chitosan. This is then followed by the formation of a C-N bond to the respective β-carbon of the

adjunct double bond in the glutaraldehyde polymer by another amino group from each of the BMP2 molecule and chitosan molecule.

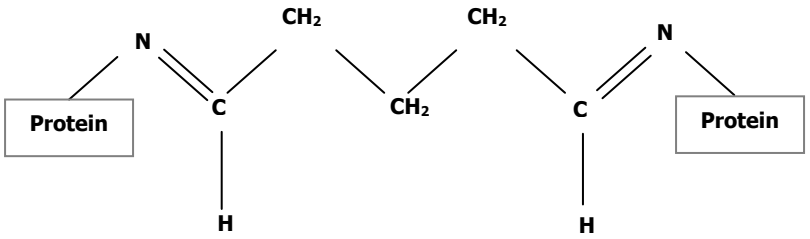

(a)

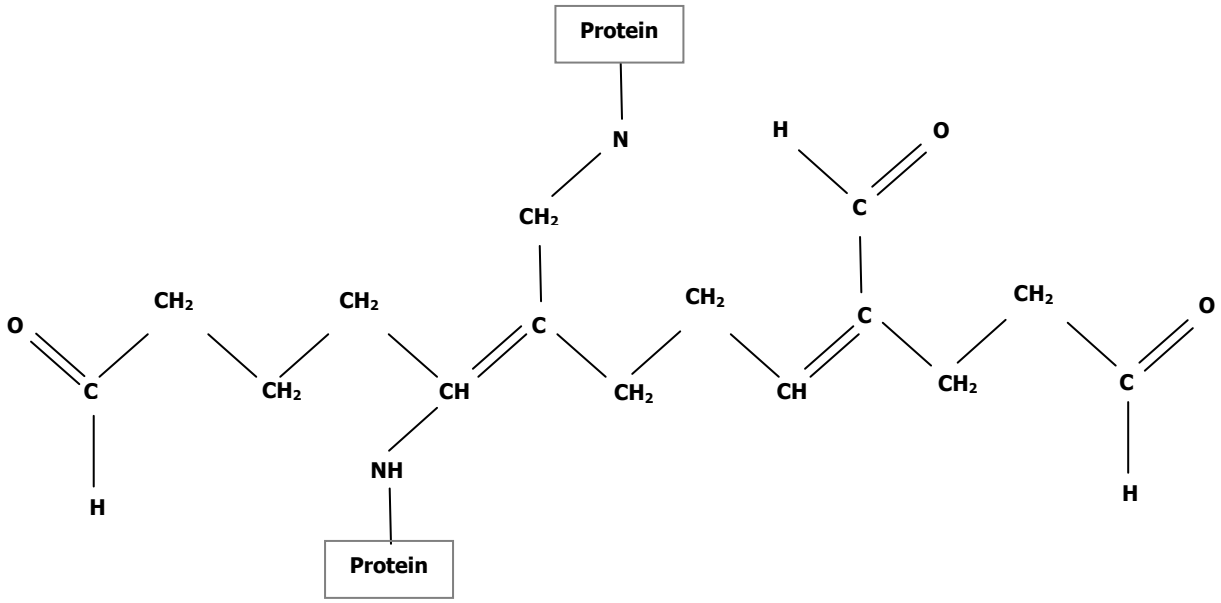

(b)

Fig. 5.4a and Fig. 5.4b. The schematic in (a) illustrates the crosslinking of lysine residues from two protein molecules by monomeric glutaraldehyde. The schematic in (b) illustrates the suggested end product obtained from the reaction of polymeric glutaraldehyde with lysine residues of the crosslinked proteins under alkaline conditions.

Efficiency of glutaraldehyde-mediated crosslinking

The stability and surface density of BMP2 adsorbed onto the Ti-CS substrate has been shown to be approximately 1% of the BMP2 from the coating solution as described in Chapter 3. Approximately 2% per day of the stably adsorbed BMP2 is released into solution after the initial spike of loosely bound BMP2 detachment from the substrate surface. In this study, glutaraldehyde crosslinking of BMP2 to chitosan enables a relatively higher density of BMP2 to be attached on the Ti-CS surface. The covalently bound BMP2 molecules are also more stably attached. By day 9, about 95% of the originally attached BMP2 remain adhered to the substrate surface.

Glutaraldehyde crosslinking does not compromise the biological activity of BMP2

Covalent crosslinking of BMP2 using glutaraldehyde does not compromise the biological activity of this growth factor. The hMSCs grown on the substrate differentiated into osteoblasts by day 7, as confirmed by the ALP activity, as well as by the expression of the bone-related genes of the differentiated cells.

Conclusion

The adsorption of BMP2 onto the chitosan-grafted titanium (Ti-CS) substrate surface is possibly mediated by electrostatic forces. Although a simple and convenient method to use, physical adsorption results in a substrate with a low surface density of BMP2. The attachment of BMP2 molecules mediated by electrostatic forces is relatively weak compared with covalent linkage, resulting in the progressive loss of BMP2 from the substrate surface. In the present study, glutaraldehyde is used to crosslink BMP2 to the Ti-CS substrate surface. Crosslinking enables a relatively higher surface density of BMP2 to be grafted on the substrate surface, as compared with using the adsorption method. The BMP2 molecules are also more firmly attached. The results show that glutaraldehyde crosslinking does not adversely affect the ability of BMP2 to induce the differentiation of hMSCs into osteoblasts. Thus, glutaraldehyde crosslinking is an effective method to achieve a firm and dense coating of biologically active BMP2 on the Ti-CS substrate.

Chapter 6

Simulation of implant bacterial infection

Effect of Sphingosine-1-phosphate on LPS-treated human mesenchymal stem cell-derived osteoblasts cultured on bone morphogenetic protein-2-linked chitosan-grafted titanium substrate

Introduction

Bone implant failures are mainly due to bacterial infection at the implant site or failure of osseointegration of bone tissue with the implant surface. A logical approach to circumvent these two problems would be to surface modify the implant material to render it osteogenic and anti-bacterial. Despite efforts to prevent initial bacteria adhesion on an implant surface, bacteria from the patient's own skin or mucosa may enter the wound site during surgical insertion of a bone implant. The attached bacteria then secrete a thick extracellular matrix, leading to the formation of a biofilm. The thick extracellular matrix delays the penetration of antimicrobial agents, making the bacteria very resistant to host defence mechanisms and antibiotics. Implant-related infection can lead to osteomyelitis, localized bone destruction and eventually implant failure. Effective treatment of implant-related infections is hindered by the evolution of antibiotic-resistant bacteria. Thus, besides the development of implant surfaces that inhibitsbacterial adhesion, there is also a need to seek an effective way to down-modulate the inflammatory response should an infection occur. This may enhance the chances of a successful implant while treatment for the infection is continued. Besides endotoxins from bacterial infections, trace amounts of endotoxins like LPS have been detected on commercially pure implant surfaces [169]. In this chapter, a study is done to investigate the effect of sphingosine-1-phosphate (S1P) on LPS-treated differentiating osteoblasts grown on the Ti-CS-BMP2(gluta) substrate. This improved substrate (described in Chapter 5) is used to simulate an opportunistic bacterial infection that occurs despite the chemical

treatment done to render the substrate anti-bacterial. Glutaraldehyde-crosslinking of BMP2 to the chitosan-coated surface of the substrate will ensure that a sufficient amount of BMP2 is available for osteoblast differentiation. Together, these two features of the improved substrate make it a suitable substrate for examining the effects of LPS on the differentiating osteoblasts. A prior discussion on the relevant aspects of the osteoimmunology in this study to enable a better appreciation of the potential therapeutic benefit of S1P to differentiating osteoblasts exposed to LPS has been presented in chapter 1, wherein the interaction of the bacterial endotoxin LPS with the CD14/TLR4/MD2 receptor complex, TNFα and S1P have been discussed. One aim of the present study is to find out if S1P can rapidly downregulate the expression of TLR4 and TNFα after prolonged LPS exposure, and thereby induce LPS tolerance in differentiating osteoblasts. Another aim of the present study is find out whether S1P can upregulate the expression of the bone-related genes, Runx2 and OCN, thereby maintaining the bone cell characteristics of developing osteoblasts during prolonged LPS exposure.

Materials and methods

Materials and methods specific to this chapter are described below. All the other materials and methods used in this chapter are described in Chapter 2 (General materials and methods) and Chapter 5 (Glutaraldehyde crosslinking of BMP2 to chitosan-grafted titanium substrate).

In order to avoid implicating factors due to patient variability, patient bone marrow-derived mesenchymal stem cells and patient bone chip-derived osteoblasts were not used in this study. Instead, appropriately characterized human mesenchymal stem cells (hMSC) and human osteoblasts (hFOB) were purchased from Lonza, USA, a commercial source and used for all the experiments in this study.

Preparation of the Ti-CS-BMP2(gluta) substrate

The preparation of the Ti-CS-BMP2(gluta) substrate is described in chapter 5.

After the preparation of the Ti-CS-BMP2(gluta) substrates, the following were subsequently done, and the procedures are described in chapter 2:

Stability and surface density of BMP2 on the Ti-CS-BMP2(gluta) substrate

Culture of hMSCs

Culture of hFOBs

Differentiation of hMSCs into osteoblasts on the Ti-CS-BMP2(gluta) substrate

The procedure is described in chapter 5.

Treatment with LPS and LPS/S1P

After 7 days of differentiation in osteogenic medium, the hMSC-derived osteoblasts growing on the Ti-CS-BMP2(gluta) substrates were subjected to LPS treatment or LPS/S1P treatment. Treatment was done for 1 day to simulate a short LPS exposure and 7 days to simulate a prolonged LPS exposure.

LPS treatment

LPS was added to the osteogenic medium to a concentration of 10 μg / ml. Half of the medium was removed and replaced with similarly LPS-supplemented medium every 2 days.

LPS/S1P treatment

LPS and S1P were added to the osteogenic medium to a concentration of 10 μg / ml and 1 μg / ml respectively. Half of the medium was removed and replaced with similarly LPS/S1P-supplemented medium every 2 days.

Reverse transcription-polymerase chain reaction

RNA was extracted from cells on day 1 (short LPS exposure) and day 7 (prolonged LPS exposure) of culture using the NucleoSpin® RNA / Protein isolation kit (Macherey-Nagel, GmbH, Germany) according to the manufacturer's instructions. Each sample of RNA was diluted 50X with DEPC (diethypyrocarbonate) water and the RNA concentration was measured using the NanoDrop ND1000 spectrophotometer. 1 μg of each sample of total RNA was used for the RT-PCR reaction. Reverse transcription of mRNA to cDNA and subsequent cDNA amplification was done using the TITANIUM™ One-step RT-PCR Kit (Clontech Laboratories, Inc., US), through one cycle at 50^{o}C for 1h and 94^{o}C for 5 minutes. This was followed by 32 cycles at 94^{o}C for 30 seconds, 60^{o}C for 30 seconds and 68^{o}C for 1 minute, with a final extension at 68^{o}C for 2 minutes. The expression of glyceraldehyde 3-phosphate dehydrogenase (GAPDH) was used to check RNA integrity. The amplified products were subjected to electrophoresis in a 2% agarose gel and stained with ethidium bromide (Sigma-Aldrich, Singapore). Densitometry was done to quantify the relative levels of the bone-related genes, Runx2, OCN and RANKL, the LPS receptor, TLR4, and the inflammatory cytokine, TNFα, all normalized to the respective levels of GADPH. Primers used for the cDNA amplification and the annealing temperatures are listed in Table 6.11. RT-PCR of the gene expression levels of TLR4, TNFα, Runx2, OCN and RANKL are shown in Fig. 6.6a – e.

Results

RT-PCR

RT-PCR was carried out to assess the relative expression levels of the relevant genes, normalized to the respective GAPDH levels, after treatment with LPS or with LPS/S1P.

Expression of TLR4

LPS treatment - TLR4 levels on D1 and D7

This comparison is done to determine if the osteoblasts (OB) develop LPS tolerance upon prolonged LPS exposure. Table 6.1 and Fig. 6.1 show that the TLR4 level on D7 is significantly lower ($p < 0.05$) than that on D1 (denoted by # on Fig. 6.1). This suggests that the OBs have probably developed LPS tolerance.

LPS/S1P treatment – TLR4 levels on D1

This comparison of the TLR4 levels on D1 (short LPS exposure) is to determine if S1P has any effect on the LPS-treated OBs. Table 6.2 and Fig. 6.1 show that LPS/S1P-treated OBs have a significantly lower ($p < 0.05$) TLR4 level than LPS-treated cells (denoted by * on Fig. 6.1). This suggests that S1P is able to rapidly induce LPS tolerance in the OBs.

Table 6.1. Comparision of TLR4 expression between D1 and D7 of LPS treatment.

	D1	D7
Mean	0.407	0.352
S.D.	0.020	0.020

p value of difference between D1 and D7: <0.05

Table 6.2. Comparision of TLR4 expression between LPS and LPS/S1P treatments on D1.

	LPS	LPS/S1P
Mean	0.364	0.214
S.D.	0.010	0.010

p value of difference between treatments: <0.05

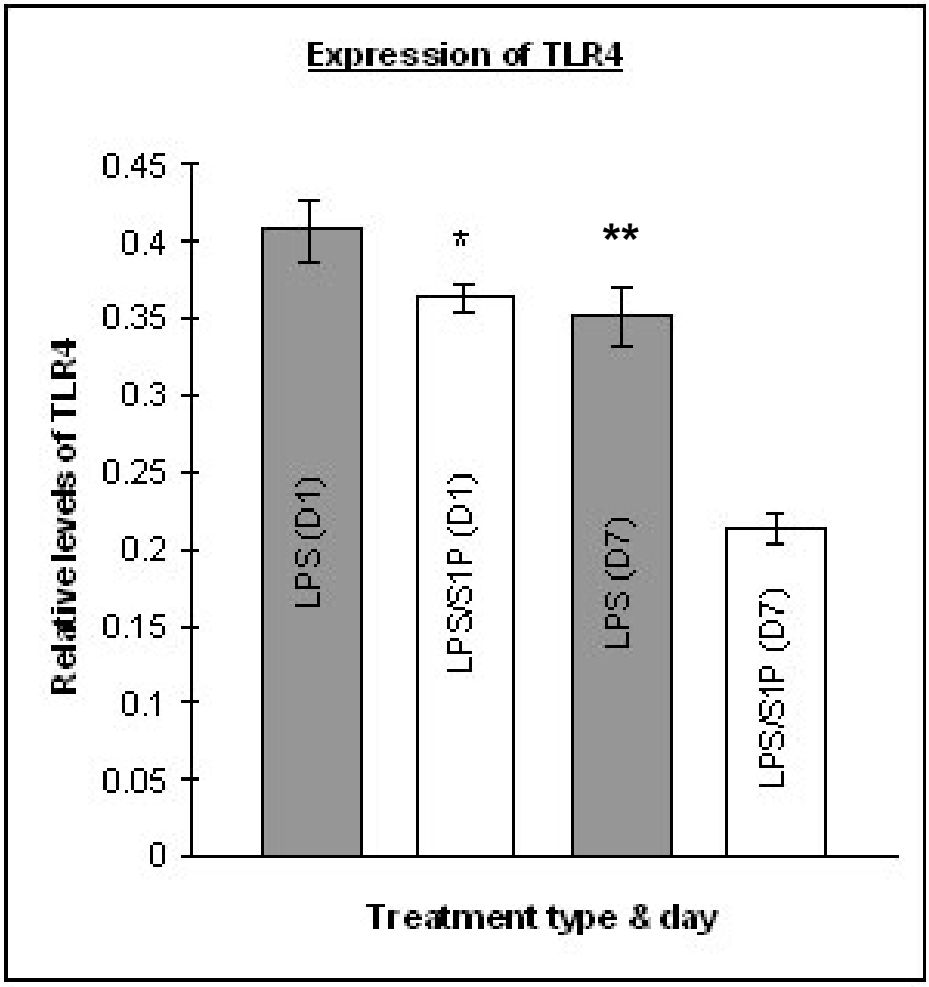

Fig. 6.1. The expression of the LPS receptor, TLR4, is significantly downregulated (n = 3) ($P < 0.05$) by day 7 during prolonged LPS treatment (denoted by **), indicating that the hMSC-derived OBs could have developed LPS tolerance. However, TLR4 expression in the OBs subjected to LPS/S1P treatment (denoted by *) is significantly downregulated (n = 3) ($p < 0.05$) by day 1. Hence, S1P-mediated down-modulation of TLR4 expression suggests that S1P is able to confer protection against LPS damage in OBs by rapidly inducing LPS tolerance. Error bars represent the standard deviation of each group.

Expression of TNFα

LPS treatment - TNFα levels on D1 and D7

This comparison is done to determine the effect of prolonged LPS treatment on TNFα expression in the OBs. Table 6.3 and Fig. 6.2 show that the TNFα level on D7 is significantly lower ($p < 0.05$) than that on D1 (denoted by** on Fig. 6.2). This suggests that the OBs have probably developed LPS tolerance.

LPS/S1P treatment – TNFα levels on D1

This comparison of the TNFα levels on D1 (short LPS exposure) is to determine if S1P has any effect on the expression of this inflammatory cytokine following LPS treatment of the OBs. Table 6.4 and Fig. 6.2 show that LPS/S1P-treated OBs have a significantly lower ($p < 0.05$) TNFα level than LPS-treated cells (denoted by * on Fig. 6.2). The results strongly suggest that S1P is able to protect the OBs against LPS-induced damage by rapidly downregulating TNFα expression.

Table 6.3. Comparision of TNFα expression between D1 and D7 of LPS treatment.

	D1	D7
Mean	0.159	0.124
S.D.	0.020	0.020

p value of difference between D1 and D7: <0.05

Table 6.4. Comparision of TNFα expression between LPS and LPS/S1P treatments on D1.

	LPS	LPS/S1P
Mean	0.131	0.084
S.D.	0.040	0.020

p value of difference between treatments: < 0.05

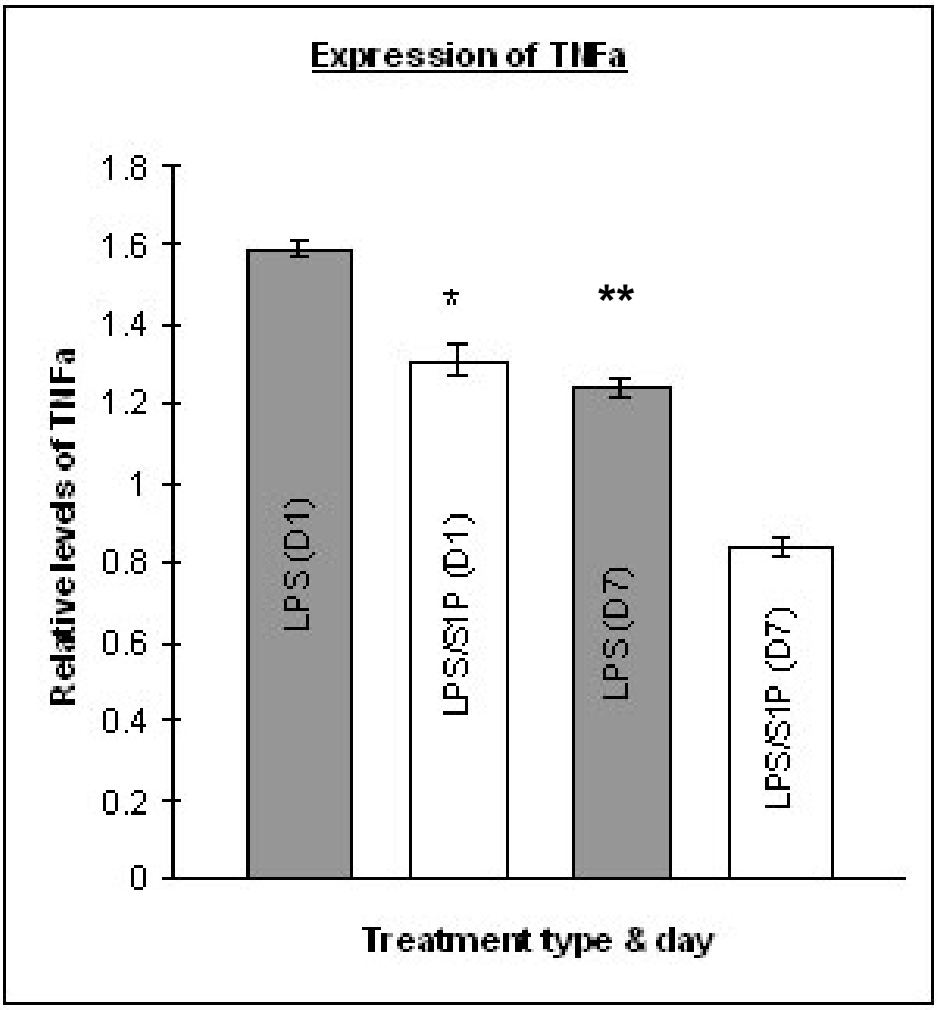

Fig. 6.2. The inflammatory cytokine TNFα is downregulated by about 12% by day 7 (n = 3) ($p < 0.05$) indicating that the OBs probably has developed LPS tolerance (denoted by **). However, LPS/S1P treatment mediates the down-modulation of TNFα by about 44% by day 1 (n = 3) (denoted by *). This suggests that S1P may protect the OBs against LPS-induced damage by mediating the rapid downregulation of TNFα expression. Error bars represent the standard deviation of each

Expression of Runx2

LPS treatment – Runx2 levels on D1 and D7

This comparison is done to determine the effect of prolonged LPS exposure on the Runx2 expression level of the OBs. Table 6.5 and Fig. 6.3 show that the Runx2 level on D7 is significantly lower ($p < 0.05$) than that on D1 (denoted by * on Fig. 6.3). This suggests that prolonged LPS exposure could have a detrimental effect on the bone cell characteristics of the OBs.

LPS/S1P treatment – Runx2 levels on D7

Prolonged LPS has been shown above to have an undesirable effect on Runx2 expression. This comparison of the Runx2 levels on D7 is to determine if S1P has any effect on the expression of this transcription factor in the OBs following prolonged LPS treatment. Table 6.6 and Fig. 6.3 show that LPS/S1P-treated OBs have a significantly higher Runx2 expression level ($p < 0.05$) than LPS-treated cells (denoted by ** on Fig. 6.3). This suggests that S1P is able to restore Runx2 expression in the OBs and thus maintain their bone cell characteristics during prolonged LPS exposure.

Table 6.5. Comparision of Runx2 expression between D1 and D7 of LPS treatment.

	D1	D7
Mean	1.240	0.840
S.D.	0.030	0.020

P value of difference between D1 and D7: < 0.05

Table 6.6. Comparision of Runx2 expression between LPS and LPS/S1P treatments on D7.

	LPS	LPS/S1P
Mean	1.320	1.080
S.D.	0.020	0.040

p value of difference between treatments: <0.05

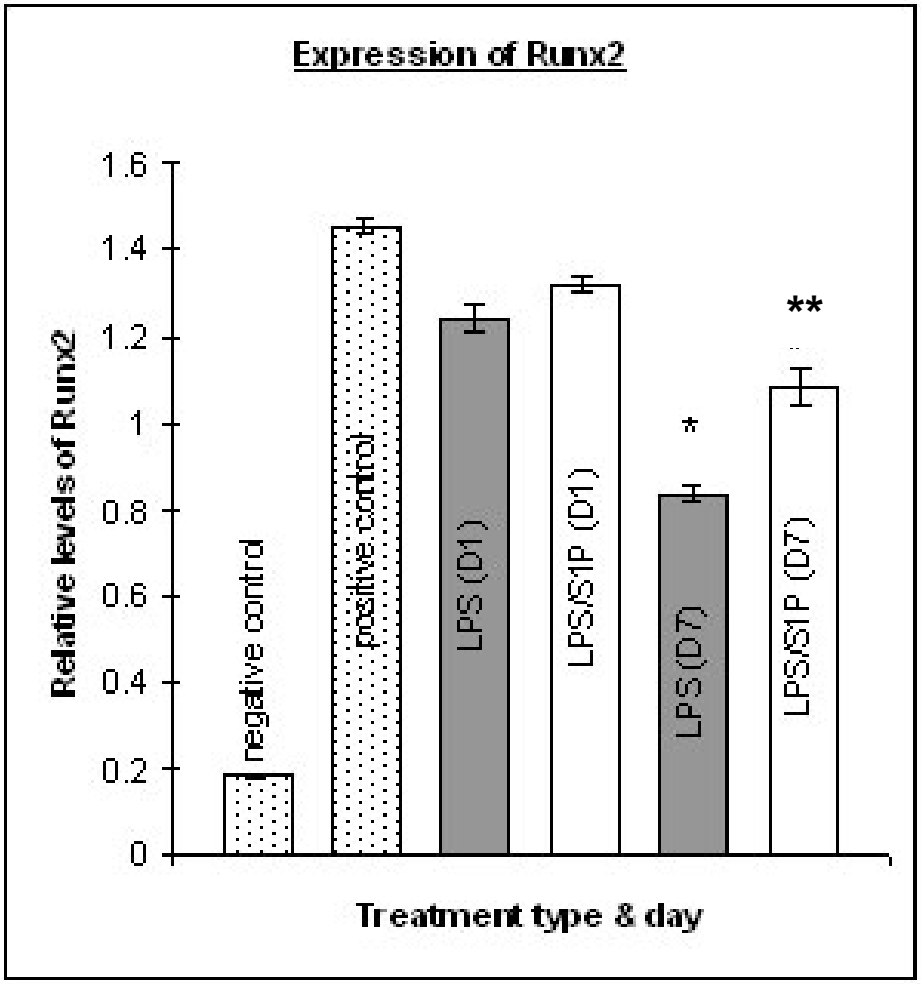

Fig. 6.3. Runx2 expression is downregulated following prolonged LPS treatment (n = 3) (denoted by *). However, in the LPS/S1P treatment, Runx2 expression level is significantly higher than that in the LPS treatment (n = 3) ($p < 0.05$) (denoted by **). S1P is probably able to maintain OB differentiation despite prolonged LPS exposure. Untreated hMSC are used as the negative control (n = 3) and hFOB cells are used as the positive control (n = 3). Error bars represent the standard deviation of each group.

Expression of OCN

LPS treatment – OCN levels on D1 and D7

This comparison is done to determine the effect of prolonged LPS exposure on the OCN expression level of the OBs. Table 6.7 and Fig. 6.4 show that the Runx2 level on D7 is significantly lower ($p < 0.05$) than that on D1 (denoted by * on Fig. 6.4). The results again suggest that prolonged LPS exposure could have a detrimental effect on the bone cell characteristics of the OBs.

LPS/S1P treatment – OCN levels on D7

Prolonged LPS has been shown above to have an undesirable effect on OCN expression. This comparison of the OCN levels on D7 is to determine if S1P has any effect on the expression of this bone-specific protein in the OBs following prolonged LPS treatment. Table 6.8 and Fig. 6.4 show that LPS/S1P-treated OBs have a significantly higher OCN expression level ($p < 0.05$) than LPS-treated cells (denoted by ** on Fig. 6.4). The results thus again suggest that S1P is able to restore OCN expression in the OBs and thus maintain their bone cell characteristics during prolonged LPS exposure.

Table 6.7. Comparision of OCN expression between D1 and D7 of LPS treatment.

	D1	D7
Mean	0.625	0.366
S.D.	0.040	0.020

P value of difference between D1 and D7: < 0.05

Table 6.8. Comparision of OCN expression between LPS and LPS/S1P treatments on D7.

	LPS	LPS/S1P
Mean	0.600	0.438
S.D.	0.020	0.040

p value of difference between treatments: <0.05

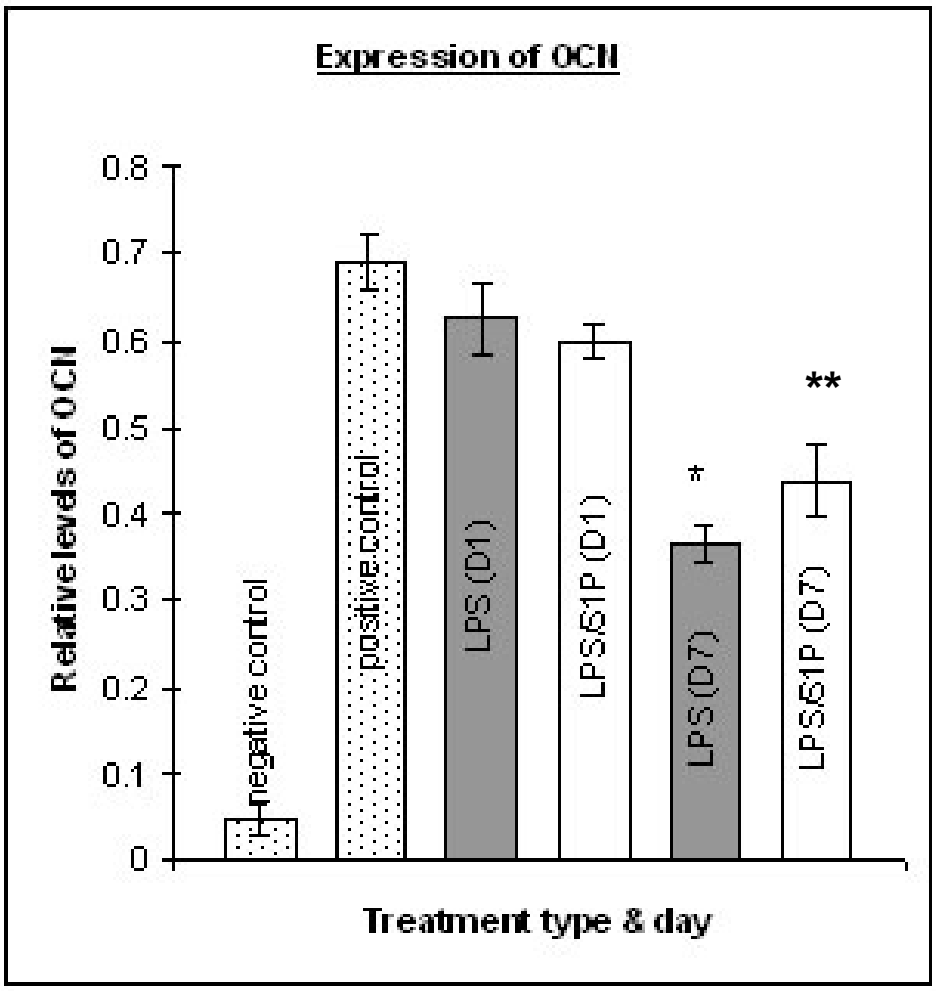

Fig. 6.4. Prolonged LPS exposure downregulates OCN gene expression (n = 3) (denoted by *). However, LPS/S1P treatment appears to restore the OCN gene expression (n = 3) ($p < 0.05$) (denoted by **). S1P is probably able to maintain OB differentiation despite prolonged LPS exposure. Untreated hMSCs are used as the negative control (n = 3) and hFOB cells are used as the positive control (n = 3). Error bars represent the standard deviation of each group.

Expression of RANKL

LPS treatment – RANKL levels on D1 and D7

This comparison is done to determine the effect of prolonged LPS treatment on RANKL expression in the OBs. Table 6.9 and Fig. 6.5 show that the RANKL level on D7 is significantly higher ($p < 0.05$) than that on D1 (denoted by * on Fig. 6.5).

LPS/S1P treatment – RANKL levels on D7

Prolonged LPS exposure has been shown above to upregulate the expression of RANKL. This comparison of the RANKL levels on D7 is to determine if S1P has any effect on the expression of RANKL following prolonged LPS treatment of the OBs. Table 6.10 and Fig. 6.5 show that LPS/S1P-treated OBs have a significantly higher ($p < 0.05$) RANKL level than LPS-treated cells (denoted by ** on Fig. 6.5). This indicates that S1P may enhance the effect of LPS in upregulating the expression of RANKL.

Table 6.9. Comparision of RANKL expression between D1 and D7 of LPS treatment.

	D1	D7
Mean	0.349	0.421
S.D.	0.020	0.030

P value of difference between D1 and D7: <0.05

Table 6.10. Comparision of RANKL expression between LPS and LPS/S1P treatments on D7.

	LPS	LPS/S1P
Mean	0.354	0.502
S.D.	0.020	0.030

p value of difference between treatments: <0.05

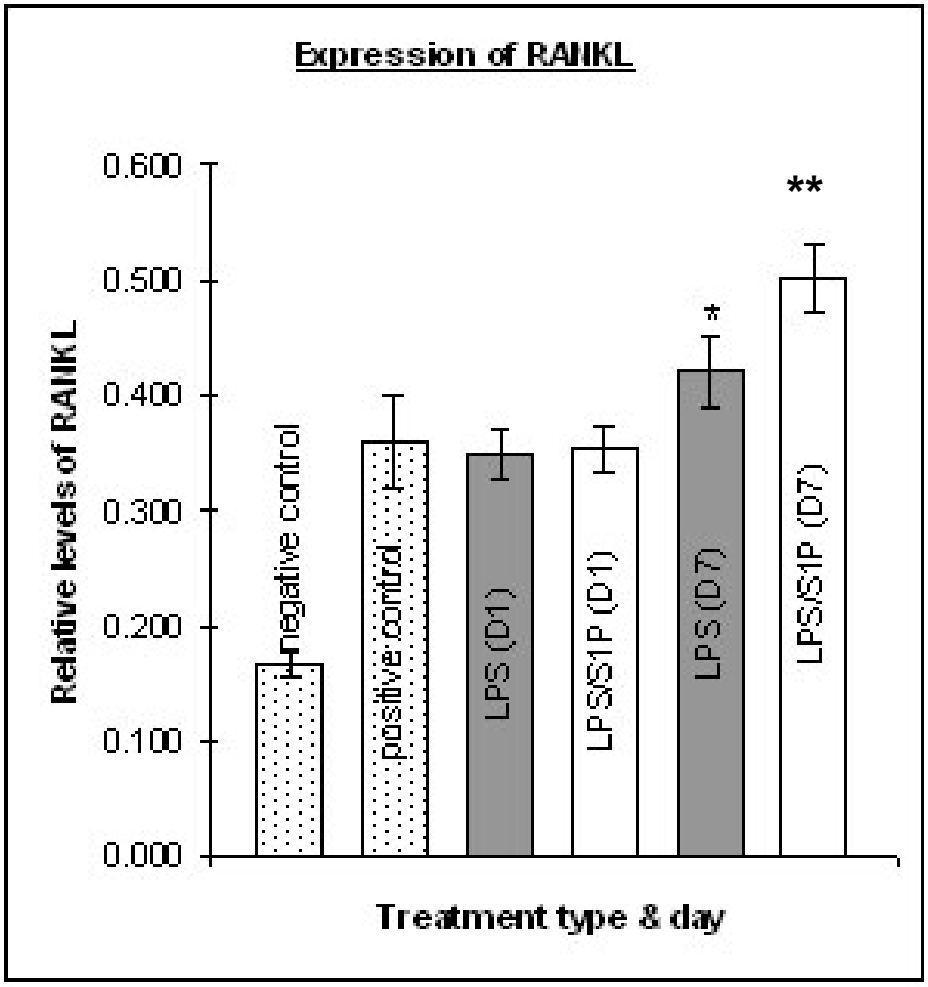

Fig. 6.5. Prolonged LPS treatment upregulates RANKL expression in the differentiating OBs (n = 3) ($p < 0.05$) (denoted by *). LPS/S1P treatment induces a significantly higher level of RANKL expression than with LPS alone (n = 3) ($p < 0.05$) (denoted by **). S1P probably enhances the effect of LPS in upregulating RANKL gene expression. Untreated hMSCs are used as the negative control (n = 3) and hFOB cells are used as the positive control (n = 3). Error bars represent the standard deviation of each group.

Table 6.11. Primers used for the RT-PCR.

Gene (Ascension number)	Sequence		T_{anneal} (^oC)	Product size (bp)
RUNX2 (NM_004348)	Forward	tttgcactgggtcatgtgtt	60	156
	Reverse	tggctgcattgaaaagactg	60	
Osteocalcin (NM_199173)	Forward	gtgcagagtccagcaaaggt	60	175
	Reverse	tcagccaactcgtcacagtc	60	
RANKL (AB064269)	Forward	agagcgcagatggatcctaa	60	180
	Reverse	ttccttttgcacagctcctt	60	
TLR4 (NM_138554)	Forward	tgagcagtcgtgctggtatc	60	167
	Reverse	cagggcttttctgagtcgtc	60	
TNFα (NM_003808)	Forward	agctattatgcgcccgtcta	60	234
	Reverse	aagcagggcttgatcagaaa	60	
GAPDH (NM_002046)	Forward	gtcagtggtggacctgacct	60	420
	Reverse	aggggtctacatggcaactg	60	

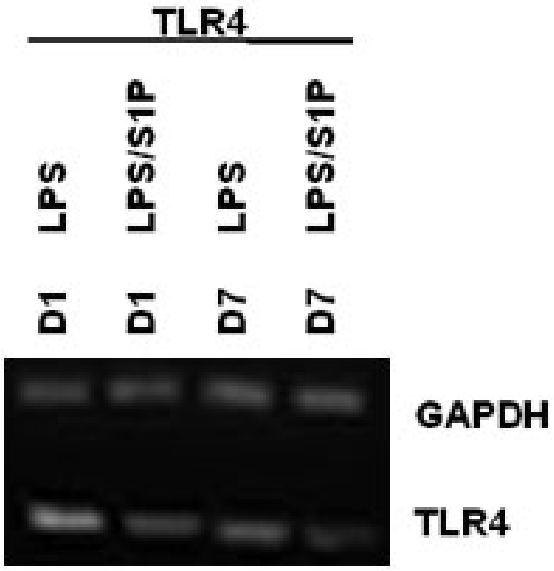

Fig. 6.6a. Gene expression level of TLR4.

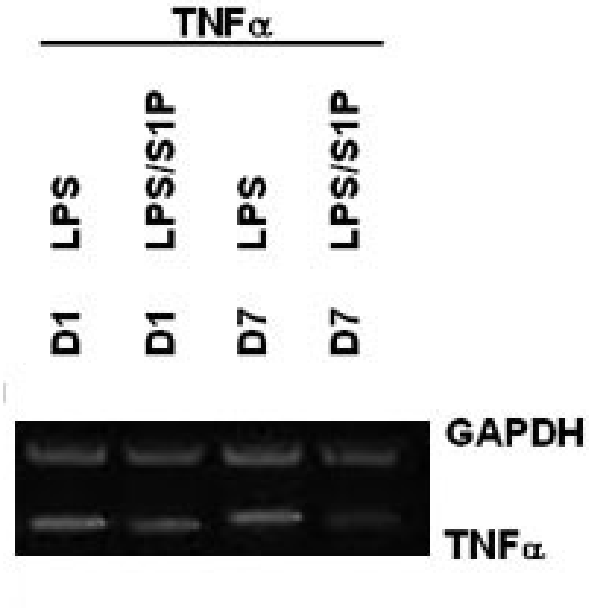

Fig. 6.6b. Gene expression level of TNFα.

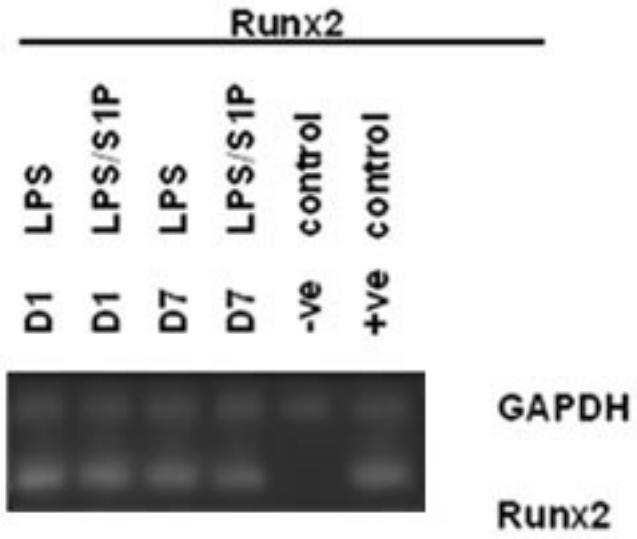

Fig. 6.6c. Gene expression level of Runx2.

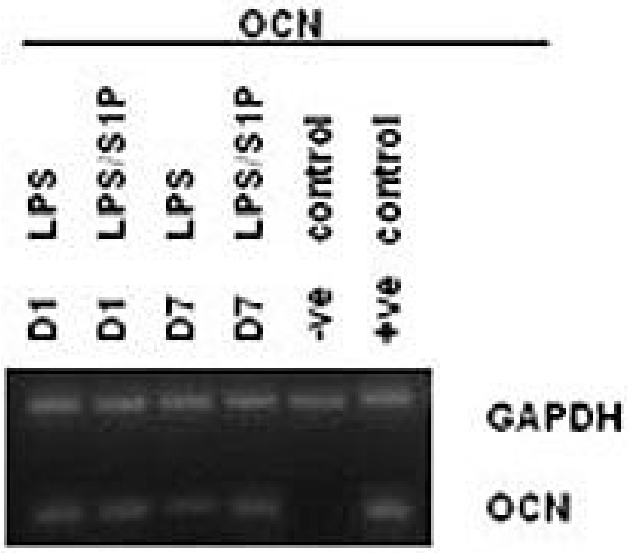

Fig. 6.6d. Gene expression level of OCN.

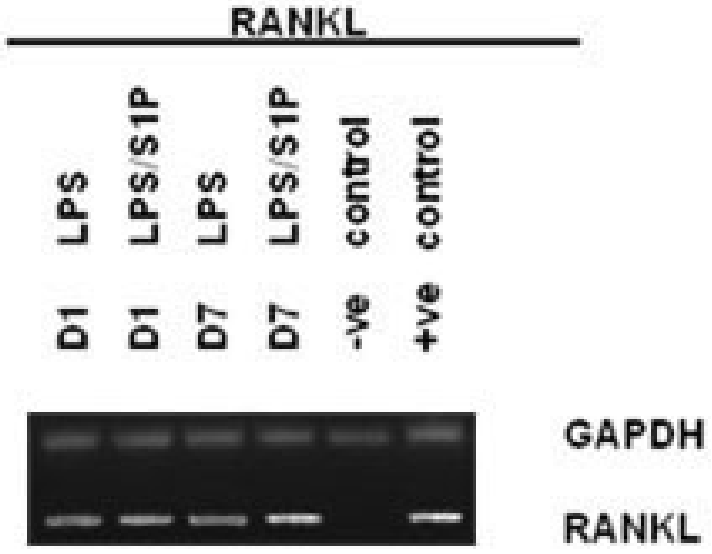

Fig. 6.6e. Gene expression level of RANKL.

Discussion

Effect of S1P on LPS-treated, hMSC-derived OBs differentiating on Ti-CS-BMP2(gluta) substrates

In murine OBs, the phenomena of LPS-induced tolerance has been observed [170]. LPS activates NFκB through TLR4 signaling to induce cytokine production and increased bactericidal activities. Chronically infected human osteocytes have also been found to express anti-microbial peptides [171]. Thus, LPS-induced tolerance is believed to be a mechanism to protect the host from hyperactivation of the innate immunity system. In macrophages, LPS-tolerance results in the downregulation of the receptor, TLR4 [172]. Similarly, in hMSC-derived osteoprogenitors, prolonged exposure to LPS downregulated the gene expression of TLR4 [173]. This is believed to be an adaptive response of OBs to an environment that is rich in microbial flora. The gene expression of the TLR4 receptor in differentiating OBs growing on Ti-CS-BMP2(gluta) substrates is downregulated by about 21% during prolonged LPS treatment (day 7), as shown in Fig. 6.1. This indicates that the OBs similarly develop LPS tolerance after prolonged LPS exposure. However, LPS/S1P treatment induced the downregulation of TLR4 by about 17% by day 1, suggesting that S1P can probably induce LPS tolerance in differentiating OBs rapidly, and maintain the protection throughout the duration of LPS exposure (Fig. 6.2). The level of the inflammatory cytokine TNFα is correspondingly downregulated by day 7 of LPS exposure (Fig. 6.3). This suggests that hMSC-derived OBs may possess the ability to resist bacterial endotoxins like LPS. However, LPS/S1P treatment

reduces TNFα levels by 44% by day 1. This strongly suggests that S1P is able to rapidly induce LPS tolerance in the differentiating OBs. Taking into consideration the results in the present study and evidence from the work of others, S1P may have an anti-inflammatory effect on OBs which are differentiating on Ti-CS-BMP2(gluta) substrates and are exposed to LPS.

LPS exposure has been shown to downregulate the expression of Runx2 in OBs [174]. Differentiating OBs in the present study behave similarly following LPS treatment (Fig. 6.5). However, in the current study, the expression level of Runx2 is upregulated with S1P treatment despite prolonged LPS exposure. Similarly, OCN expression is reduced upon LPS exposure but with S1P treatment, the OCN expression level is upregulated even after prolonged LPS exposure (Fig. 6.6). Thus, the results suggest that, by gradual or partial restoration of the expression of bone genes in the differentiating OBs, S1P helps to maintain their bone cell characteristics.

RANKL is a member of the TNF superfamily and shares much homology with TNFα [175]. Interaction of RANKL with its receptor, RANK, on osteoclast precursors stimulates the differentiation of osteoclasts and increase peri-implant bone resorption [176]. In inflammatory osteolysis, TNFα increases the expression of RANKL [175]. LPS treatment of differentiating OBs growing on the Ti-CS-BMP2(gluta) substrates similarly induces the increased level of RANKL expression as shown in Fig. 6.9. Unfortunately, S1P also induces RANKL upregulation [98]. S1P treatment of the day 7 differentiating OBs exposed to LPS also showed an increase in RANKL level as shown in Fig. 6.10. However,

increased RANKL expression may not be a clinically serious complication. RANKL levels can be managed by the administration of a monoclonal antibody against RANKL [177]. One such antibody is Denosumab, is a neutralizing fully human IgG_2 antibody that targets specifically human RANKL to bring about a decrease in osteoclastogenesis [178].

Conclusion

Bone implant failures are mainly caused by poor osseointegration between implant and bone tissue, and by bacterial infection. Despite efforts to minimize chances of initial bacterial adhesion on an implant surface, implant-related infections do occasionally occur. A bacterial infection can result in osteomyelitis and localized bone destruction, eventually leading to implant failure. Besides the development of antibacterial implant surfaces, there is also a need to seek an effective way to down-modulate an inflammatory response should an implant-related infection occur. In the present study, it is found that sphingosine-1-phosphate (S1P) rapidly downregulates osteoblast expression of TLR4 and TNFα, following LPS exposure. This suggests that S1P is able to induce LPS tolerance in differentiating osteoblasts. Thus, S1P is likely to play an anti-inflammatory role in differentiating Ti-CS-BMP2(gluta) OBs exposed to LPS, by downregulating the gene expression of TLR4 and TNFα. The lower expression level of TLR4 probably reduces the sensitivity of the OBs to LPS, and consequently also reduces the expression level of TNFα. During prolonged LPS exposure, S1P treatment also upregulates the expression of Runx2 and osteocalcin. Hence, S1P possibly helps to maintain the integrity of the OBs in an LPS environment. The findings from the present study indicate that S1P through its dual beneficial effect on osteoblasts exposed to LPS may be of potential therapeutic use in implant-related infections.

Chapter 7

Angiogenic patch to promote vascularization around the healing bone

Poly lactic-co-glycolic acid as a controlled release delivery device

Introduction

Biodegradable polymers play an important role in providing a temporary support for cell growth and differentiation. Ideally, biodegradable polymers must possess the mechanical properties to suit the application and maintain the *in vivo* ambient environment. They must also degrade into products that are harmless to the cells and tissues in the body after a suitable length of time. Poly lactic-co-glycolic acid (PLGA) is one such polymer which has been used to make sutures and other implantable structures, as well as 3-dimensional scaffolds as a support for tissue engineering [179]. In order to enhance initial cell attachment and cell differentiation on PLGA scaffolds, it is usually necessary to functionalize the scaffold surface with bioactive molecules [180, 181]. The adjustable degradation rate of PLGA presents an attractive option to make PLGA-based controlled release delivery devices. PLGA can be grafted with bioactive molecules, to be released gradually to support cell differentiation. Unfortunately, the functionalization of PLGA usually requires extensive chemical modification. Chemical surface modification of PLGA can compromise its mechanical strength [182]. Similarly, chemical modification of bioactive molecules may adversely alter their ability to bind onto their respective cell surface receptors, and thus decrease their biological activity [181]. Thus, a method of anchoring bioactive molecules in their native form to a substrate, which can also control the release of the molecules into solution, would be favoured. In the present study, work was carried out to investigate the coating of an angiogenic factor, vascular endothelial growth factor (VEGF), on unmodified PLGA suture substrates to support the

differentiation of human mesenchymal stem cells (hMSCs) into endothelial cells (ECs).

Materials and methods

Materials and methods specific to this chapter are described below. All the other materials and methods used in this chapter are described in Chapter 2 (General materials and methods).

In order to avoid implicating factors due to patient variability, patient bone marrow-derived mesenchymal stem cells were not used in this study. Instead, appropriately characterized human mesenchymal stem cells (hMSC) were purchased from Lonza, USA, a commercial source and used in all the experiments in the present study.

Materials

Ethicon™ Coated VICRYL™ (polyglactin 910) (W9321) PLGA sutures with a glycolic to lactic acid ratio of 90:10 were purchased from Johnson & Johnson International. Gelatin was purchased from Sigma-Aldrich Chemical Co. (Singapore). Recombinant human VEGF was obtained from R&D Systems (US). The degradation of PLGA in solution was assessed by measuring the pH of the solution using a inoLab pH meter. PE-conjugated CD133 antibody was purchased from eBioscience (San Diego, US). FITC-conjugated polyclonal goat anti-mouse IgG antibody was purchased from AbD Serotec (UK). Flk1-PE was purchased from R&D Systems (US). Unconjugated monoclonal mouse anti-human von Willebrand Factor (vWF) antibody was obtained from Abcam (UK). Unconjugated mouse-anti-human Tie2 antibody was purchased from Santa Cruz (US). The intensity and stability of VEGF coated onto the suture substrate

surface were assessed using a human VEGF ELISA kit purchased from Bender MedSystems (Austria). BD Matrigel™ Basement Membrane Matrix was obtained from BD Biosciences (US).

Preparation of the PLGA-VEGF substrates

The PLGA-VEGF substrates were prepared by stitching sutures onto a square grid 1 cm X 1 cm marked on the base of a plastic weighing boat, to form a suture mat on plastic base. The suture substrates were sterilised by soaking in 70% ethanol for 1 h, rinsed with copious amounts of ultrapure water and allowed to air-dry in a sterile environment. Each substrate was then coated with a solution of 50 ng of VEGF in 50 μl of a mixture comprising 0.1% gelatin and 1% low-melting agarose in the ratio 1:1, and allowed to dry at room temperature overnight. The substrates were then gently rinsed with PBS and allowed to dry. A second thin coating of the gelatine / agarose mixture was then layered over each substrate. The substrates were rinsed with PBS and allowed to dry before use. All the biological assays were done in duplicates, and each assay was done twice. Fig. 7.1 and Fig. 7.2 are illustrations of the suture substrates.

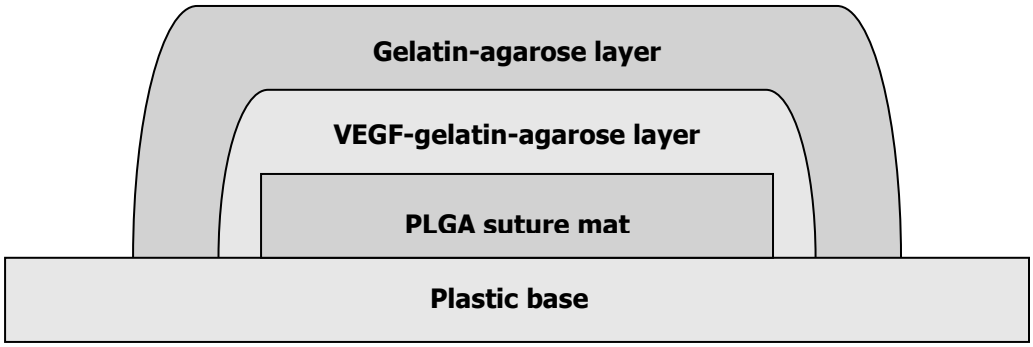

Fig. 7.1 This schematic shows the cross-section of the suture substrate.

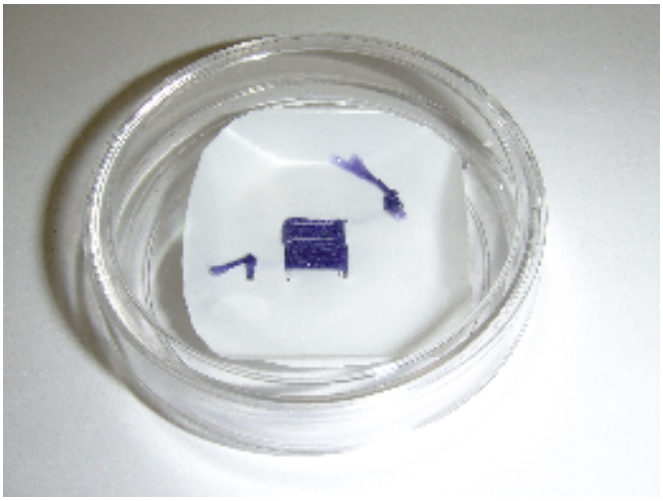

Fig. 7.2 Photograph of the finished PLGA-VEGF suture substrate before being trimmed to size.

Assessment of the degradation rate of PLGA in solution

PLGA suture substrates were prepared as described above. The degradation rate of PLGA in water, PBS and MEM-α supplemented with 10% FBS, was assessed by measuring the change in pH of the respective solutions. One piece of substrate each was placed in 10 ml of the respective solution, and the pH of each solution was measured on days 1, 5, 10, 15, 20 and 25.

Stability of coated VEGF on suture substrates

For the assessment of the stability of VEGF on the suture substrates, the substrates were trimmed to size and placed individually in a 24-well plate containing 1 ml of PBS per well. The amount of VEGF released from each substrate surface into solution was assessed on days 1, 5, 10, 15, 20 and 25. At each respective point in time, 50 μl of PBS was removed from a well marked with the respective time-point. The amount of VEGF in solution was then measured using the Bender Medsystems human VEGF ELISA kit, following the manufacturer's instructions. The colour intensity of the reaction mixture was measured at 450 nm using an absorbance plate reader. The amount of VEGF in the solution was determined using a series of VEGF solutions of known concentrations as standards which were prepared using a VEGF stock supplied in the ELISA kit. The amount of VEGF at each point in time was then expressed as a percentage of the initial amount of VEGF coated on each suture substrate.

Cell culture

Human mesenchymal stem cells (hMSC) were seeded into cell culture flasks and cultured in a medium comprising Minimal Essential Medium-alpha (MEM-α), supplemented with 10% foetal bovine serum (FBS), L-glutamine (2mmol/l), penicillin (100 U/ml) and streptomycin sulphate (100 μg/ml), and incubated at 37^{o}C in a humidified atmosphere of 5% CO_2 and 95% air. Unattached cells were removed on the following day. Half of the culture medium was replaced by a fresh aliquot of medium once every 2 days. The attached cells were allowed to grow to about 75% confluence. Cell colonies that were formed were identified and individually removed by gentle trypsinization, seeded into a new flask each and allowed to grow to about 75% confluence before being used. Passage 2 hMSCs were used throughout the present study. Attached cells were detached by trypsinization and resuspended in fresh culture medium for subsequent experiments described below.

Flow cytometry

Cells were detached by trypsinization and then incubated in PBS with 2% FBS for 10 minutes in an ice bath. 1μl of the CD133-PE antibody was added to the cells, suspended in 100μl of PBS with 2% FBS, in separate tubes. After incubation for 10 minutes in an ice bath in the dark, the cells were washed, resuspended in 1 ml of PBS, and analysed using flow cytometry. A total of 10,000 events were collected for the analysis.

Preparation of culture medium containing VEGF

For the preparation of VEGF-containing medium, the suture was stitched onto both sides of each plastic substrate and coated with VEGF. In subsequent discussions, these substrates will be termed double-sided substrates. Five pieces of double-sided substrates were placed into a small petri dish, such that the substrates were completely submerged in 3 ml of culture medium containing 2% serum.

Effect of VEGF release from suture substrate on MSC differentiation

hMSCs were seeded onto cover slips, each placed in a single well of a 6-well plate at a density of 5 000 cells / cm^2. Unattached cells were removed the following day, and the cells were allowed to grow for another 2 days. The cover slips were then removed from the 6-well plate and individually placed centrally in a petri dish containing 5 pieces of VEGF-coated double-sided substrates which were lined along the inner circumference of the dish. The negative controls comprised a petri dish with cells in normal medium and another dish with cells grown in medium that had uncoated substrates immersed in it. A dish without any substrate but containing culture medium supplemented with 10 ng / ml of VEGF and 2% serum served as the positive control. The experiment was carried out for 14 days. Half of the medium was removed and replaced with fresh medium every third day.

Immunofluorescent (IF) microscopy

Cells cultured on the cover slips were fixed in methanol at -20^{o}C for 10 min and then rinsed with PBS. Following which, the cells were incubated with the relevant fluorochrome-conjugated antibody (1:300) for 1 h. For von Willebrand Factor (vWF) staining and Tie2 staining, where unconjugated primary antibodies were used, the cells were rinsed in PBS and further stained with FITC-conjugated goat anti-mouse secondary antibody (1:300) for 1 h. The cells were then viewed using a fluorescent microscope (Olympus IX71), at a magnification of 100X (for VEGFR2) and 200X (for Tie2, vWF and CD31).

In vitro capillary-like tube formation assay

The assay was performed using 50 μl of BD Matrigel in each well of a 96-well dish at 4^{o}C. The matrigel was left at room temperature for 1 h to allow it to solidify before use. Cells grown on the cover slips were detached with trypsin and the excess trypsin was removed by centrifugation. The cells were resuspended in normal cell culture medium and 2 000 cells in 50 μl of medium was plated onto the Matrigel. The cells were then incubated for 3 h and the capillary-like tube formation was examined under a light microscope.

Results

Assessment of the degradation rate of PLGA in solution

The degradation rate of PLGA sutures in water, PBS and cell culture medium was monitored by measuring changes in the pH of the respective solutions over 25 days (Fig. 7.3). The pH values show a decrease of about 1.09 (water), 1.56 (PBS) and 0.93 (MEM) after 25 days. The buffering capacity of the cell culture medium has probably contributed to the smaller change in pH as compared with the other two media.

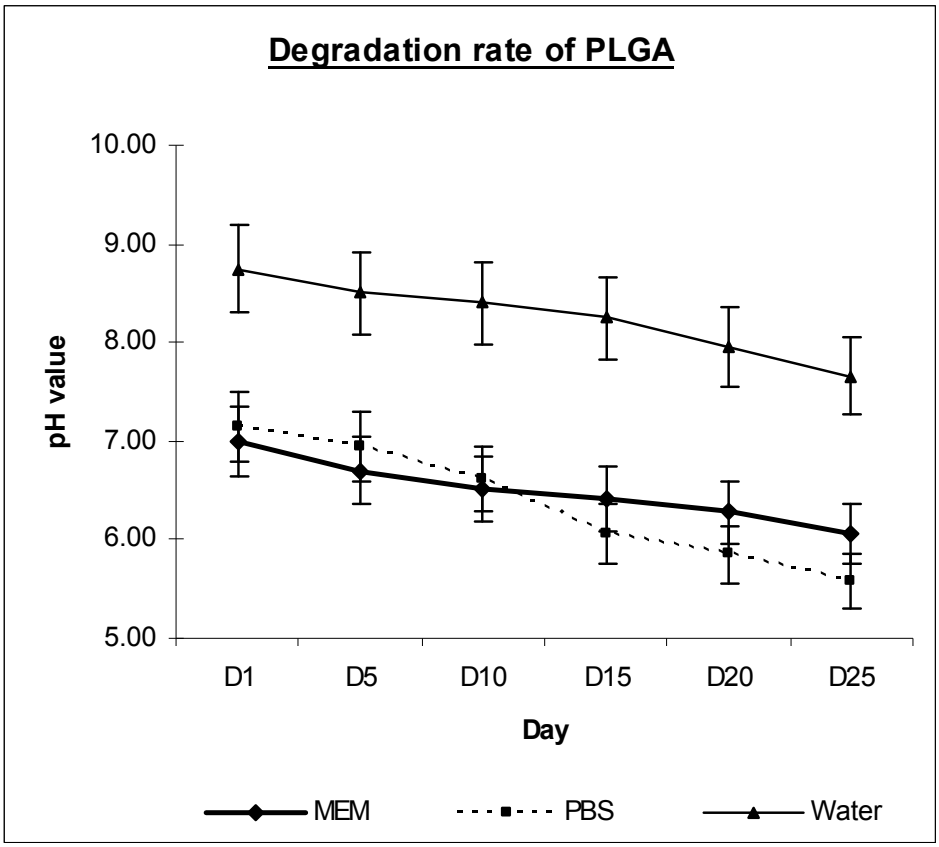

Fig. 7.3 The degradation rate of PLGA sutures in water, PBS and cell culture medium was monitored by changes in the pH of the respective solutions over 25 days (n = 2). Error bars represent the standard deviations. The change in pH is the smallest in MEM, indicating that MEM probably has a higher buffering capacity as compared with the other two media.

Stability of coated VEGF on suture substrates

The substrates were coated with a high concentration of VEGF in a VEGF-gelatin-agarose mixture to ensure that the entire substrate surface was covered with the angiogenic factor. A thin layer of gelatin-agarose mixture was layered over the substrate to protect the VEGF from being removed due to abrasion, and to facilitate an even rate of diffusion of VEGF into solution. VEGF was progressively released into solution and its concentration reached a peak at day 15 (Fig. 7.4). Subsequently by day 25, VEGF concentration began to decline.

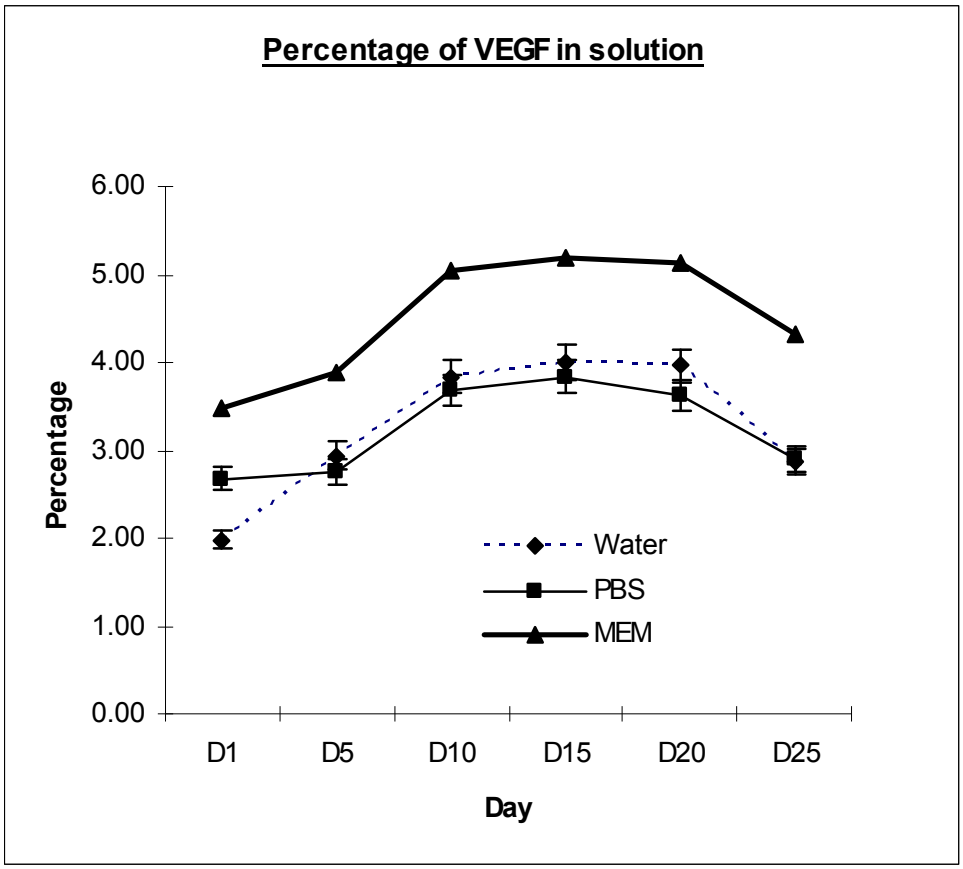

Fig. 7.4. Concentration of VEGF in solution, expressed as percentage of the initial coating concentration of VEGF on the suture substrate (n = 2). Error bars represent the standard deviations. VEGF is progressively released and its concentration in solution reaches a peak at about day 15, which corresponds to approxiamately 2.6 ng / ml (MEM), 2 ng / ml (PBS) and 2 ng / ml (water) per substrate.

Flow cytometry

Passage 2 hMSCs were subjected to flow cytometry analysis to check for the presence of endothelial cell progenitors. No detectable CD133+ cells were found.

In vitro differentiation of hMSCs into endothelial cells

The hMSCs express the endothelial cell markers, Flk-1 (VEGFR-2), Tie2 and vWF after a 7-day culture in medium with VEGF released from the VEGF suture substrates (Fig. 7.5a – 7.5c). After a 14-day differentiation, the differentiated cells also show a weak expression of CD31 (Fig. 7.5d). The ability of the differentiated cells to form a capillary network on semi-solid medium was demonstrated in an *in vitro* angiogenesis assay using Matrigel (Fig. 7.6a). A visual count revealed that about 90% of the cells exposed to VEGF form tube-like structures. hMSCs in the negative controls did not form any capillary network and remained as single cells on the Matrigel (Fig. 7.6b).

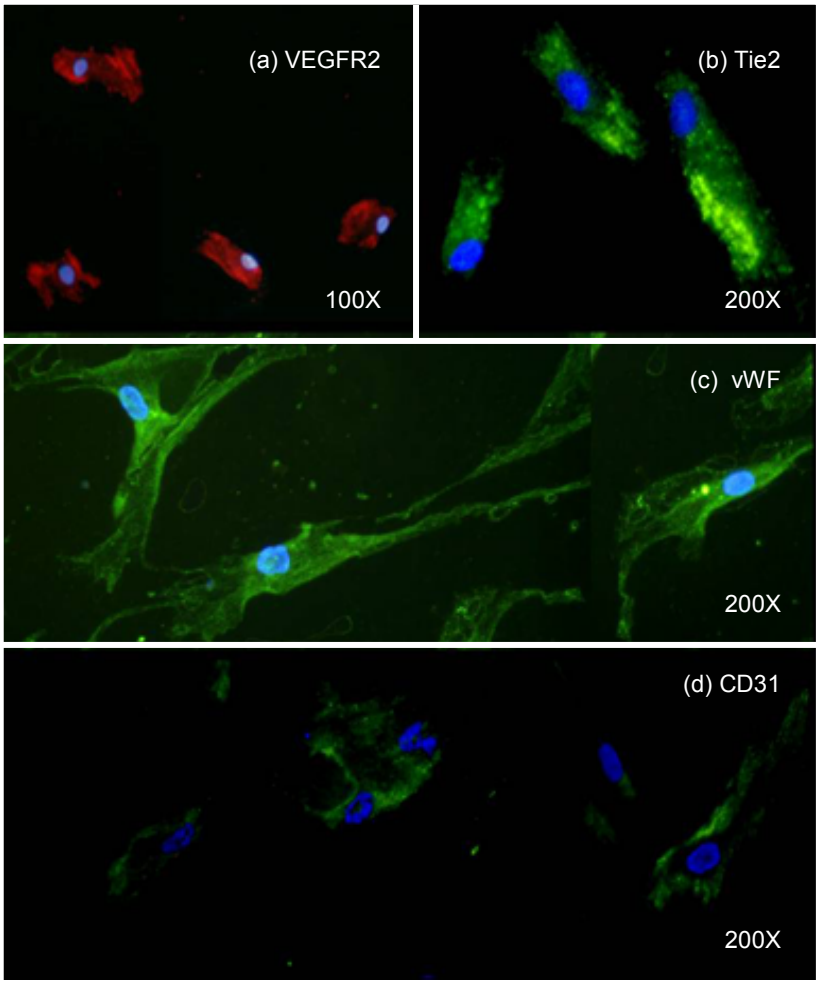

Fig. 7.5. Immunofluorescent staining reveals that the hMSC-derived cells show expression of EC markers, VEGFR2 (Flk-1), Tie2 and vWF (Fig. 7.5a – 7.5c) after a 7-day differentiation. The weak expression of the late EC marker, CD31, was detected after a further 7 days of differentiation (Fig. 7.5d).

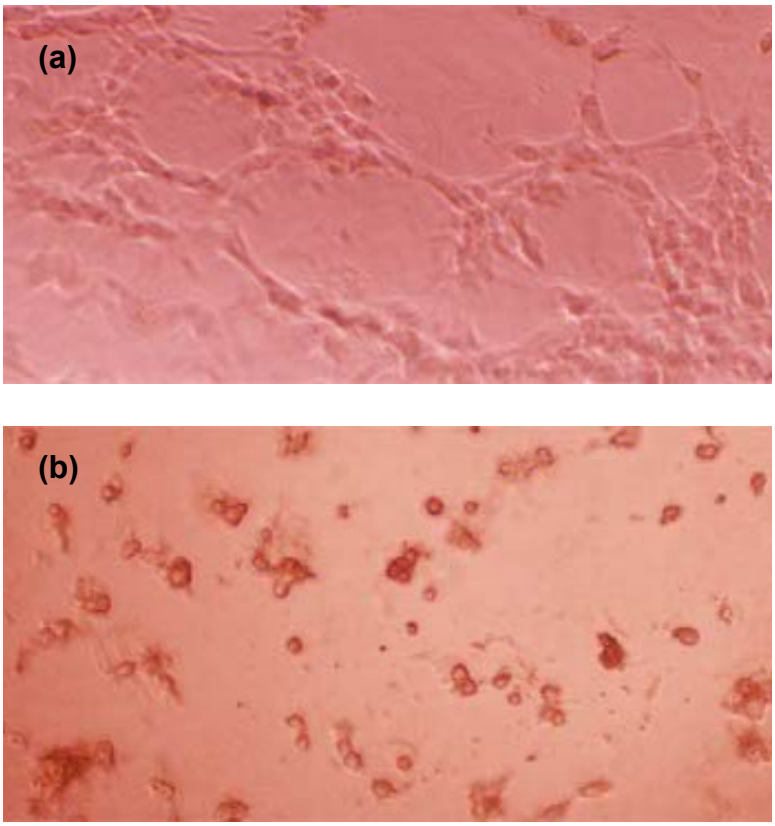

Fig. 7.6. Endothelial cells differentiated from hMSCs display a capillary network formation on Matrigel. A visual count reveals that about 90% of the cells form the network (Fig. 7.6a). Untreated hMSCs remain as isolated, single cells on the Matrigel surface (Fig. 7.6b).

Discussion

PLGA is a synthetic biodegradable polymeric material which has been used as a material for sutures, and for the fabrication of scaffolds in tissue engineering to provide temporary support for cellular survival and tissue development. It has a controllable degradation rate, possesses suitable mechanical strength, and is also an easy material to mould into different shapes [180, 181]. Its adjustable degradation rate also makes it suitable to be used as a controlled release delivery device. Unfortunately, PLGA usually needs to be chemically modified so that other molecules may be covalently grafted onto its surface. Chemical modification may consequently weaken the mechanical strength of PLGA [179, 182]. Similarly, most bioactive molecules which are intended to be grafted onto PLGA usually also need to be chemically modified [183, 184]. For example, VEGF can be oxidized using periodate oxidation for subsequent grafting onto dihydrazide modified PLGA [181]. However, chemical modification of a bioactive molecule may inactivate it or alter its effective biological function. The oxidized forms of two human VEGF isoforms, $VEGF_{165}$ and $VEGF_{121}$, have been reported to lose their ability to bind to the VEGF receptor, VEGFR-2 [180]. While cell-surface heparan-sulphate proteoglycans can restore the VEGFR-2 binding ability of oxidized $VEGF_{165}$ by playing a chaperone-like role, the same process cannot restore the VEGFR-2 binding ability of oxidized $VEGF_{121}$. Thus, the reported decrease in activity of $VEGF_{121}$ could probably be due to oxidative damage. Hence, a method to functionalize a biodegradable material without compromising its mechanical strength and

degradation properties would be an advantage. Similarly, bioactive molecules should be attached to a matrix without any alteration to their chemical structure which may consequently compromise their biological activity. In the present study, a simple and effective method of coating PLGA sutures with VEGF was used. PLGA degrades by hydrolysis into its constituent lactic and glycolic acids [63]. As degradation proceeds, the presence of more acidic groups may thus autocatalyze the hydrolysis process. For this reason, it can be expected that the release kinetics of any bioactive molecule, in this case, VEGF, will be affected. The degradation of the PLGA sutures was studied by monitoring the changes in the pH of each of the solutions in which the sutures were submerged. The results show that the PLGA suture substrates underwent a gradual degradation process. The degradation in cell culture medium had the smallest change in pH. This could be due to the greater buffering capacity of the culture medium. The control of pH *in vivo* could be an important consideration if PLGA were to be used as a delivery device, as large pH changes may affect the degradation rate of PLGA. The *in vivo* environment is dynamic: as PLGA degrades, blood flow and tissue fluid surrounding the implant site would probably remove the products of degradation, and thus prevent the accumulation of the acidic break-down products. This would reduce the rate of autocatalytic degradation of the PLGA implant, and consequently prevent a massive release of the attached VEGF. In the present study, the degradation rate of PLGA was correlated with the release profile of VEGF from the PLGA substrate over a similar length of time. VEGF is chosen because it plays a key role in vasculogenesis and angiogenesis. Owing

to this important role, VEGF is often used in the *in vitro* differentiation of haematopoietic stem cells or endothelial progenitor cells into endothelial cells [185-187]. VEGF is known to have a short half-life in solution [188]. Hence, it is paramount that VEGF must be continually released at an optimal rate so that there are sufficient biologically active quantities of it in solution to mediate EC differentiation. The results show that VEGF is progressively released from the substrate surface and reached a peak on day 15. This indicates that our PLGA suture substrate is capable of the sustained release of amounts of biologically active VEGF.

The hMSCs have been characterized by flow cytometry and confirmed by the supplier to express MSC markers including CD105. Using flow cytometry, a further check was done to ensure that there were no endothelial progenitors present among the hMSCs. The presence of CD133+ cells was not detected. The aim of the present study is to test if the VEGF released from the suture substrates can induce the differentiation of the CD105+ hMSCs into ECs. The results show that the hMSC-derived cells expressed VEGFR2 (Flk-1), Tie2 and vWF after 7 days of VEGF-mediated differentiation. However, CD31, which has been implicated in various biological phenomena, including cell migration, angiogenesis, transendothelial migration and modulation of integrin-mediated cell adhesion, was not detected on the differentiated cells after a 7-day VEGF treatment. This is consistent with similar observations reported by other researchers [189, 190]. After a further 7 days of differentiation, the weak expression of CD31 was detected, indicating that this marker is expressed late in

EC differentiation. Based on this finding, an *in vitro* angiogenesis assay was carried out. hMSC-derived cells differentiated for 14 days in medium with VEGF released from the suture substrates plated onto a Matrigel surface. The formation of a capillary network was observed 3 h after cell plating. A visual count showed that about 90% of the treated cells form the tube-like network. Similarly, about 90% of hMSCs cultured in normal medium supplemented with 10 ng / ml (positive control) form a capillary network on Matrigel. Undifferentiated hMSCs in medium without VEGF (negative control) remained as single cells on the Matrigel. As the hMSCs had been ascertained to be non-CD133+, the possibility that the differentiated cells originated from a small population of endothelial progenitors can be excluded. Thus, the results indicate that the method used in the present study to coat the PLGA substrate with VEGF can retain the biological activity of this growth factor, and progressively release it to mediate EC differentiation.

Various other methods of immobilizing bioactive molecules onto substrates have been reported, with most of them requiring extensive modification to the substrate surface and to the bioactive molecules. Despite the potential risks that chemical and genetic modifications pose to the performance of both the substrates and the bioactive molecules, there have been some encouraging results. Basic fibroblast growth factor (bFGF) loaded within heparin conjugated PLGA microspheres has been shown to be released gradually *in vivo* to support angiogenesis [191]. Heparin is a highly sulphated glycosaminoglycan that has binding affinities to various growth factors. Heparin also helps to mitigate

the mitogenic activity of growth factors through the growth regulation of fibroblast and endothelial cells [192]. Thus, heparin is commonly used in the fabrication of matrices for the controlled release of growth factors [200, 201]. Others have combined condensed plasmid DNA encoding osteogenic growth factors and angiogenic growth factors, together with bone marrow stromal cells for loading into PLGA scaffolds. These scaffolds have been used for the *in vivo* induction of bone tissue regeneration and blood vessel formation [193]. Although not as potentially risky as cellular transplantation of virus-mediated genetically modified cells, substrate-immobilized plasmid DNA may result in the continuous secretion of a high level of a growth factor. Thus, plasmid DNA encoding an angiogenic factor like bFGF may accelerate the growth of pre-existing tumours or occult cancer, although bFGF is only weakly oncogenic [203-208]. Furthermore, continuous delivery of a relatively high concentration of bFGF can possibly worsen diabetic retinopathy [194]. A growth factor can also be anchored to a substrate using a cysteine tag [195]. However, this method involves the genetic modification of VEGF and its expression in *Escherichia coli*. The modified VEGF carries a cysteine tag that allows it to be conjugated to fibronectin using a cross-linking agent. Although fusion tag conjugates may be an attractive alternative to immobilize bioactive molecules onto implantable substrates, it involves extensive genetic modification and relies on the use of micro-organisms to express the modified protein.

Conclusion

PLGA is a suitable biodegradable polymer to be used for tissue engineering applications. Its tunable degradation rate enables it to be tailored to suit its application. The ease of moulding PLGA into structures with suitable mechanical strength and its degradation into harmless products in the body make it a potentially excellent controlled release delivery device. However, the extensive chemical modification of PLGA during the functionalization process could potentially compromise its mechanical strength as well as render the attached bioactive molecules non-functional. In the present study, the method of anchoring VEGF on unmodified PLGA suture substrates can enable the gradual release of the angiogenic factor from the substrate into the solution, to induce the differentiation of hMSCs into ECs.

Each additional step in a modification procedure can potentially compromise the performance of an implantable device, as well as increase the risk potential associated with its application. It is therefore reasonable to be concerned that extensively modified implants and bioactive molecules can be potentially hazardous *in vivo*. Thus, simple functionalization procedures should be as widely adopted as possible. The method of immobilizing VEGF onto PLGA substrates reported here possesses the advantage of ease of fabrication and poses a relatively minimal risk *in vivo*. Thus, this method can serve as a model for the attachment of other bioactive molecules onto various types of substrates, especially for the fabrication of controlled release devices.

Chapter 8

Concluding chapter for this thesis

Conclusion

The continual search for advanced orthopaedic biomaterials

The conceptual evolution of orthopaedic biomaterials has taken place over three generations, from the first generation of bioinert materials, through the second generation of bioactive and resorbable materials, to the third generation materials that are engineered to stimulate specific cellular responses at the molecular level. This continual biomaterial evolution has taken the process toward the development of materials capable of instructive and smart functions. The fundamental strategy of smart biomaterials design remains largely the same as in the late 1960s when Larry Hench designed biomaterials containing calcium and phosphate in proportions similar to bone mineral [3]. Currently, the strategy has taken on a new dimension - to design smart biomaterials that can direct biological entities to entirely regenerate tissues. The aim is to create a synthetic tissue or organ that can function as the original natural counterpart. This ambition has taken biomedical engineering research to the molecular, cellular and macroscopic levels in investigating biological mechanisms occurring in tissues and organs, and biomaterial interfaces. Hence, the trend in biomaterials development is shifting towards creating biologically active systems that can interact with the biological environment. Thus, from tissue engineering with biomaterials as scaffolds combined with autologous cells, the interest has shifted toward creating smart biomaterials by incorporating bioactive molecules or peptide sequences into delivery substrates [196, 197]. The controlled release of bioactive molecules into the local environment or the attached peptide sequences serve to instruct the behaviour of adhered cells. The surface

chemistry of a substrate has also been shown to modulate cellular behaviour. This is illustrated by the example of a class of biphasic calcium phosphate ceramic which can induce osteogenesis at non-osseous sites *in vivo*, without the need for attached cells on the ceramic or the delivery of incorporated bioactive molecules [198]. Thus the surface chemistry of a biomaterial may be exploited to create a surface that interacts with the biological environment. A biomaterial surface can be engineered to allow the selective adsorption of morphogenetic proteins that induce osteogenesis.

The evolving strategies

The current strategy in tissue repair is to design biocompatible constructs that restores the damaged function and stimulate specific biological responses [3]. The idea of a biomaterial that mimics biological responses is an exciting one. Orthopaedic biomimetic materials have been developed for hard and soft tissue repair. The relatively new field of tissue engineering combines a biomaterial with cells to create an artificial tissue to replace damaged or diseased tissue. Tissue engineering is thus an interdisciplinary field that puts together engineering principles and methods and life sciences to develop biological substitutes that restore, maintain and improve the function of damaged tissues and organs [199]. Progress in biomaterial design have progressed to the stage where attempts are made at fabricating materials that can instruct physico-chemical and biological processes at biomaterial interfaces [3]. Osteoinductive biomaterials are able to direct bone formation *in vivo* but the mechanism of osteoinduction still remains

unclear [3]. Despite this, important parameters like the pore size of osteoinductive materials have been identified [200]. Also important are other biomaterial parameters that influence the formation of hard and soft skeletal tissue. These parameters need to be taken into consideration in the design of smart biomaterials. Some biomaterials undergo spontaneous degradation, hence the degradation mechanism need to be understood, especially if bioactive molecules are incorporated into the design of these biomaterials. Degradation affects the release kinetics of loaded drugs and growth factors, an important parameter that has been considered in chapter 7. A degradable biomaterial with a well-tuned degradation rate can be effectively used to deliver drugs and bioactive molecules to a localized region of the healing bone. The presence of proteins on the surface of a biomaterial can affect protein adsorption on the substrate surface and consequently influence cellular behaviour [201, 202]. The charge and concentration of adsorbed proteins can determine their coverage on the substrate surface [203]. The quantity and conformation of adsorbed serum proteins on biomaterial surfaces could influence ionic exchanges and consequently biological activity, and thus determine cellular activity [204, 205]. Thus, ligands can be attached onto biomaterial surfaces to serve to attract cell types with the appropriate cell surface receptors. Other than surface physico-chemical properties, the topography of biomaterials is also another important parameter which can be manipulated to induce specific cellular functions [3]. Other ways to enable smart biomaterials include creating multi-component 3-

dimensional scaffolds, as well as attachment of different bioactive molecules to a scaffold to create a multi-function substrate [3].

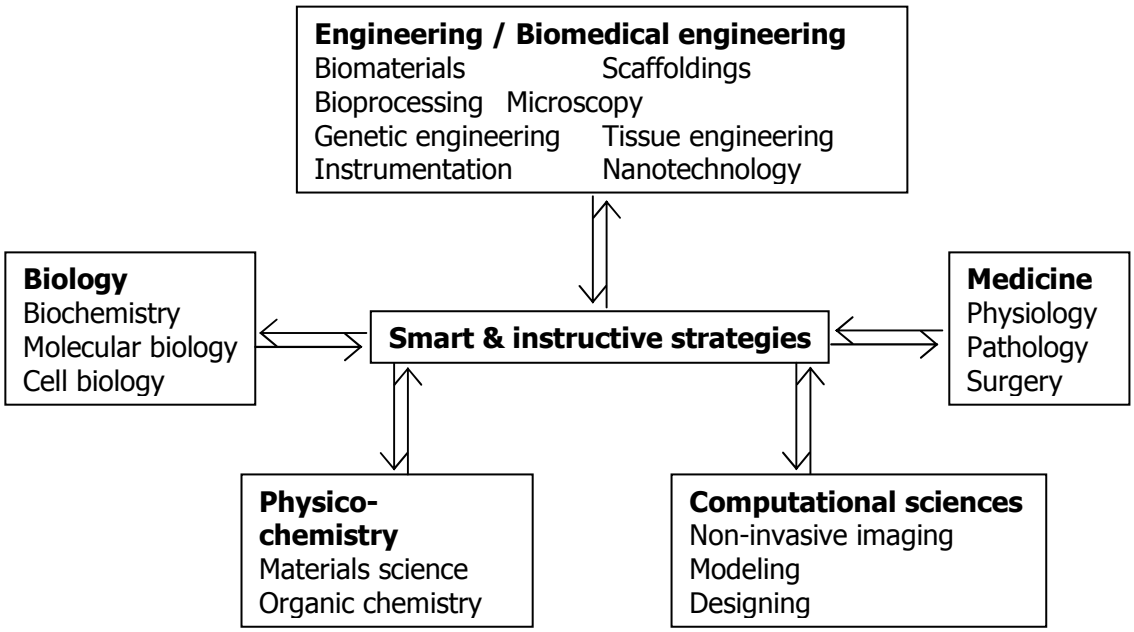

Fig. 8.1. The convergence of scientific disciplines and technologies enables smart and instructive strategies for tissue regeneration. (Adapted from Barrère *et. al. Materials Science and Engineering: R: Reports* **59** (2008), pp. 38-71.)

Potential revolutionary biomaterials

More revolutionary developments in biomaterials could involve the incorporation of nanotechnology with tissue engineering [206]. The creation of self-assembling peptides can be realized with an understanding of the three-dimensional structures of existing biomolecues and the availability of automated chemical synthesis processes [207-211]. Smart peptides can respond to environmental cues and self-assemble into nanofilaments and nanoropes offer much promise [212, 213]. These revolutionary smart biomaterials can interact intelligently with cells and peptide sequences, which can potentially be applied to orthopaedic implant materials.

Smart biomaterials that can respond to the body environment are potential candidates for the fabrication of extra-cellular matrix (ECM). Biologically, natural ECM confers mechanical strength to the cell and maintains its integrity. ECM components are intimately involved in the transduction of cellular signals that control tissue-specfic gene expressions mediated by growth factors [197, 214, 215]. ECM made of smart biomaterials that mimic natural ECM would add a new dimension in tissue engineering. Such artificial ECM, unlike natural ones like decellularized ECM, can potentially be safely used in vivo without causing immunogenecity [206].

The convergence of scientific disciplines and technologies

The evolution of biomaterials has been made possible through the convergence of a multitude of scientific disciplines and technologies (Fig. 8.1) [3].

The amalgamation of knowledge from biology, physico-chemistry, computational sciences, medicine and engineering / biomedical engineering paves a promising direction in which he design of biomaterials currently moves. In the design of bone implants, smart and instructive strategies is the way forward, towards the emergence of a generation of orthopaedic biomaterials that can direct self-healing of bone defects.

The contributions of this project

The work done in the present thesis has enabled a better appreciation of the capabilities of specifically functionalized biomaterials and their potential to be used for the fabrication of implants. The cell-based assays have also enabled a better understanding of the molecular and cellular events that occur in the differentiating cells which are attached on the substrate surface. The present work forms the basis for future work on bone cell differentiation on metallic substrates. The work done on the PLGA-VEGF substrate is a proof of concept to illustrate the use of a resorbable biomaterial as a controlled release delivery device for orthopaedic applications. It, too, forms the basis for future work on using PLGA or any other resorbable biomaterial as a carrier for bioactive molecules. Together, the work in the present thesis paves the way for further highly detailed work to be performed, for the creation of smart implants for orthopaedic applications, which are able to instruct the self-healing of bone defects.

Limitations of this project

Despite the contributions of this project, there are undeniably limitations. Limited technical, financial and time resources necessarily restrict the techniques employed, and the biological work done. While the techniques of depositing a BMP2 coat on the titanium substrate, including the improved method mentioned in chapter 5, result in a stably attached BMP2 layer under *in vitro* conditions, this may not be the case under surgical conditions. The gelatin-agarose layer used to coat the VEGF adsorbed on the PLGA substrate surface can similarly be easily displaced under surgical conditions. A protective coating over the VEGF adsorbed on the PLGA surface serves as a reservoir to evenly release the VEGF. However, a more durable coating material needs to be used. All the biological assays were carried out under *in vitro* conditions. The response of the cells attached on the titanium substrates *in vitro* may not reflect the response of the cells *in vivo* in the presence of the cytokine milieu. The same can be said of the response of the endothelial cells in the case of the PLGA-VEGF substrate.

Possible future work

The work in the present thesis has shown that the creation of smart biomaterials for directing the self-healing of bone is feasible. However, the BMP2 coat on the titanium substrate need to be stably attached enough to withstand abrasive forces. One possible way to enhance the stability of the BMP2 layer is to sand-blast the substrate surface. Sand-blasting creates tiny indentations on the substrate surface where BMP2 molecules may be attached. The indentations serve to shield the BMP2 molecules from abrasions. The gelatin-agarose gel coating on the PLGA-VEGF substrate can be replaced by a more durable and resorbable crosslinked polyacrylamide gel. However, acrylamide must be handled with caution. Polyacrylamide is not toxic but unpolymerized acrylamide could be present in the polymerized acrylamide. Thus, the polyacrylamide used should be of similar quality as those used to make soft contact lenses. Understandably, the technology used to make polyacrylamide of contact lens quality may not be available in a biomedical research laboratory, and could be a potential limitation unless a commercial supply is available. Possible future work can also be done to examine the osteogenic effects of the Ti-CS-BMP2(gluta) substrate and the angiogenic effects of the PLGA-VEGF substrate *in vivo*. An investigation into the immunological responses induced by the implantation of these two substrates should also be done. Immune responses have an integral role in the process of bone healing. Hence, a detailed study of the osteoimmunology of bone healing *in vivo* will yield

useful information for improving the functionalization process of the two types of substrates examined by the present author.

Bibliography

[1] K. Miyazono, S. Maeda and T. Imamura, Coordinate regulation of cell growth and differentiation by TGF-beta superfamily and Runx proteins, *Oncogene* **23** (2004), pp. 4232-4237.

[2] B. I. Rini and E. J. Small, Biology and clinical development of vascular endothelial growth factor-targeted therapy in renal cell carcinoma, *J Clin Oncol* **23** (2005), pp. 1028-1043.

[3] T. A. M. F. Barrère, K. de Groot, C.A. van Blitterswijk, Advanced biomaterials for skeletal tissue regeneration: Instructive and smart functions, *Materials Science and Engineering: R: Reports* **59** (2008), pp. 38-71.

[4] J. W. Costerton, P. S. Stewart and E. P. Greenberg, Bacterial biofilms: a common cause of persistent infections, *Science (New York, N.Y* **284** (1999), pp. 1318-1322.

[5] L. L. Hench, Biomaterials, *Science (New York, N.Y* **208** (1980), pp. 826-831.

[6] J. Brettle, A survey of the literature on metallic surgical implants, *Injury* **2** (1970), pp. 26-39.

[7] W. Al Hertani, J. P. Waddell and G. I. Anderson, The effect of partial vs. full hydroxyapatite coating on periprosthetic bone quality around the canine madreporic femoral stem, *J Biomed Mater Res* **53** (2000), pp. 518-524.

[8] U. Breine, B. Johansson, P. J. Roylance, H. Roeckert and J. M. Yoffey, Regeneration of Bone Marrow. A Clinical and Experimental Study Following Removal of Bone Marrow by Curettage, *Acta Anat (Basel)* **59** (1964), pp. 1-46.

[9] B. Daley, A. T. Doherty, B. Fairman and C. P. Case, Wear debris from hip or knee replacements causes chromosomal damage in human cells in tissue culture, *J Bone Joint Surg Br* **86** (2004), pp. 598-606.

[10] G. J. Thompson and D. A. Puleo, Ti-6Al-4V ion solution inhibition of osteogenic cell phenotype as a function of differentiation timecourse in vitro, *Biomaterials* **17** (1996), pp. 1949-1954.

[11] P. Ducheyne, S. Radin, M. Heughebaert and J. C. Heughebaert, Calcium phosphate ceramic coatings on porous titanium: effect of structure and composition on electrophoretic deposition, vacuum sintering and in vitro dissolution, *Biomaterials* **11** (1990), pp. 244-254.

[12] R. F. C. M. Francisco J.C. Braga, Edson de A. Filho, Antonio C. Guastaldi, Surface modification of Ti dental implants by Nd:YVO4 laser irradiation, *Applied Surface Science* **253** (2007), pp. 9203-9208.

[13] S. D. R. Krishnan, R. Kesavamoorthy, C. Babu Rao, A.K. Tyagi, Baldev Raj and Metallurgy and Materials Group, Laser surface modification and characterization of air plasma sprayed alumina coatings *Surface and Coatings Technology* **200** (2006), pp. 2791-2799.

[14] F. M. Tadashi Kokubo, Hyun-Min Kim, Takashi Nakamura, Spontaneous Formation of Bonelike Apatite Layer on Chemically Treated Titanium Metals, *Journal of the American Ceramic Society* **79** (1996), pp. 1127-1129.

[15] P. Li and K. de Groot, Calcium phosphate formation within sol-gel prepared titania in vitro and in vivo, *J Biomed Mater Res* **27** (1993), pp. 1495-1500.

[16] C. Ohtsuki, H. Iida, S. Hayakawa and A. Osaka, Bioactivity of titanium treated with hydrogen peroxide solutions containing metal chlorides, *J Biomed Mater Res* **35** (1997), pp. 39-47.

[17] R. K. Kulkarni, E. G. Moore, A. F. Hegyeli and F. Leonard, Biodegradable poly(lactic acid) polymers, *J Biomed Mater Res* **5** (1971), pp. 169-181.

[18] R. K. Kulkarni, K. C. Pani, C. Neuman and F. Leonard, Polylactic acid for surgical implants, *Arch Surg* **93** (1966), pp. 839-843.

[19] W. J. Ciccone, 2nd, C. Motz, C. Bentley and J. P. Tasto, Bioabsorbable implants in orthopaedics: new developments and clinical applications, *J Am Acad Orthop Surg* **9** (2001), pp. 280-288.

[20] R. von Oepen and W. Michaeli, Injection moulding of biodegradable implants, *Clin Mater* **10** (1992), pp. 21-28.

[21] S. Li and S. McCarthy, Further investigations on the hydrolytic degradation of poly (DL-lactide), *Biomaterials* **20** (1999), pp. 35-44.

[22] M. Vert, Li, S.M., G. Spenlehhauer, P. Guerin Bioresorbability and biocompatibility of aliphatic polyesters, *J. Mater. Sci. Mater. Med.* **3** (1992), pp. 432-446.

[23] A. Gopferich, Mechanisms of polymer degradation and erosion, *Biomaterials* **17** (1996), pp. 103-114.

[24] I. Grizzi, H. Garreau, S. Li and M. Vert, Hydrolytic degradation of devices based on poly(DL-lactic acid) size-dependence, *Biomaterials* **16** (1995), pp. 305-311.

[25] S. Li, Hydrolytic degradation characteristics of aliphatic polyesters derived from lactic and glycolic acids, *J Biomed Mater Res* **48** (1999), pp. 342-353.

[26] J. M. Brady, D. E. Cutright, R. A. Miller and G. C. Barristone, Resorption rate, route, route of elimination, and ultrastructure of the implant site of polylactic acid in the abdominal wall of the rat, *J Biomed Mater Res* **7** (1973), pp. 155-166.

[27] J. C. Middleton and A. J. Tipton, Synthetic biodegradable polymers as orthopedic devices, *Biomaterials* **21** (2000), pp. 2335-2346.

[28] L. L. Hench and J. M. Polak, Third-generation biomedical materials, *Science (New York, N.Y* **295** (2002), pp. 1014-1017.

[29] Z. Ma, C. Gao, Y. Gong, J. Ji and J. Shen, Immobilization of natural macromolecules on poly-L-lactic acid membrane surface in order to improve its cytocompatibility, *J Biomed Mater Res* **63** (2002), pp. 838-847.

[30] M. V. S. M. Li, Morphological Changes Resulting from the Hydrolytic Degradation of Stereocopolymers Derived from L- and DL-Lactides, *Macromolecules* **27** (1994), pp. 3107-3110.

[31] C. M. Agrawal and R. B. Ray, Biodegradable polymeric scaffolds for musculoskeletal tissue engineering, *J Biomed Mater Res* **55** (2001), pp. 141-150.

[32] K. Kato, Y. Eika and Y. Ikada, Deposition of a hydroxyapatite thin layer onto a polymer surface carrying grafted phosphate polymer chains, *J Biomed Mater Res* **32** (1996), pp. 687-691.

[33] P. Hardouin, K. Anselme, B. Flautre, F. Bianchi, G. Bascoulenguet and B. Bouxin, Tissue engineering and skeletal diseases, *Joint Bone Spine* **67** (2000), pp. 419-424.

[34] H. Hutmacher, Schliephake, A Review of Material Properties of Biodegradable and Bioresorbable Polymers and Devices for GTR and GBR Applications, *Int J Oral Maxillofac Implants* **11** (1996), pp. 667-678.

[35] J. S. Temenoff and A. G. Mikos, Review: tissue engineering for regeneration of articular cartilage, *Biomaterials* **21** (2000), pp. 431-440.

[36] X. Wang, J. Ma, Y. Wang and B. He, Structural characterization of phosphorylated chitosan and their applications as effective additives of calcium phosphate cements, *Biomaterials* **22** (2001), pp. 2247-2255.

[37] A. Yokoyama, S. Yamamoto, T. Kawasaki, T. Kohgo and M. Nakasu, Development of calcium phosphate cement using chitosan and citric acid for bone substitute materials, *Biomaterials* **23** (2002), pp. 1091-1101.

[38] J. C. Banwart, M. A. Asher and R. S. Hassanein, Iliac crest bone graft harvest donor site morbidity. A statistical evaluation, *Spine* **20** (1995), pp. 1055-1060.

[39] J. C. Fernyhough, J. J. Schimandle, M. C. Weigel, C. C. Edwards and A. M. Levine, Chronic donor site pain complicating bone graft harvesting from the posterior iliac crest for spinal fusion, *Spine* **17** (1992), pp. 1474-1480.

[40] J. A. Goulet, L. E. Senunas, G. L. DeSilva and M. L. Greenfield, Autogenous iliac crest bone graft. Complications and functional assessment, *Clin Orthop Relat Res* (1997), pp. 76-81.

[41] K. Cai, K. Yao, Y. Cui, et al., Surface modification of poly (D,L-lactic acid) with chitosan and its effects on the culture of osteoblasts in vitro, *J Biomed Mater Res* **60** (2002), pp. 398-404.

[42] Y. M. Chen, Y. C. Chung, L. W. Wang, K. T. Chen and S. Y. Li, Antibacterial properties of chitosan in waterborne pathogen, *J Environ Sci Health A Tox Hazard Subst Environ Eng* **37** (2002), pp. 1379-1390.

[43] S. P. Massia, J. Stark and D. S. Letbetter, Surface-immobilized dextran limits cell adhesion and spreading, *Biomaterials* **21** (2000), pp. 2253-2261.

[44] S. P. Massia and J. Stark, Immobilized RGD peptides on surface-grafted dextran promote biospecific cell attachment, *J Biomed Mater Res* **56** (2001), pp. 390-399.

[45] R. E. Y. Marchant, S.; Szakalas-Gratzl, G., Interactions of plasma proteins with a novel polysaccharide surfactant physisorbed to polyethylene *J Biomater Sci Polym Ed* **6** (1995), pp. 549-564.

[46] E. Osterberg, K. Bergstrom, K. Holmberg, et al., Protein-rejecting ability of surface-bound dextran in end-on and side-on configurations: comparison to PEG, *J Biomed Mater Res* **29** (1995), pp. 741-747.

[47] D. Miksa, E. R. Irish, D. Chen, R. J. Composto and D. M. Eckmann, Dextran functionalized surfaces via reductive amination: morphology, wetting, and adhesion, *Biomacromolecules* **7** (2006), pp. 557-564.

[48] B. Crepon, J. Jozefonvicz, V. Chytry, B. Rihova and J. Kopecek, Enzymatic degradation and immunogenic properties of derivatized dextrans, *Biomaterials* **12** (1991), pp. 550-554.

[49] M. C. D. Richard A. Frazier, Gert Matthijs, Clive J. Roberts, Etienne Schacht, Saul J. B. Tendler, and Philip M. Williams, In Situ Surface Plasmon

Resonance Analysis of Dextran Monolayer Degradation by Dextranase, *Langmuir* **13** (1997), pp. 7115-7120.

[50] A. Domb and A. G. Mikos, Matrices and scaffolds for drug delivery in tissue engineering, *Adv Drug Deliv Rev* **59** (2007), pp. 185-186.

[51] E. Fattal, S. Pecquet, P. Couvreur and A. Andremont, Biodegradable microparticles for the mucosal delivery of antibacterial and dietary antigens, *Int J Pharm* **242** (2002), pp. 15-24.

[52] C. Fonseca, S. Simoes and R. Gaspar, Paclitaxel-loaded PLGA nanoparticles: preparation, physicochemical characterization and in vitro anti-tumoral activity, *J Control Release* **83** (2002), pp. 273-286.

[53] T. Hickey, D. Kreutzer, D. J. Burgess and F. Moussy, Dexamethasone/PLGA microspheres for continuous delivery of an anti-inflammatory drug for implantable medical devices, *Biomaterials* **23** (2002), pp. 1649-1656.

[54] K. H. Matthews, H. N. Stevens, A. D. Auffret, M. J. Humphrey and G. M. Eccleston, Lyophilised wafers as a drug delivery system for wound healing containing methylcellulose as a viscosity modifier, *Int J Pharm* **289** (2005), pp. 51-62.

[55] L. Mu and S. S. Feng, A novel controlled release formulation for the anticancer drug paclitaxel (Taxol): PLGA nanoparticles containing vitamin E TPGS, *J Control Release* **86** (2003), pp. 33-48.

[56] M. Murillo, C. Gamazo, M. Goni, J. Irache and M. Blanco-Prieto, Development of microparticles prepared by spray-drying as a vaccine delivery system against brucellosis, *Int J Pharm* **242** (2002), pp. 341-344.

[57] J. Panyam and V. Labhasetwar, Biodegradable nanoparticles for drug and gene delivery to cells and tissue, *Adv Drug Deliv Rev* **55** (2003), pp. 329-347.

[58] S. P. Rigby, C. F. Van der Walle and J. H. Raistrick, Determining drug spatial distribution within controlled delivery tablets using MFX imaging, *J Control Release* **96** (2004), pp. 97-100.

[59] M. S. Romero-Cano and B. Vincent, Controlled release of 4-nitroanisole from poly(lactic acid) nanoparticles, *J Control Release* **82** (2002), pp. 127-135.

[60] Y. Yamaguchi, M. Takenaga, A. Kitagawa, Y. Ogawa, Y. Mizushima and R. Igarashi, Insulin-loaded biodegradable PLGA microcapsules: initial burst release controlled by hydrophilic additives, *J Control Release* **81** (2002), pp. 235-249.

[61] K. A. Athanasiou, G. G. Niederauer and C. M. Agrawal, Sterilization, toxicity, biocompatibility and clinical applications of polylactic acid/polyglycolic acid copolymers, *Biomaterials* **17** (1996), pp. 93-102.

[62] S. V. Frank Alexis, Santosh Kumar Rath, Leong-Huat Gan, Some insight into hydrolytic scission mechanisms in bioerodible polyesters, *Journal of Applied Polymer Science*

102 (2006), pp. 3111-3117.

[63] G. M. Çatiker E, Güner A. , Degradation of PLA, PLGA homo- and copolymers in the presence of serum albumin: A spectroscopic investigation., *Polymer International* **49** (2000), pp. 728-734.

[64] M. S. Shive and J. M. Anderson, Biodegradation and biocompatibility of PLA and PLGA microspheres, *Adv Drug Deliv Rev* **28** (1997), pp. 5-24.

[65] B. S. Zolnik, P. E. Leary and D. J. Burgess, Elevated temperature accelerated release testing of PLGA microspheres, *J Control Release* **112** (2006), pp. 293-300.

[66] A. C. Grayson, M. J. Cima and R. Langer, Size and temperature effects on poly(lactic-co-glycolic acid) degradation and microreservoir device performance, *Biomaterials* **26** (2005), pp. 2137-2145.

[67] L. Lu, S. J. Peter, M. D. Lyman, et al., In vitro and in vivo degradation of porous poly(DL-lactic-co-glycolic acid) foams, *Biomaterials* **21** (2000), pp. 1837-1845.

[68] T. G. Park, Degradation of poly(lactic-co-glycolic acid) microspheres: effect of copolymer composition, *Biomaterials* **16** (1995), pp. 1123-1130.

[69] C. M. Kolf, E. Cho and R. S. Tuan, Mesenchymal stromal cells. Biology of adult mesenchymal stem cells: regulation of niche, self-renewal and differentiation, *Arthritis research & therapy* **9** (2007), p. 204.

[70] N. Beyer Nardi and L. da Silva Meirelles, Mesenchymal stem cells: isolation, in vitro expansion and characterization, *Handbook of experimental pharmacology* (2006), pp. 249-282.

[71] Y. Muguruma, T. Yahata, H. Miyatake, et al., Reconstitution of the functional human hematopoietic microenvironment derived from human mesenchymal stem cells in the murine bone marrow compartment, *Blood* **107** (2006), pp. 1878-1887.

[72] J. Ringe, S. Strassburg, K. Neumann, et al., Towards in situ tissue repair: human mesenchymal stem cells express chemokine receptors CXCR1, CXCR2 and CCR2, and migrate upon stimulation with CXCL8 but not CCL2, *J Cell Biochem* **101** (2007), pp. 135-146.

[73] T. Nakase and H. Yoshikawa, Potential roles of bone morphogenetic proteins (BMPs) in skeletal repair and regeneration, *Journal of bone and mineral metabolism* **24** (2006), pp. 425-433.

[74] E. M. Langenfeld and J. Langenfeld, Bone morphogenetic protein-2 stimulates angiogenesis in developing tumors, *Mol Cancer Res* **2** (2004), pp. 141-149.

[75] J. Street, M. Bao, L. deGuzman, et al., Vascular endothelial growth factor stimulates bone repair by promoting angiogenesis and bone turnover, *Proceedings of the National Academy of Sciences of the United States of America* **99** (2002), pp. 9656-9661.

[76] J. M. Kanczler and R. O. Oreffo, Osteogenesis and angiogenesis: the potential for engineering bone, *Eur Cell Mater* **15** (2008), pp. 100-114.

[77] C. Suri, P. F. Jones, S. Patan, et al., Requisite role of angiopoietin-1, a ligand for the TIE2 receptor, during embryonic angiogenesis, *Cell* **87** (1996), pp. 1171-1180.

[78] C. Frelin, A. Ladoux and G. D'Angelo, Vascular endothelial growth factors and angiogenesis, *Annales d'endocrinologie* **61** (2000), pp. 70-74.

[79] Y. Tsuzuki, D. Fukumura, B. Oosthuyse, C. Koike, P. Carmeliet and R. K. Jain, Vascular endothelial growth factor (VEGF) modulation by targeting hypoxia-inducible factor-1alpha--> hypoxia response element--> VEGF cascade differentially regulates vascular response and growth rate in tumors, *Cancer research* **60** (2000), pp. 6248-6252.

[80] G. Augustin, A. Antabak and S. Davila, The periosteum. Part 1: anatomy, histology and molecular biology, *Injury* **38** (2007), pp. 1115-1130.

[81] H. P. Gerber, T. H. Vu, A. M. Ryan, J. Kowalski, Z. Werb and N. Ferrara, VEGF couples hypertrophic cartilage remodeling, ossification and angiogenesis during endochondral bone formation, *Nat Med* **5** (1999), pp. 623-628.

[82] G. Gliki, C. Wheeler-Jones and I. Zachary, Vascular endothelial growth factor induces protein kinase C (PKC)-dependent Akt/PKB activation and phosphatidylinositol 3'-kinase-mediates PKC delta phosphorylation: role of PKC in angiogenesis, *Cell biology international* **26** (2002), pp. 751-759.

[83] J. Yu, D. Bian, C. Mahanivong, R. K. Cheng, W. Zhou and S. Huang, p38 Mitogen-activated protein kinase regulation of endothelial cell migration depends on urokinase plasminogen activator expression, *The Journal of biological chemistry* **279** (2004), pp. 50446-50454.

[84] J. Chai, M. K. Jones and A. S. Tarnawski, Serum response factor is a critical requirement for VEGF signaling in endothelial cells and VEGF-induced angiogenesis, *Faseb J* **18** (2004), pp. 1264-1266.

[85] N. C. Keramaris, G. M. Calori, V. S. Nikolaou, E. H. Schemitsch and P. V. Giannoudis, Fracture vascularity and bone healing: a systematic review of the role of VEGF, *Injury* **39 Suppl 2** (2008), pp. S45-57.

[86] V. Albrecht, T. P. Hofer, B. Foxwell, M. Frankenberger and L. Ziegler-Heitbrock, Tolerance induced via TLR2 and TLR4 in human dendritic cells: role of IRAK-1, *BMC immunology* **9** (2008), p. 69.

[87] C. Alexander and E. T. Rietschel, Bacterial lipopolysaccharides and innate immunity, *Journal of endotoxin research* **7** (2001), pp. 167-202.

[88] R. Medzhitov, Toll-like receptors and innate immunity, *Nature reviews* **1** (2001), pp. 135-145.

[89] R. Medzhitov, P. Preston-Hurlburt and C. A. Janeway, Jr., A human homologue of the Drosophila Toll protein signals activation of adaptive immunity, *Nature* **388** (1997), pp. 394-397.

[90] O. Takeuchi, K. Hoshino, T. Kawai, et al., Differential roles of TLR2 and TLR4 in recognition of gram-negative and gram-positive bacterial cell wall components, *Immunity* **11** (1999), pp. 443-451.

[91] K. W. Kim, M. L. Cho, S. H. Lee, et al., Human rheumatoid synovial fibroblasts promote osteoclastogenic activity by activating RANKL via TLR-2 and TLR-4 activation, *Immunology letters* **110** (2007), pp. 54-64.

[92] F. Liotta, R. Angeli, L. Cosmi, et al., Toll-like receptors 3 and 4 are expressed by human bone marrow-derived mesenchymal stem cells and can inhibit their T-cell modulatory activity by impairing Notch signaling, *Stem cells (Dayton, Ohio)* **26** (2008), pp. 279-289.

[93] R. Shimazu, S. Akashi, H. Ogata, et al., MD-2, a molecule that confers lipopolysaccharide responsiveness on Toll-like receptor 4, *The Journal of experimental medicine* **189** (1999), pp. 1777-1782.

[94] M. S. Nanes, Tumor necrosis factor-alpha: molecular and cellular mechanisms in skeletal pathology, *Gene* **321** (2003), pp. 1-15.

[95] L. Gilbert, X. He, P. Farmer, et al., Expression of the osteoblast differentiation factor RUNX2 (Cbfa1/AML3/Pebp2alpha A) is inhibited by tumor necrosis factor-alpha, *The Journal of biological chemistry* **277** (2002), pp. 2695-2701.

[96] M. Gowen, B. R. MacDonald and R. G. Russell, Actions of recombinant human gamma-interferon and tumor necrosis factor alpha on the proliferation and osteoblastic characteristics of human trabecular bone cells in vitro, *Arthritis and rheumatism* **31** (1988), pp. 1500-1507.

[97] W. Zou, I. Hakim, K. Tschoep, S. Endres and Z. Bar-Shavit, Tumor necrosis factor-alpha mediates RANK ligand stimulation of osteoclast differentiation by an autocrine mechanism, *J Cell Biochem* **83** (2001), pp. 70-83.

[98] J. Ryu, H. J. Kim, E. J. Chang, H. Huang, Y. Banno and H. H. Kim, Sphingosine 1-phosphate as a regulator of osteoclast differentiation and osteoclast-osteoblast coupling, *The EMBO journal* **25** (2006), pp. 5840-5851.

[99] T. Hla, Signaling and biological actions of sphingosine 1-phosphate, *Pharmacol Res* **47** (2003), pp. 401-407.

[100] M. J. Kluk and T. Hla, Signaling of sphingosine-1-phosphate via the S1P/EDG-family of G-protein-coupled receptors, *Biochimica et biophysica acta* **1582** (2002), pp. 72-80.

[101] S. Pyne and N. J. Pyne, Sphingosine 1-phosphate signalling in mammalian cells, *The Biochemical journal* **349** (2000), pp. 385-402.

[102] S. Spiegel and S. Milstien, Sphingosine 1-phosphate, a key cell signaling molecule, *The Journal of biological chemistry* **277** (2002), pp. 25851-25854.

[103] S. Spiegel and S. Milstien, Sphingosine-1-phosphate: an enigmatic signalling lipid, *Nat Rev Mol Cell Biol* **4** (2003), pp. 397-407.

[104] A. Grey, X. Xu, B. Hill, et al., Osteoblastic cells express phospholipid receptors and phosphatases and proliferate in response to sphingosine-1-phosphate, *Calcified tissue international* **74** (2004), pp. 542-550.

[105] T. Roelofsen, R. Akkers, W. Beumer, et al., Sphingosine-1-phosphate acts as a developmental stage specific inhibitor of platelet-derived growth factor-induced chemotaxis of osteoblasts, *J Cell Biochem* **105** (2008), pp. 1128-1138.

[106] O. Oyama, N. Sugimoto, X. Qi, et al., The lysophospholipid mediator sphingosine-1-phosphate promotes angiogenesis in vivo in ischaemic hindlimbs of mice, *Cardiovascular research* **78** (2008), pp. 301-307.

[107] L. S. Sefcik, C. E. Petrie Aronin, K. A. Wieghaus and E. A. Botchwey, Sustained release of sphingosine 1-phosphate for therapeutic arteriogenesis and bone tissue engineering, *Biomaterials* **29** (2008), pp. 2869-2877.

[108] X. Peng, P. M. Hassoun, S. Sammani, et al., Protective effects of sphingosine 1-phosphate in murine endotoxin-induced inflammatory lung injury,

American journal of respiratory and critical care medicine **169** (2004), pp. 1245-1251.

[109] M. A. Eskan, B. G. Rose, M. R. Benakanakere, M. J. Lee and D. F. Kinane, Sphingosine 1-phosphate 1 and TLR4 mediate IFN-beta expression in human gingival epithelial cells, *J Immunol* **180** (2008), pp. 1818-1825.

[110] I. Teige, A. Treschow, A. Teige, et al., IFN-beta gene deletion leads to augmented and chronic demyelinating experimental autoimmune encephalomyelitis, *J Immunol* **170** (2003), pp. 4776-4784.

[111] J. E. Hughes, S. Srinivasan, K. R. Lynch, R. L. Proia, P. Ferdek and C. C. Hedrick, Sphingosine-1-phosphate induces an antiinflammatory phenotype in macrophages, *Circulation research* **102** (2008), pp. 950-958.

[112] C. Xin, S. Ren, B. Kleuser, et al., Sphingosine 1-phosphate cross-activates the Smad signaling cascade and mimics transforming growth factor-beta-induced cell responses, *The Journal of biological chemistry* **279** (2004), pp. 35255-35262.

[113] H. Zhang, M. Oh, C. Allen and E. Kumacheva, Monodisperse chitosan nanoparticles for mucosal drug delivery, *Biomacromolecules* **5** (2004), pp. 2461-2468.

[114] Z. Shi, K. G. Neoh, E. T. Kang, C. Poh and W. Wang, Titanium with Surface-Grafted Dextran and Immobilized Bone Morphogenetic Protein-2 for Inhibition of Bacterial Adhesion and Enhancement of Osteoblast Functions, *Tissue Eng Part A* (2008).

[115] Z. Shi, K. G. Neoh, E. T. Kang, C. Poh and W. Wang, Bacterial adhesion and osteoblast function on titanium with surface-grafted chitosan and immobilized RGD peptide, *Journal of biomedical materials research* **86** (2008), pp. 865-872.

[116] Z. Shi, K. G. Neoh and E. T. Kang, Antibacterial activity of polymeric substrate with surface grafted viologen moieties, *Biomaterials* **26** (2005), pp. 501-508.

[117] K. G. N. Zhilong Shi, En-Tang Kang, Chyekhoon Poh, Wilson Wang., Titanium with Surface-Grafted Dextran and Immobilized Bone Morphogenetic Protein-2 for Inhibition of Bacterial Adhesion and Enhancement of Osteoblast Functions, *Tissue Engineering Part A* **15** (2009), pp. 417-426.

[118] S. Ohnishi, H. Ohgushi, S. Kitamura and N. Nagaya, Mesenchymal stem cells for the treatment of heart failure, *International journal of hematology* **86** (2007), pp. 17-21.

[119] E. I. Rabea, M. E. Badawy, C. V. Stevens, G. Smagghe and W. Steurbaut, Chitosan as antimicrobial agent: applications and mode of action, *Biomacromolecules* **4** (2003), pp. 1457-1465.

[120] Z. Shi, K. G. Neoh, E. T. Kang, C. Poh and W. Wang, Bacterial adhesion and osteoblast function on titanium with surface-grafted chitosan and immobilized RGD peptide, *Journal of biomedical materials research* (2007).

[121] J. Hall, R. G. Sorensen, J. M. Wozney and U. M. Wikesjo, Bone formation at rhBMP-2-coated titanium implants in the rat ectopic model, *Journal of clinical periodontology* **34** (2007), pp. 444-451.

[122] H. Schliephake, A. Aref, D. Scharnweber, S. Bierbaum, S. Roessler and A. Sewing, Effect of immobilized bone morphogenic protein 2 coating of titanium implants on peri-implant bone formation, *Clinical oral implants research* **16** (2005), pp. 563-569.

[123] X. Fan, L. Lin, J. L. Dalsin and P. B. Messersmith, Biomimetic anchor for surface-initiated polymerization from metal substrates, *Journal of the American Chemical Society* **127** (2005), pp. 15843-15847.

[124] D. S. Kommireddy, S. M. Sriram, Y. M. Lvov and D. K. Mills, Stem cell attachment to layer-by-layer assembled TiO2 nanoparticle thin films, *Biomaterials* **27** (2006), pp. 4296-4303.

[125] G. Plickert, M. Kroiher and A. Munck, Cell proliferation and early differentiation during embryonic development and metamorphosis of Hydractinia echinata, *Development (Cambridge, England)* **103** (1988), pp. 795-803.

[126] Y. Yang, J. D. Bumgardner, R. Cavin, D. L. Carnes and J. L. Ong, Osteoblast precursor cell attachment on heat-treated calcium phosphate coatings, *Journal of dental research* **82** (2003), pp. 449-453.

[127] H. J. Ronold, S. P. Lyngstadaas and J. E. Ellingsen, Analysing the optimal value for titanium implant roughness in bone attachment using a tensile test, *Biomaterials* **24** (2003), pp. 4559-4564.

[128] H. J. Buhring, V. L. Battula, S. Treml, B. Schewe, L. Kanz and W. Vogel, Novel markers for the prospective isolation of human MSC, *Annals of the New York Academy of Sciences* **1106** (2007), pp. 262-271.

[129] N. Quirici, D. Soligo, P. Bossolasco, F. Servida, C. Lumini and G. L. Deliliers, Isolation of bone marrow mesenchymal stem cells by anti-nerve growth factor receptor antibodies, *Experimental hematology* **30** (2002), pp. 783-791.

[130] T. Matsunaga, K. Yanagiguchi, S. Yamada, N. Ohara, T. Ikeda and Y. Hayashi, Chitosan monomer promotes tissue regeneration on dental pulp wounds, *Journal of biomedical materials research* **76** (2006), pp. 711-720.

[131] S. Yamada, N. Ohara and Y. Hayashi, Mineralization of matrix vesicles isolated from a human osteosarcoma cell line in culture with water-soluble chitosan-containing medium, *Journal of biomedical materials research* **66** (2003), pp. 500-506.

[132] B. Kulterer, G. Friedl, A. Jandrositz, et al., Gene expression profiling of human mesenchymal stem cells derived from bone marrow during expansion and osteoblast differentiation, *BMC genomics* **8** (2007), p. 70.

[133] D. Campoccia, L. Montanaro and C. R. Arciola, The significance of infection related to orthopedic devices and issues of antibiotic resistance, *Biomaterials* **27** (2006), pp. 2331-2339.

[134] E. A. Jones, S. E. Kinsey, A. English, et al., Isolation and characterization of bone marrow multipotential mesenchymal progenitor cells, *Arthritis and rheumatism* **46** (2002), pp. 3349-3360.

[135] E. A. Jones, A. English, K. Henshaw, et al., Enumeration and phenotypic characterization of synovial fluid multipotential mesenchymal progenitor cells in inflammatory and degenerative arthritis, *Arthritis and rheumatism* **50** (2004), pp. 817-827.

[136] M. Kassem and B. M. Abdallah, Human bone-marrow-derived mesenchymal stem cells: biological characteristics and potential role in therapy of degenerative diseases, *Cell Tissue Res* (2007).

[137] Y. Liu, K. de Groot and E. B. Hunziker, BMP-2 liberated from biomimetic implant coatings induces and sustains direct ossification in an ectopic rat model, *Bone* **36** (2005), pp. 745-757.

[138] Y. Liu, E. B. Hunziker, P. Layrolle, J. D. De Bruijn and K. De Groot, Bone morphogenetic protein 2 incorporated into biomimetic coatings retains its biological activity, *Tissue engineering* **10** (2004), pp. 101-108.

[139] J. Fu, J. Ji, W. Yuan and J. Shen, Construction of anti-adhesive and antibacterial multilayer films via layer-by-layer assembly of heparin and chitosan, *Biomaterials* **26** (2005), pp. 6684-6692.

[140] I.-K. K. Man Woo Huh, Du Hyun Lee, Woo Sik Kim, Dong Ho Lee, Lee Soon Park, Kyung Eun Min, Kwan Ho Seo, Surface characterization and antibacterial activity of chitosan-grafted poly(ethylene terephthalate) prepared by plasma glow discharge, *J Appl Polym Sci* **81** (2001), pp. 2769-2778.

[141] H. K. No, N. Y. Park, S. H. Lee and S. P. Meyers, Antibacterial activity of chitosans and chitosan oligomers with different molecular weights, *International journal of food microbiology* **74** (2002), pp. 65-72.

[142] Z. Shi, K. G. Neoh, E. T. Kang and W. Wang, Antibacterial and mechanical properties of bone cement impregnated with chitosan nanoparticles, *Biomaterials* **27** (2006), pp. 2440-2449.

[143] P. Ducy, Cbfa1: a molecular switch in osteoblast biology, *Dev Dyn* **219** (2000), pp. 461-471.

[144] T. Komori, [Cbfa1/Runx2, an essential transcription factor for the regulation of osteoblast differentiation], *Nippon rinsho* **60 Suppl 3** (2002), pp. 91-97.

[145] T. M. Schroeder, E. D. Jensen and J. J. Westendorf, Runx2: a master organizer of gene transcription in developing and maturing osteoblasts, *Birth Defects Res C Embryo Today* **75** (2005), pp. 213-225.

[146] O. Pullig, G. Weseloh, D. Ronneberger, S. Kakonen and B. Swoboda, Chondrocyte differentiation in human osteoarthritis: expression of osteocalcin in normal and osteoarthritic cartilage and bone, *Calcified tissue international* **67** (2000), pp. 230-240.

[147] S. Gronthos, A. C. Zannettino, S. E. Graves, S. Ohta, S. J. Hay and P. J. Simmons, Differential cell surface expression of the STRO-1 and alkaline phosphatase antigens on discrete developmental stages in primary cultures of human bone cells, *J Bone Miner Res* **14** (1999), pp. 47-56.

[148] M. Mizuno and Y. Kuboki, Osteoblast-related gene expression of bone marrow cells during the osteoblastic differentiation induced by type I collagen, *Journal of biochemistry* **129** (2001), pp. 133-138.

[149] D. A. Puleo and A. Nanci, Understanding and controlling the bone-implant interface, *Biomaterials* **20** (1999), pp. 2311-2321.

[150] M. Morra, Biochemical modification of titanium surfaces: peptides and ECM proteins, *Eur Cell Mater* **12** (2006), pp. 1-15.

[151] J. M. Bobbitt, Periodate oxidation of carbohydrates, *Advances in carbohydrate chemistry* **48** (1956), pp. 1-41.

[152] Hermanson, Editor, *Bioconjugate Techniques*, Academic Press, San Diego, CA, USA (2004).

[153] T. Y. Lim, W. Wang, Z. Shi, C. K. Poh and K. G. Neoh, Human bone marrow-derived mesenchymal stem cells and osteoblast differentiation on titanium with surface-grafted chitosan and immobilized bone morphogenetic protein-2, *J Mater Sci Mater Med* **20** (2009), pp. 1-10.

[154] C. M. Digirolamo, D. Stokes, D. Colter, D. G. Phinney, R. Class and D. J. Prockop, Propagation and senescence of human marrow stromal cells in culture: a simple colony-forming assay identifies samples with the greatest potential to propagate and differentiate, *British journal of haematology* **107** (1999), pp. 275-281.

[155] A. Herbertson and J. E. Aubin, Dexamethasone alters the subpopulation make-up of rat bone marrow stromal cell cultures, *J Bone Miner Res* **10** (1995), pp. 285-294.

[156] A. Herbertson and J. E. Aubin, Cell sorting enriches osteogenic populations in rat bone marrow stromal cell cultures, *Bone* **21** (1997), pp. 491-500.

[157] N. Jaiswal, S. E. Haynesworth, A. I. Caplan and S. P. Bruder, Osteogenic differentiation of purified, culture-expanded human mesenchymal stem cells in vitro, *J Cell Biochem* **64** (1997), pp. 295-312.

[158] D. G. Phinney, G. Kopen, W. Righter, S. Webster, N. Tremain and D. J. Prockop, Donor variation in the growth properties and osteogenic potential of human marrow stromal cells, *J Cell Biochem* **75** (1999), pp. 424-436.

[159] D. J. Rickard, M. Kassem, T. E. Hefferan, G. Sarkar, T. C. Spelsberg and B. L. Riggs, Isolation and characterization of osteoblast precursor cells from human bone marrow, *J Bone Miner Res* **11** (1996), pp. 312-324.

[160] A. K. Shah, J. Lazatin, R. K. Sinha, T. Lennox, N. J. Hickok and R. S. Tuan, Mechanism of BMP-2 stimulated adhesion of osteoblastic cells to titanium alloy, *Biol Cell* **91** (1999), pp. 131-142.

[161] M. E. Nimni, D. Cheung, B. Strates, M. Kodama and K. Sheikh, Chemically modified collagen: a natural biomaterial for tissue replacement, *J Biomed Mater Res* **21** (1987), pp. 741-771.

[162] I. Migneault, C. Dartiguenave, M. J. Bertrand and K. C. Waldron, Glutaraldehyde: behavior in aqueous solution, reaction with proteins, and application to enzyme crosslinking, *BioTechniques* **37** (2004), pp. 790-796, 798-802.

[163] A. V. I. Walt D. R., The chemistry of enzyme and protein immobilization with glutaraldehyde, *Trends in Analytical Chemistry* **13** (1994), pp. 425-430.

[164] Y. Wine, N. Cohen-Hadar, A. Freeman and F. Frolow, Elucidation of the mechanism and end products of glutaraldehyde crosslinking reaction by X-ray structure analysis, *Biotechnology and bioengineering* **98** (2007), pp. 711-718.

[165] Z. Wang, G. Zhu, Q. Huang, et al., X-ray studies on cross-linked lysozyme crystals in acetonitrile-water mixture, *Biochimica et biophysica acta* **1384** (1998), pp. 335-344.

[166] M. I. Toshio Tashima, Yoshihiro Kuroda, Shigemasa Yagi, Terumichi Nakagawa, Structure of a new oligomer of glutaraldehyde produced by aldol condensation reaction, *The Journal of Organic Chemistry* **56** (1991), pp. 694-697.

[167] A. J. Habeeb and R. Hiramoto, Reaction of proteins with glutaraldehyde, *Archives of biochemistry and biophysics* **126** (1968), pp. 16-26.

[168] H. H. Weetall, Immobilized enzymes: analytical applications, *Analytical chemistry* **46** (1974), pp. 602A-604A p.

[169] A. A. Ragab, R. Van De Motter, S. A. Lavish, et al., Measurement and removal of adherent endotoxin from titanium particles and implant surfaces, *J Orthop Res* **17** (1999), pp. 803-809.

[170] K. Maruyama, G. Sano and K. Matsuo, Murine osteoblasts respond to LPS and IFN-gamma similarly to macrophages, *Journal of bone and mineral metabolism* **24** (2006), pp. 454-460.

[171] P. H. Warnke, I. N. Springer, P. A. Russo, et al., Innate immunity in human bone, *Bone* **38** (2006), pp. 400-408.

[172] S. Sato, F. Nomura, T. Kawai, et al., Synergy and cross-tolerance between toll-like receptor (TLR) 2- and TLR4-mediated signaling pathways, *J Immunol* **165** (2000), pp. 7096-7101.

[173] I. F. Mo, K. H. Yip, W. K. Chan, H. K. Law, Y. L. Lau and G. C. Chan, Prolonged exposure to bacterial toxins downregulated expression of toll-like receptors in mesenchymal stromal cell-derived osteoprogenitors, *BMC cell biology* **9** (2008), p. 52.

[174] K. Nomiyama, C. Kitamura, T. Tsujisawa, et al., Effects of lipopolysaccharide on newly established rat dental pulp-derived cell line with odontoblastic properties, *Journal of endodontics* **33** (2007), pp. 1187-1191.

[175] J. Lam, Y. Abu-Amer, C. A. Nelson, D. H. Fremont, F. P. Ross and S. L. Teitelbaum, Tumour necrosis factor superfamily cytokines and the pathogenesis of inflammatory osteolysis, *Annals of the rheumatic diseases* **61 Suppl 2** (2002), pp. ii82-83.

[176] A. Sabokbar, O. Kudo and N. A. Athanasou, Two distinct cellular mechanisms of osteoclast formation and bone resorption in periprosthetic osteolysis, *J Orthop Res* **21** (2003), pp. 73-80.

[177] G. Schett and J. P. David, Denosumab--a novel strategy to prevent structural joint damage in patients with RA?, *Nature clinical practice* **4** (2008), pp. 634-635.

[178] S. B. Cohen, R. K. Dore, N. E. Lane, et al., Denosumab treatment effects on structural damage, bone mineral density, and bone turnover in rheumatoid arthritis: a twelve-month, multicenter, randomized, double-blind, placebo-controlled, phase II clinical trial, *Arthritis and rheumatism* **58** (2008), pp. 1299-1309.

[179] Wen, Development of poly (lactic-co-glycolic acid)-collagen

scaffolds for tissue engineering, *Materials*

Science and Engineering C **27** (2006), pp. 285-292.

[180] M. Nakamura, Y. Abe and T. Tokunaga, Pathological significance of vascular endothelial growth factor A isoform expression in human cancer, *Pathology international* **52** (2002), pp. 331-339.

[181] J. L. Sharon and D. A. Puleo, Immobilization of glycoproteins, such as VEGF, on biodegradable substrates, *Acta biomaterialia* **4** (2008), pp. 1016-1023.

[182] Chu, Hydrolytic degradation of polyglycolic acid: Tensile strength and crystallinity study, *Journl of Applied Polymer Science* **26** (1980), pp. 1727-1734.

[183] E. S. Lee, K. Na and Y. H. Bae, Polymeric micelle for tumor pH and folate-mediated targeting, *J Control Release* **91** (2003), pp. 103-113.

[184] B. Stella, S. Arpicco, M. T. Peracchia, et al., Design of folic acid-conjugated nanoparticles for drug targeting, *Journal of pharmaceutical sciences* **89** (2000), pp. 1452-1464.

[185] U. M. Gehling, S. Ergun, U. Schumacher, et al., In vitro differentiation of endothelial cells from AC133-positive progenitor cells, *Blood* **95** (2000), pp. 3106-3112.

[186] N. Quirici, D. Soligo, L. Caneva, F. Servida, P. Bossolasco and G. L. Deliliers, Differentiation and expansion of endothelial cells from human bone marrow CD133(+) cells, *British journal of haematology* **115** (2001), pp. 186-194.

[187] M. Reyes, T. Lund, T. Lenvik, D. Aguiar, L. Koodie and C. M. Verfaillie, Purification and ex vivo expansion of postnatal human marrow mesodermal progenitor cells, *Blood* **98** (2001), pp. 2615-2625.

[188] A. B. Ennett, D. Kaigler and D. J. Mooney, Temporally regulated delivery of VEGF in vitro and in vivo, *Journal of biomedical materials research* **79** (2006), pp. 176-184.

[189] D. E. Jackson, The unfolding tale of PECAM-1, *FEBS letters* **540** (2003), pp. 7-14.

[190] J. Oswald, S. Boxberger, B. Jorgensen, et al., Mesenchymal stem cells can be differentiated into endothelial cells in vitro, *Stem cells (Dayton, Ohio)* **22** (2004), pp. 377-384.

[191] H. J. Chung, H. K. Kim, J. J. Yoon and T. G. Park, Heparin immobilized porous PLGA microspheres for angiogenic growth factor delivery, *Pharmaceutical research* **23** (2006), pp. 1835-1841.

[192] H. Lee, R. A. Cusick, F. Browne, et al., Local delivery of basic fibroblast growth factor increases both angiogenesis and engraftment of hepatocytes in tissue-engineered polymer devices, *Transplantation* **73** (2002), pp. 1589-1593.

[193] Y. C. Huang, D. Kaigler, K. G. Rice, P. H. Krebsbach and D. J. Mooney, Combined angiogenic and osteogenic factor delivery enhances bone marrow stromal cell-driven bone regeneration, *J Bone Miner Res* **20** (2005), pp. 848-857.

[194] M. Bensaid, F. Malecaze, H. Prats, F. Bayard and J. P. Tauber, Autocrine regulation of bovine retinal capillary endothelial cell (BREC) proliferation by BREC-derived basic fibroblast growth factor, *Experimental eye research* **48** (1989), pp. 801-813.

[195] M. V. Backer, V. Patel, B. T. Jehning, K. P. Claffey and J. M. Backer, Surface immobilization of active vascular endothelial growth factor via a cysteine-containing tag, *Biomaterials* **27** (2006), pp. 5452-5458.

[196] D. G. Anderson, S. Levenberg and R. Langer, Nanoliter-scale synthesis of arrayed biomaterials and application to human embryonic stem cells, *Nature biotechnology* **22** (2004), pp. 863-866.

[197] M. P. Lutolf and J. A. Hubbell, Synthetic biomaterials as instructive extracellular microenvironments for morphogenesis in tissue engineering, *Nature biotechnology* **23** (2005), pp. 47-55.

[198] H. Yuan, M. Van Den Doel, S. Li, C. A. Van Blitterswijk, K. De Groot and J. D. De Bruijn, A comparison of the osteoinductive potential of two calcium phosphate ceramics implanted intramuscularly in goats, *J Mater Sci Mater Med* **13** (2002), pp. 1271-1275.

[199] R. Langer and J. P. Vacanti, Tissue engineering, *Science (New York, N.Y* **260** (1993), pp. 920-926.

[200] P. Habibovic, H. Yuan, M. van den Doel, T. M. Sees, C. A. van Blitterswijk and K. de Groot, Relevance of osteoinductive biomaterials in critical-sized orthotopic defect, *J Orthop Res* **24** (2006), pp. 867-876.

[201] T. A. Horbett and M. B. Schway, Correlations between mouse 3T3 cell spreading and serum fibronectin adsorption on glass and hydroxyethylmethacrylate-ethylmethacrylate copolymers, *J Biomed Mater Res* **22** (1988), pp. 763-793.

[202] W. Norde and J. Lyklema, Why proteins prefer interfaces, *J Biomater Sci Polym Ed* **2** (1991), pp. 183-202.

[203] M. K. K. Kawasaki, H. Matsumura, W. Norde, A comparison of the adsorption of saliva proteins and some typical proteins onto the surface of hydroxyapatite, *Colloids and Surfaces B: Biointerfaces* **32** (2003), pp. 321-334.

[204] A. El-Ghannam, P. Ducheyne and I. M. Shapiro, Effect of serum proteins on osteoblast adhesion to surface-modified bioactive glass and hydroxyapatite, *J Orthop Res* **17** (1999), pp. 340-345.

[205] E. C. M. Rouahi, O. Gallet, A. Jada, K. Anselme, Physico-chemical characteristics and protein adsorption potential of hydroxyapatite particles: Influence on in vitro biocompatibility of ceramics after sintering, *Colloids and Surfaces B: Biointerfaces* **47** (2006), pp. 10-19.

[206] M. E. Furth, A. Atala and M. E. Van Dyke, Smart biomaterials design for tissue engineering and regenerative medicine, *Biomaterials* **28** (2007), pp. 5068-5073.

[207] R. Fairman and K. S. Akerfeldt, Peptides as novel smart materials, *Current opinion in structural biology* **15** (2005), pp. 453-463.

[208] M. O. Guler, L. Hsu, S. Soukasene, D. A. Harrington, J. F. Hulvat and S. I. Stupp, Presentation of RGDS epitopes on self-assembled nanofibers of branched peptide amphiphiles, *Biomacromolecules* **7** (2006), pp. 1855-1863.

[209] J. D. Hartgerink, E. Beniash and S. I. Stupp, Peptide-amphiphile nanofibers: a versatile scaffold for the preparation of self-assembling materials,

Proceedings of the National Academy of Sciences of the United States of America **99** (2002), pp. 5133-5138.

[210] D. E. Wagner, C. L. Phillips, W. M. Ali, et al., Toward the development of peptide nanofilaments and nanoropes as smart materials, *Proceedings of the National Academy of Sciences of the United States of America* **102** (2005), pp. 12656-12661.

[211] X. Zhao and S. Zhang, Fabrication of molecular materials using peptide construction motifs, *Trends in biotechnology* **22** (2004), pp. 470-476.

[212] E. Beniash, J. D. Hartgerink, H. Storrie, J. C. Stendahl and S. I. Stupp, Self-assembling peptide amphiphile nanofiber matrices for cell entrapment, *Acta biomaterialia* **1** (2005), pp. 387-397.

[213] G. A. Silva, C. Czeisler, K. L. Niece, et al., Selective differentiation of neural progenitor cells by high-epitope density nanofibers, *Science (New York, N.Y* **303** (2004), pp. 1352-1355.

[214] R. L. Juliano and S. Haskill, Signal transduction from the extracellular matrix, *The Journal of cell biology* **120** (1993), pp. 577-585.

[215] H. Birkedal-Hansen, Proteolytic remodeling of extracellular matrix, *Current opinion in cell biology* **7** (1995), pp. 728-735.